ACS MATERIALS LETTERS

www.acsmaterialsletters.org

REVIEW

Technological Evolution of Image Sensing Designed by Nanostructured Materials

Muhammad Aamir Iqbal,*[,θ] Maria Malik,[θ] Top Khac Le,[θ] Nadia Anwar, Sunila Bakhsh, Wajeehah Shahid, Samiah Shahid, Shaheen Irfan, Mohammed Al-Bahrani, Kareem Morsy, Huy-Binh Do, Vinoth Kumar Ponnusamy,* and Phuong V. Pham*

Cite This: *ACS Materials Lett.* 2023, 5, 1027−1060

Read Online

ACCESS | Metrics & More | Article Recommendations

ABSTRACT: **Imaging sensing holds a remarkable place in modern electronics and optoelectronics for the complementary metal-oxide-semiconductor integration of high-speed optical communications and photodetection with the merits of high-speed operation, cost-effectiveness, and noncomplex fabrication. The optimum quality of image sensing relies on noise, sensitivity, power consumption, voltage operation, and speed imaging to access and compete with the state-of-the-art image sensing devices in the industry. Many studies have been conducted to address these issues; however, performance has not yet been optimized and solutions are still in the works. In this review, we briefly provide information on recent advances in image sensing using nanostructured emerging materials through nanofabrication integration including the technology evolution on traditional and modern technology platforms, general mechanisms, classification, and actual applications as well as existing limitations. Finally, new challenges and perspectives for the future trends of image sensing and their possible solutions are also discussed.**

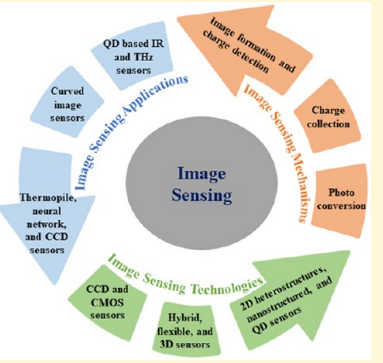

1. INTRODUCTION

The Cambrian explosion, or fast evolution, occurred about 540 million years ago and resulted in the diversification of living organisms into different species. The emergence of diverse sense organs, the most significant of which was the eye's evolution, was one of the causes of this diversification. With the advent of modern technological devices, a similar tendency has emerged. As the world becomes more digital, mobile cameras act as the retinas and complementary metal-oxide-semiconductor (CMOS) or contact image sensor (CIS) to capture the images just like the eyeballs. Researchers were able to quickly process, copy, and preserve vast volumes of visual data by adopting image sensing technologies. Because of the enormous amount of data manipulated on mobile devices, application processor and memory storage device capacity and performance have again exploded. Additionally, people began to place greater value on cameras, which caused mobile devices to become more varied. Consequently, research in image sensing has been drastically increasing annually in the past decade (see Figure 1).

> In this review, we briefly provide information on recent advances in image sensing using nanostructured emerging materials through nanofabrication integration including the technology evolution on traditional and modern technology platforms

> As the world becomes more digital, mobile cameras act as the retinas and complementary metal-oxide-semiconductor (CMOS) or contact image sensor (CIS) to capture the images just like the eyeballs.

Received: October 26, 2022
Accepted: February 22, 2023

https://doi.org/10.1021/acsmaterialslett.2c01011
ACS Materials Lett. 2023, 5, 1027−1060

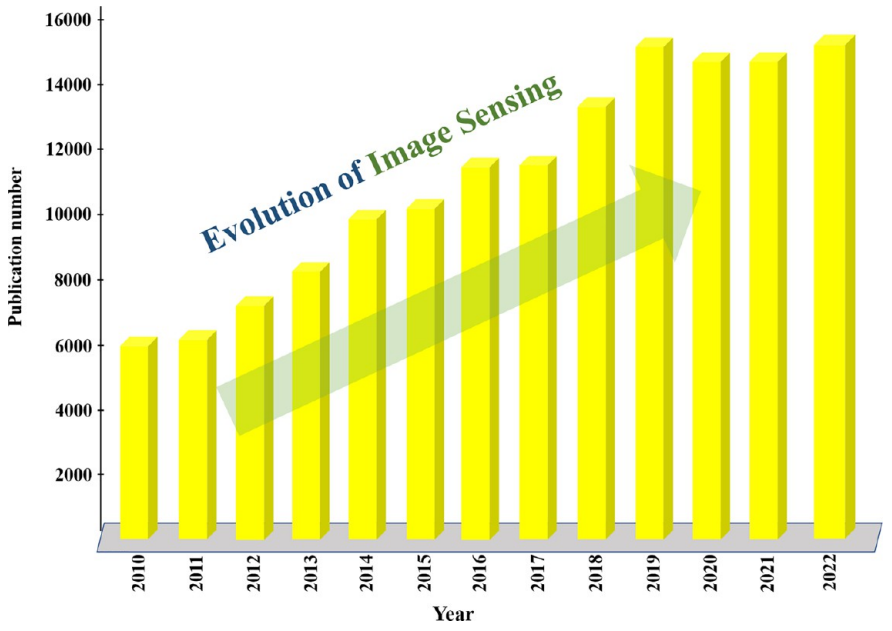

Figure 1. Shedding light on the publication number of image sensing from 2010 to 2022. (Source: Web of Science).

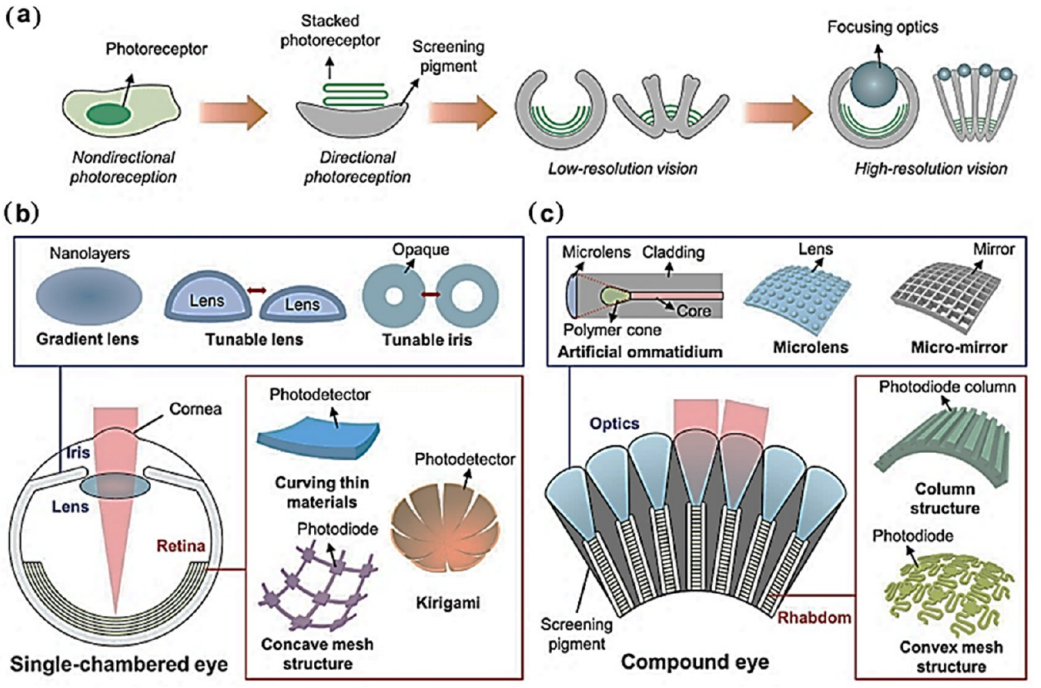

Figure 2. Schematic description and the development of eyes from nondirectional photoreceptors to high-resolution vision, as represented by: (a) single-chambered eyes (left), and compound eyes (right). The major components of bioinspired imaging systems are: (b) single-chambered eyes, and (c) compound eyes. Reproduced with permission from ref 1. Copyright 2018 Wiley.

Through electrical gadgets, the changes that took place during the Cambrian period have been reflected in our daily lives. Additionally, the recent COVID-19 epidemic, which ushered in the "contact-free" era, has spurred diversification and given the electronic device industry a boost in growth. Though the pandemic will eventually come to an end, the tendency will persist. The emergence of the eye was driven by the requirement for the capacity to handle progressively more difficult sensory tasks. The complexity of information processing necessitates more advanced sensory organs, as the amount of information increases. Figure 2 depicts a schematic description of the development of eyes from nondirectional photoreceptors to high-resolution vision as well as the major components of bioinspired imaging systems.[1] When light's photon energy is higher than the semiconductor's bandgap energy, it forms an e^-/h^+ pair as it travels through the optical system and into the photodiode. Depending on the light's intensity, accumulating and interpreting this information enables the creation of a 2D image. Silicon has been found to be a very useful material, with a bandgap energy of 1.1 eV that covers the entire spectrum of the human eye, opening up new avenues for detection and imaging applications.[2]

https://doi.org/10.1021/acsmaterialslett.2c01011
ACS Materials Lett. 2023, 5, 1027−1060

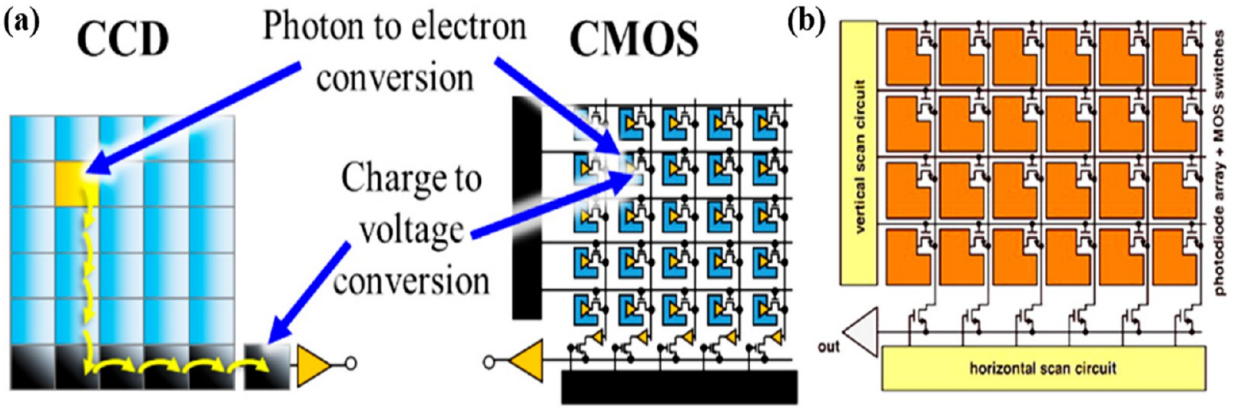

Figure 3. Structural comparison of: (a) CCD and (b) CMOS image sensor. Reproduced with permission from ref 6. Copyright 2020 MDPI. (b) schematic layout of a CIS image sensing device. Reproduced with permission from ref 7. Copyright 2008, Elsevier.

It is necessary to magnify signals from a tiny amount of light while suppressing nonlight signals (noise) as much as possible to see clearly in low light. Additionally, seeing in bright light calls for receiving a lot of light and clearly differentiating it. These qualities are measured by metrics such as dynamic range (DR) and signal-to-noise ratio (SNR). There has been a lot of work done to amplify signals and reduce unwanted noise in the area of low-light SNR. Researchers are currently working to improve these qualities and illuminace to the level of 5 lx, which is a very gloomy environment. The human eye's intrascene and interscene DR are normally 120 and 180 dB, respectively, following the contemporary smartphone's intrascene and interscene DR of 70 and 120 dB, respectively, which is being improved constantly, whereas pixel size and resolution are the main determinants of these features.[3] It is desirable that the pixel size be smaller to get a better CIS resolution. The most important thing is to keep the aforementioned qualities constant even as the pixel size decreases.

Nanostructured materials (NMs) are important in a variety of practical applications such as nanoelectronics and nanophotonics, as well as textile engineering, owing to their unique characteristics such as optical absorptions, electrical conductivity, and photothermal properties.[4] The understanding that most solid properties are dependent on microstructure, such as chemical compositions and atomic structure, as well as the size of a solid in one, two, or three dimensions is the most fundamental result in solid physics and chemistry. Furthermore, if one or more of these characteristics change, the solid's properties also change. When a solid atomic structure deviates from a few interatomic spacings in one, two, or three dimensions, the most well-known model of the relationship between the atomic structure and bulk material is used.[5]

Imaging electronics, in addition to imaging optics, play an important role in an imaging system's presentation. The finest system performance comes from properly integrating all components, including the camera, capture board, software, and wires. The phototubes, Vidicon and Plumbicon, were once utilized as image sensors in cameras; however, they are no longer in use. They have left a permanent stamp on sensor size and format nomenclature; therefore, all machine vision sensors nowadays are categorized as either charge-coupled devices (CCDs) or CMOS images. The performance of a CCD is critical for detection accuracy and terminal sensitivity. With the advancement in CCD technology, the pixel pitch and pixel size have decreased. However, due to the limitations of shift registers, the fill factor of charge-coupled devices has not been developed considerably, resulting in a reduced CCD incident light consumption rate. The incorporation and advancement in metasurfaces with optics in recent years has provided a novel answer to this challenge. To understand the structural illustartion, Figure 3 depicts the schematic structure of analog and digital CCD (see Figure 3a) and CIS (CMOS image sensing) (see Figure 3b) devices, respectively.[6,7]

CMOS is a digital device by definition: resetting or activating pixels, amplifications, and charge conversion to selection or multiplexing can all be accomplished in each site, and it consists of a photodiode along with three transistors. Because of fabrication loopholes in various charges to voltage conversion circuits, they result in fast CMOS-sensor speeds but low sensitivity due to important fixed design noise. A photon detector is a crucial component of optical logical systems such as electrochemiluminescence (ECL), where it is used to determine the signal intensity. In ECL investigations, the detector would cover a wavelength range of around 400−700 nm to precisely receive photon signals.[7] The photoelectric effect, which involves the formation, separation, and transit of photoinduced charge carriers as well as the extraction of these charge carriers to the external circuit can be used in semiconductor-based photodetectors (PDs). The metal-oxide semiconductor is commonly used as a building block in photoelectric devices due to its unique electrical and optoelectronic properties; however, the trade-off between improving the photoresponse and reducing decay times limits the practical application of PDs based on metal-oxide semiconductors. Scholars have suggested numerous schemes to modulate charge carriers' behaviors, which can improve the photoelectric performance of related PDs, including light absorption modification, the design of innovative PD heterostructures, and the construction of detailed geometry and electrode configuration.[8]

Although perovskite materials-based sensing for near UV to near IR light can exist as a promising alternative to silicon in photodiode imaging, but there is a lack of detailed investigations into that device built on a metal/Si substrates, preventing direct integration by CMOS and silicon electronics. Perovskites are typically difficult to process to meet the requirements of effective photodiode imaging due to their significant surface roughness and severe pinholes. These problems result in a high dark current and inconsistent dark or photocurrent consistency. The use of room-temperature

https://doi.org/10.1021/acsmaterialslett.2c01011
ACS Materials Lett. 2023, 5, 1027−1060

crystallization perovskite systems to control film crystallization kinetics on a CMOS compatible metal or silicon substrate results in lower dark current and higher (dark to photo) current consistency of the perovskite photodiode. The self-powered device has a higher response of 0.2 A/W at 940 nm, an immense active range of 100 dB, and a fast-fall time of 2.27 s, all of which are superior to the far-most Si-based imaging sensors.[9] Finally, recent studies succesfully demostrated the imaging application and photodetection response in a recent study.has been by incorporating the integrated photodiode array. In terms of spectral coverage, low resolutions, non-transparency, nonflexibility, and complementary CMOS inconsistency, traditional semiconductors, which are silicon (Si) as well as indium−gallium-arsenide (InGaAs)-based photodetectors, have hit a wall in modern electronics and photonics.[10,11] However, the working mechanisms of several types of image sensing devices and their large-scale applications are briefly discussed in this review.

2. TECHNOLOGICAL EVOLUTION OF IMAGE SENSING: AN OVERVIEW ON CURRENT STATUS

An image sensor is a type of optoelectronic device that makes use of the photoconductivity of semiconductor materials to transform pictorial data into an associated electrical signal, called an image. It is now a major tool for applications in biological sciences, digital imaging, mineral extraction, fiber optics, surveillance systems, military reconnaissance, environmental monitoring, computer vision, aberration correction, and healthcare.[11,12] The important part of photoelectronic devices called "solid state image sensors" is used in cell phones, video cameras, vehicle imaging, surveillance, biometric devices,[13,14] short-wave surveillance,[15] and medical imaging equipment that uses infrared radiation.[16] Photosensitive materials, in general, govern the linear dynamic range (LDR) response time, spectrum sensitivity, color correctness, and resolution of image sensors, influencing the quality of imaging devices.[12]

2.1. Image Sensing Technologies. The two main technologies that have been developed for image sensing are based on CCD (charged-coupled device) and CMOS (complementary metal oxide semiconductor) image sensors. In the image sensing process, incoming photons travel to the interior of a semiconductor in such a way that many of them interact and produce electron−hole pairs. These pairs are required to split in to an electric field before recombination, providing photocurrent proportional to the intensity of incident light in multiple magnitude orders. Evaluating noise sources, noise reduction methods, and the resulting signal-to-noise ratios is a crucial component of solid-state photosensing, which brings up the fundamental driver behind the advancement of CCD technology since its invention in 1969. The CCD image sensor technology has been substituted by CMOS-compatible image sensors since the mid-2000s and is currently in a continuous process of evolution based on CCDs.[17] The need for image sensor technology is quickly extending beyond smartphones, which presently have the highest market share, and includes internet security cameras, computer vision systems used in industrial automation, and cameras for automatic vehicle driving. The roadmap of CCD and CMOS image sensors from past technologies toward better future resolution with megapixel cameras having 3D stacked sensors for improved image sensing is shown in Figure 4, showing that the pixel size of the imaging devices is continuing to decrease with the passing years while the 3D stacking of materials is proposed for future innovations.[18]

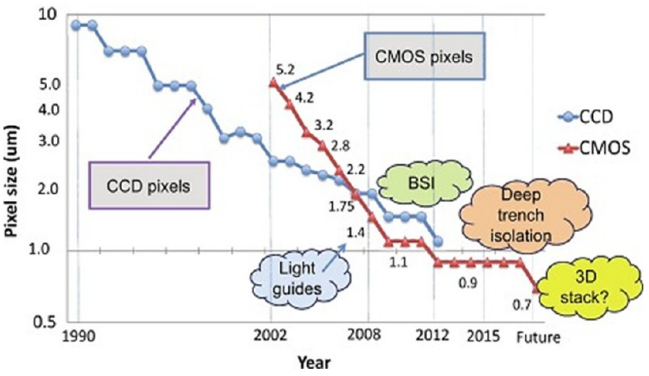

Figure 4. Road map of image sensing technological evolution. (BSI represents the backside illumination) Reproduced with permission from ref 18. Copyright 2020 Elsevier.

2.2. CCD Image Sensors. The CCD sensors can be constructed using several passive photodiode tubes that can integrate charge throughout the exposure time of the camera. The pixel-level electronics, consisting of mostly 3 or 4 transistors, is able to translate the charge stored in the photodiodes into a distinct voltage. As a result, the output of each pixel just needs to be captured and sampled by CMOS sensors.[19] CCD image sensors steady drive toward lower pixel sizes and better resolution has contributed to the production of smart cameras with more megapixels and better image quality. The availability of considerably increased memory capacity and high-speed data processing has been made possible by consistent developments in semiconductor technology, giving rise to numerous changing forms of audio- and video electronic devices. The transition of image sensors from CCDs to CMOS has recently enabled faster capture and HD (high definition) cameras, significantly expanding the market for digital cameras (Suzuki, 2010). The development of curved CCD image sensors, either as standalone devices or as contoured mosaics to form focal planes for use in telescopic astronomy and stereopanoramic-based terrestrial cameras, illustrates the significant advancements in optical design that enhance the potential role of scientific instruments. The curved CCD mosaic improved real-time remote tracking and mapping of distant entities, including galaxies, with more precision when employed in conjunction with huge cameras of high resolution.[20] CCDs remain the ideal choice for some very large (>35 mm format) imagers used in large-field-of-view digital aerial photogrammetry applications and professional photography.

2.3. CMOS Image Sensors. The performance of CMOS active pixel sensors (APS) is comparable to that of CCD sensors, and they also have benefits in terms of cost, compactness, on-chip functionality, and system power reduction. The two most common trends that aid in enhancing the performance of CMOS image sensors are altered submicrometer processes to increase image characteristics and the development of high frame rate sensors to make still and video images with improved dynamic range.[21] The constant push for increasing imaging resolution led to smaller sensor pixels. Modern commercial CMOS uses $1 \times 1\ \mu m^2$ pixels by overlaying dye-doped filters. Due to color crosstalk

https://doi.org/10.1021/acsmaterialslett.2c01011
ACS Materials Lett. 2023, 5, 1027−1060

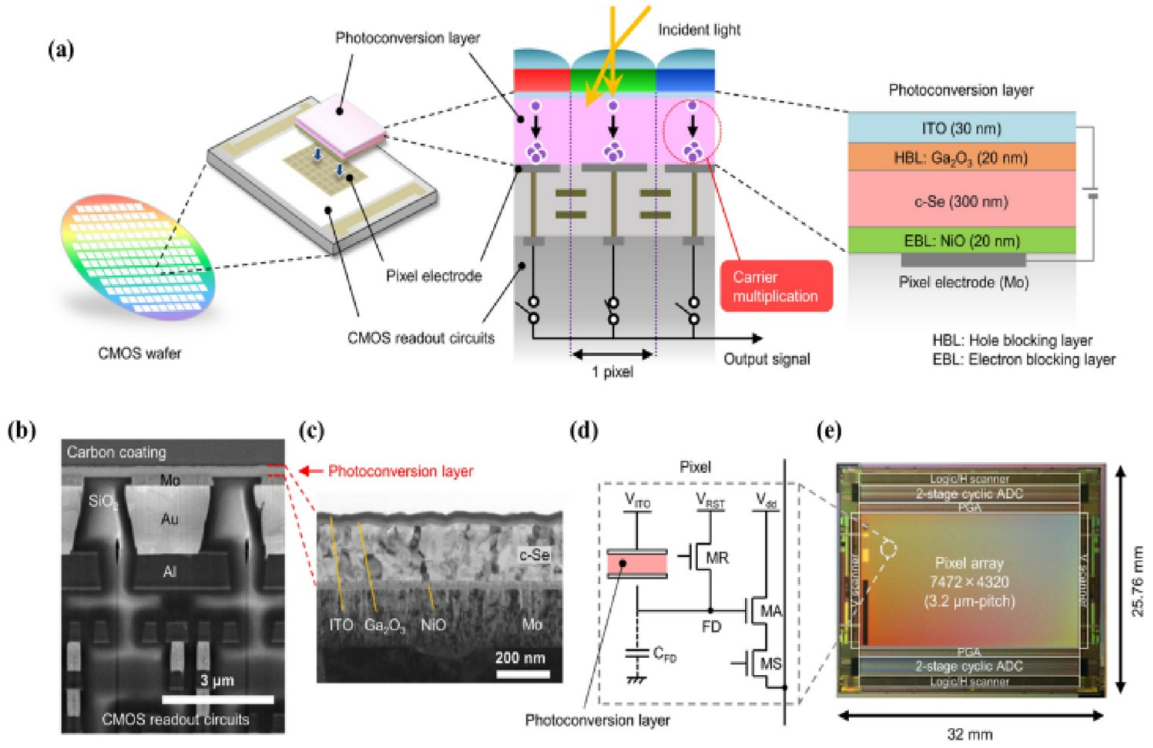

Figure 5. Structure of image sensor along with its pixel configuration: (a) Representation of stacked layer CMOS showing photoconductivity in photoconversion layer, (b) cross-sectional image of a pixel through scanning electron microscopy, (c) cross-section image of photo conversion layer using transmission electron microscopy, (d) pixel diagram, and (e) color diagram of a pitch showing photomicrograph. Adapted with permission from ref 26. Copyright 2020 Nature Publishing Group.

and precisely matched lithography operations, the reduced pixel size raises great concern for color generation.[22,23] Self-resetting pixels have been designed for an implantable CMOS and require four transistors to implement the self-resetting feature. The process of pixel fabrication can be achieved by the use of polymetal CMOS technology, resulting in a larger pixel size. Thus, through image processing, intensity-change images can be produced from the output of self-resetting pixels.[24]

Recent CMOS image sensors, unlike in the past, have become more valuable than CCDs. In comparison to CCDs, they provide the benefit of less energy consumption, lower voltage operation, on-chip functionality, and lower cost effectiveness. However, they are still less sensitive and louder than the CCDs. CMOS image sensors come in a variety of forms to meet the enormous demand in a variety of applications, including digital imaging, corporate visualization, medical and aerospace applications, electrostatic sensing, automobiles, measurement, and 3D pictorial technology by considering advancements in semiconductor technology and multimedia techniques. The development of CMOS image sensors and their potential for use with cutting-edge imaging technologies are intriguing candidates to raise living standards. Recently, CMOS has predominated in the digital camera due to the quick growth of analog digital converters (ADCs) , back illumination, and stacked CMOS continues to deliver improved functionality and an improved user experience in smart phones.[18]

2.4. Hybrid Image Sensors. Hybrid image sensing is now used for bonding at a high density in 3D integration. However, continuous interconnect down-scaling may compromise electrical performance. The impact of this technology on 3D illuminated CMOS can be assessed by monitoring device performance and robustness that demonstrate pitch bond scaling at smaller level. There was no evidence of smaller bonding by thermocycling or electromigration in the available studies, validating the reliability of fine pitch and its application for next-generation imaging devices.[25] Hybrid image sensors composed of nonsilicon photoconversion layers and CMOS field-effect transistors (CMOSFETs) have proven to have superior performance as compared to Si photodiode CMOS image sensors with Si photodiodes. Hybrid image sensors have shown a number of intriguing performance features by exploiting different aspects of non-Si photoconversion films such as high LDR, global shutter type, and high near-infrared(NIR) and X-ray sensitivity. The formation of a brighter image with enhanced signals and clear noise deterioration is shown in Figure 5.[26]

2.5. Flexible Image Sensing Technology. Flexible image sensors, as compared to conventional rigid substrate image sensors, have better shapes and can be adapted to various objects. Because of its exceptional operational capabilities, this sensor can meet the growing demands of new generations of optoelectronic and nanophotonic innovations. The flexible image sensors have a number of outstanding qualities, such as reduced weight, portability, smooth diverse integration, compatibility with wide areas, low manufacturing costs, and remarkable stretchability. Flexible devices are able to accurately and continuously capture physiological signals without interfering with daily activities, which opens the door for a variety of medical uses. Various flexible image sensing devices have been developed for applications in the fields of wearables, prosthetics, robots, and vehicles, which will benefit from the capacity of such devices to develop compact and versatile color image sensors with high sensitivity.[27−29]

https://doi.org/10.1021/acsmaterialslett.2c01011
ACS Materials Lett. 2023, 5, 1027−1060

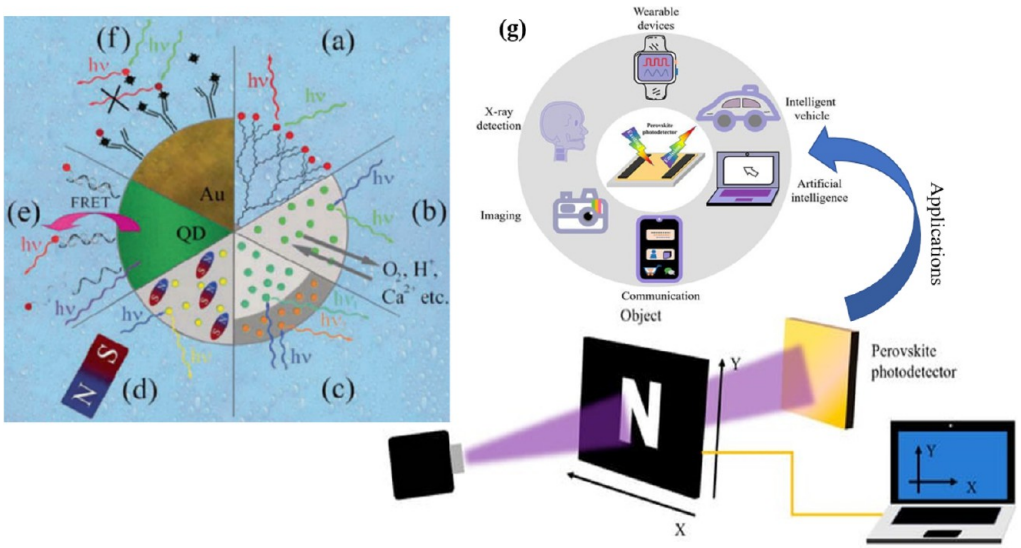

Figure 6. Pictorial presentation of optical nanostructured image sensors: (a) Macromolecule-based nanostructured image sensors, (b) polymer and sol−gel-based nanosensors, (c) core−shell system with multifunctional materials, (d) magnetic bead-based multifunctional nanosensors, (e) quantum dot-based nanosensors, and (f) metal bead-based nanosensors. (a−f) Reproduced with permission from ref 34. Copyright 2010, Springer. (g) Schematic for an image sensing system along with perovskite materials-based photodetector applications. Reproduced with permission from ref 30. Copyright 2022 MDPI.

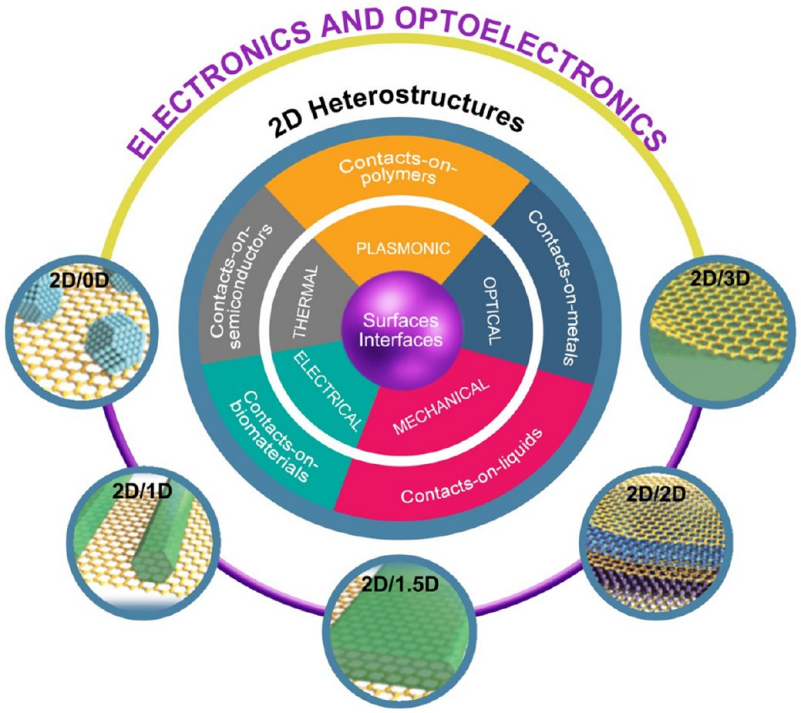

Figure 7. Pictorial illustration tuning capacity of photodetectors constructed from stacked 2D heterostructures. Reproduced with permission from ref 36. Copyright 2022 American Chemical Society.

Many useful materials have been investigated recently for their posisble use in photodetectors, including perovskite structures, organic semiconductors, 0D and 1D nanostructures such as nanotubes, rods, belts, and wires, as well as layered 2D materials. Outstanding mechanical flexibility, good detectivity, and distinctive electrical and optical properties are present in these materials with excellent biomimetic visual applications.[30−32] Flexible image sensors have been developed by employing nanowire semiconductors with a distinctively ordered structure, exceptional transparency, and excellent optoelectronic properties.[27]

2.6. Nanostructured Materials in Image Sensing. Image sensing devices with increased sensitivity, cost effectiveness, speedy reactions, faster recovery, and decreased size with operational flexibility are in high demand. These characteristics for chemical and biological sensors can be greatly enhanced by nanostructured materials. The nanostructured materials that can be used for the production of nanosensors for imaging include nanoscale wires with highly

https://doi.org/10.1021/acsmaterialslett.2c01011
ACS Materials Lett. 2023, 5, 1027−1060

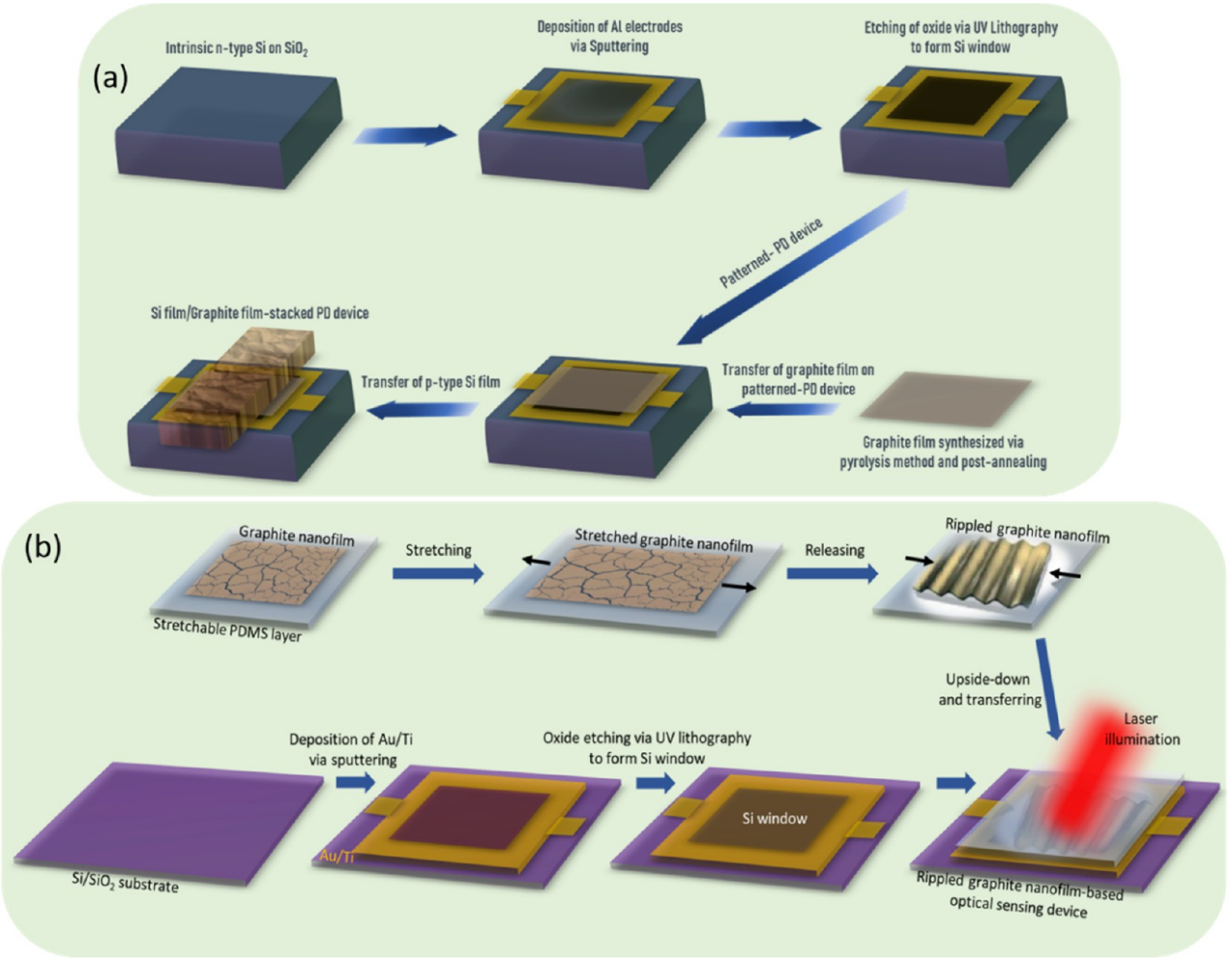

Figure 8. Fabrication process of graphene-based photodetectors: (a) Fabrication process of Si/graphite film stacked layer photodetection devices. Reproduced with permission from ref 37. Copyright 2022 MDPI. (b) Process of fabrication in rippled graphite (rGr) nanofilm-based image sensor. Reproduced with permission from ref 38. Copyright 2022 MDPI.

sensitive detectors, carbon nanotubes with a large surface area and greater electrical conductivity, metal and metal oxide nanoparticles, thin films, polymers, and biological materials.[33]

Although nanotechnology is a hot topic, the debate is continuing regarding the size of nanoparticles. Nanostructures bridge the gap between nanoscience and nanotechnology and associate the two domains. There are numerous applications in which the fine particle size can be of significant interest. However, there is a strong consensus that the size range below 100 nm offers the greatest potential.[34] The common scientific method of nanomaterial categorization is their identification with respect to their dimensions in order to fully comprehend and increase their diversity. Figure 6 depicts a pictorial presentation of optical nanostructured image sensors (see Figure 6a–f) along with a schematic for image sensing with perovskite materials-based photodetector applications (see Figure 6g).[30,34]

The nanostructures made from silver and iron oxide nanoparticles have been utilized for imaging with surface plasmon-resonance set at NIR. These nanostructures showed good photothermal, thrombolytic, and anticancer potentials at varying concentrations upon near-infrared laser irradiation, resulting in photothermal treatment of cancer and thrombosis. Moreover, these nanostructures exhibited outstanding magnetic resonance imaging(MRI) T2-signal after being bound to the surface of the thrombus or sequestered within cells, making them a suitable imaging agent for thrombus detection and cell identification without producing any toxicity.[35]

2.7. 2D Heterostructures. Recently, material scientists have constructed two-dimensional (2D) heterostructures, which are still in the early phases of development, to look for novel physical, chemical, and technological processes at very small sizes, such as the micro, nano, and picolevel (see Figure 7). By utilizing physical and chemical properties, choosing the right thickness, and stacking layers, these 2D heterostructures can be engineered to produce remarkable carrier dynamics that could play a role in widespread broadband optoelectronics at higher frequencies.[36]

Recent research on graphene-based photodetection (PD) systems has revealed the poor optical absorption of these materials. To overcome this problem, hybrid heterostructure devices have been used in the graphene-based PD device development process to increase its photoabsorption. Silicon devices are generally used in visual image sensors due to their distinct properties such as increased light absorption, larger carrier mobility, and classical CMOS integration. Designing an innovative PD device using Si film is considered a novel approach for image sensors (see Figure 8a).[37] Electronic and

https://doi.org/10.1021/acsmaterialslett.2c01011
ACS Materials Lett. 2023, 5, 1027–1060

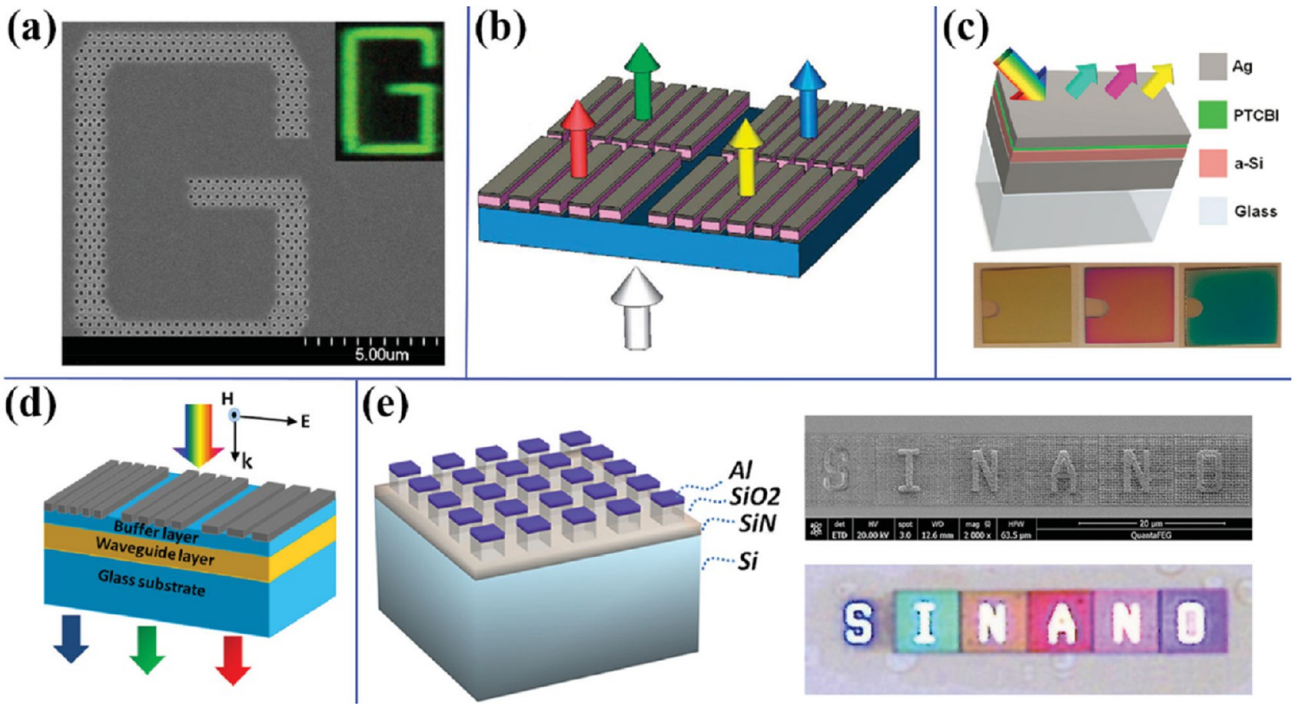

Figure 9. Nanostructured materials-based color filters: (a) Metallic array color filter based on nanohole, (b) layered color filters, (c) plane reflective color filters, (d) GMR color filters, and (e) scattering color filters. Reproduced with permission from ref 49. Copyright 2016 Wiley.

optoelectronic devices have been studied with rippled or wrinkled graphene, which revealed that an increase in ripple density of graphite nanostructures with the help of a supporting PDMS layer, the photoresponsivity also increased (see Figure 8b).[38] The graphene-based photodetector systems concentrated on hybrid technology to boost photoabsorption. However, because of their heterogeneous interfaces, such hybrid devices demand time-consuming integration procedures and a decrease in carrier mobility. When compared to a smooth nanostructure, a 100% increase in the optical detectivity of the deformable nanofilm surface occurred in the visible laser range (532 nm). Additionally, the results of the computational simulation strongly support a development in the photodetection of photodetector systems based on deformed nanofilm surfaces.[39]

2.8. Convolutional Neural Networks for Image Sensing. Convolutional neural networks (CNNs) are frequently used to process 2D array input data including image data. Since images are records of natural signals, they offer information in the form of pixel values and local connections. This attribute enables the combination of low-level features, such as edges, with higher-level features that have a semantic significance. Image analysis involves investigating pixel values and associated local connectivity in order to find powerful, distinctive representations that may be utilized for picture classification. While also being aware of their values and localized arrangements, CNN enables the learning of those representational elements of picture data to a more abstract degree. As with linear connections in an artificial neural network (ANN), convolutional operations serve as trainable kernel functions that connect the layers in a CNN. Because of the local sensitivity of a kernel function,[40] CNNs are capable of considering the local interconnectivity of the input data when learning the features from them.

2.9. Three-Dimensional Integral Imaging. The first study on three-dimensional (3D) integral imaging technology reported that this system can capture and reconstruct images using flexible sensors mounted on a flexible surface in unknown postures. The integral imaging with flexibility enables sensors to be positioned on a nonplanar surface, which may expand the vision of 3D imaging in contrast to standard integral imaging, where the sensor array is typically positioned on a plane surface.[41] The approach designed for this purpose is based on the theory of two-sided visual geometry and a camera projection model that can capture images of the positions on a flexible surface. Additionally, a number of weakly resolved 2D photos with shifts in subpixels can be used to produce a super-resolution image.[41]

2.10. Nanostructured Color Imaging Devices. The spatial resolution of color imaging technologies has grown quickly during the last few decades. This technological boom was primarily caused by the widespread use of portable devices such as mobile phones and compact optical cameras, but high resolution is also useful in industrial and environmental imaging. Pixels as small as 1 μm can be obtained by employing CMOS with dye- and pigment-based color filters. The further reduction of pixel size is a difficult procedure for which new materials and complex multistep fabrication procedures are needed. Dielectric materials can be utilized to produce high-brightness structural colors since they have fewer inherent losses, which makes these nanostructures better suited for their use in color printing. Additionally, dielectric nanostructures, contrary to plasmonics, have two different resonance types such as electric dipole and a magnetic dipole. This gives the spectral response's tunability an additional degree of freedom. Transmission can also produce structural colors because resonances cause dips in the spectra. By changing the geometrical shape of the dielectric nanostructure, the resonance position can be adjusted throughout the visible

https://doi.org/10.1021/acsmaterialslett.2c01011
ACS Materials Lett. 2023, 5, 1027−1060

spectrum and beyond. The implementation of specific color filter arrays and multispectral arrangements has all been accomplished with success using this method in which spectral filters are placed on the top position of a pixelated sensor, like CMOS, for digital color imaging. The resolution of imaging devices is a crucial component, and it is based on the pixel size. High resolution is preferred for many applications, enabling tiny spectral filters. Dielectric nanostructures have the potential to form flexible, tiny spectral filters that can be substituted for traditional pigments and color filters because of their resonant behavior and tenability.[42] The structured color filter delivers process compatibility, high compactness, vigorous stability, and an improved tenability owing to the interaction of light and nanostructures.[43,44] High-resolution imaging and displays could benefit from the outstanding ability of this technology for color printing with a much higher resolution of 100,000 dpi.[45] Moreover, some other characteristics, such as polarization and nanophotonics-based phased arrays, have recently evolved with the potential to be used in image-forming devices.[46−48] The interaction of light with nanostructured materials is the basis for the structured color. The effect of numerous nanophotons is transmitted selectively, and light is reflected to make a spectrum band. The common color filters based on nanophotons are shown in Figure 9.[49] There are many techniques that can be used for color filter spectra; however, there is no such procedure through which all efficiency characteristics, including purity and compatibility, for subsequent application in image sensing can be achieved. Research is ongoing to produce nanophotonic structure-based selective features that can be helpful for emerging image sensing technologies.

In Figure 9a, a small circle of gray is shown in a triangular plane of aluminum film of 150 nm thickness. The G letter in green color was taken by a transmission electron microscope that showed a resolution of approximately 1 μm, while Figure 9b and c show layered color filters formed by metal dielectric metal gratings and plane reflective color filters formed by Ag/PTCBI/a-Si/Ag stacks and GMR color filters of Si 3-N-4 of 100 nm thickness, respectively. Figure 9e presents scattering color filters based on aluminum nanopatches on silicon, SiO_2 as an intermediate nanolayer, the Si layer as an antireflection coating, and scanning electron microscope color images of the letters "SINANO".[49]

2.11. Quantum Dot Image Sensors. Nanotechnology has enabled the synthesis of several useful nanoparticles such as quantum dots (QDs), metallic nanoparticles, and magnetic nanoparticles. The unique electrical, optical, and magnetic characteristics displayed by these nanostructured materials have a wide range of biological uses. In particular, magnetic iron-oxide nanoparticles have shown potential as deep imaging agents for clinical tissues due to the biocompatibility of these nanoparticles.[50]

For broadband flexible imaging, QD image sensors based on hybrid nanostructures of SnS-QD/Zn_2SnO_4 nanowires have been produced. Nanowires were decorated with SnS-QD using a two-step vapor deposition process. In comparison to pure ZTO NWs, hybrid QD/NWs have a significantly higher photoconductive yield and specified detectivity in the UV region, as well as a longer photoresponse covering the UV and NIR ranges. Additionally, the polyethylene terephthalate-based hybrid QD/NW photodetector demonstrated good flexibility, folding capacity, and long-term mechanical stability. A flexible broadband image sensor is produced and mounted into a 10 × 10 array. The flexible image sensor's remarkable target identification capacity is exhibited by its ability to clearly distinguish between target pictures made up of white and red light when it is bent. The better performance of the device demonstrated the QD/NW hybrid nanostructures have great potential for use in flexible broadband imaging technologies in the future.[51]

The basic role of an image sensor is to convert light signals, or photons into electrical signals. An image sensor, also known as an "imager", is a semiconductor device that converts an optical image created by a lens into an electronic signal.

3. GENERAL MECHANISMS OF IMAGE SENSING

All image sensors rely on the photoelectric effect, which describes the interaction between photons (light) and atoms. The basic role of an image sensor is to convert light signals, or photons into electrical signals. An image sensor, also known as an "imager", is a semiconductor device that converts an optical image created by a lens into an electronic signal. An image sensor can detect a wide range of light wavelengths, from X-rays to infrared, by modifying the detector configuration or using material that is susceptible to the specific range of wavelengths. To recreate an image with a suitable resolution, an appropriate number of "pixels" is known as "picture elements" or "the minimum spatial unit of a digital image in an image sensor", which are required to be ordered in rows and

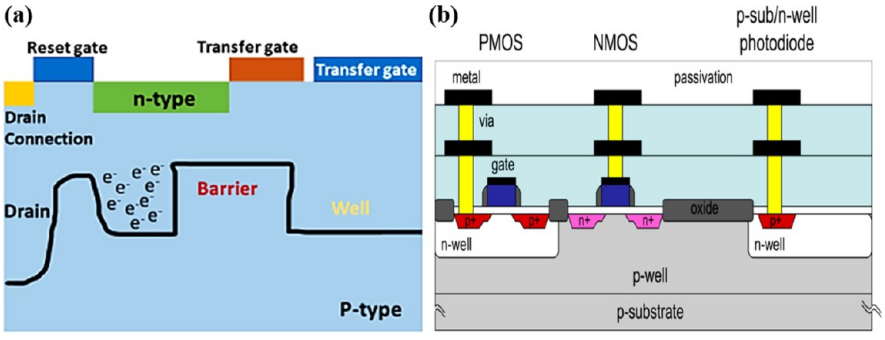

Figure 10. Working mechanisms: (a) CCD. (b) CMOS devices. Reproduced with permission from ref 54. Copyright 2008 MDPI.

https://doi.org/10.1021/acsmaterialslett.2c01011
ACS Materials Lett. 2023, 5, 1027−1060

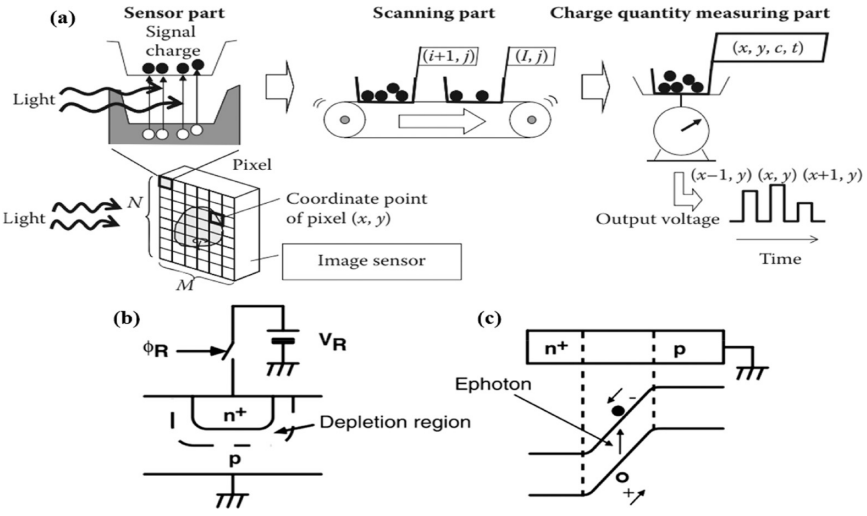

Figure 11. (a) Functional elements of an image sensor. Reproduced with permission from ref 55. Copyright 2015 CRC Press. Photodiode operation in reverse bias: (b) cross-sectional view and (c) energy band diagram. (b, c) Reproduced with permission from ref 56. Copyright 2006 Taylor and Francis.

columns. Incoming light is converted into a signal charge (electrons or holes) by these pixels, and the formation of this signal charge is dependent on the pixel's structure. A depletion region is generated in a pixel by doping silicon with a very small amount of material, which gives rise to an electron deficiency. Every pixel generates a positively charged region, which attracts photoelectrons while repelling holes. As a result, photoelectrons are accumulated in a constant depletion region inside each pixel. The recombination of photoelectrons and holes is stopped as the holes are pushed away from the depletion region.[52,53]

Figure 10a shows a CCD image sensor. When light falls on a photodiode, it creates a flow of photoelectrons, where the electrons accumulate within the p-type silicon in the potential well. However, this well attracts electrons and causes them to flow, generating electric current.[53] The transfer gate was used, and the clock signal was routed to the barrier and, well, generations. The process was repeated to create a sequence of images: the collection of charges, which is followed by a readout of the data corresponding to the number of photoelectrons collected at each photosite. There are different types of imagers available, each with its own individual readout method. Three major types of imagers that are used in scientific imaging include charge-coupled devices (CCDs), electron-multiplying CCDs (em-CCDs), and complementary metal oxide semiconductor imagers (CMOS imagers or CIS). A CMOS or CIS device working layout is shown in Figure 10b.[54]

3.1. Photoconversion. When a silicon atom is hit by an incident photon, the emitted energy of the photon is absorbed by an electron within the outermost valence band of the atom, and transfers to a higher energy level. Such mobile electrons leave holes behind and thus result in the creation of electron−hole pairs. Since the generation of electrons is due to photon absorption, they are known as "photoelectrons". Figure 11a shows the operational components of an image sensor,[55] while Figure 11b and c depicts how a photodiode works in reverse bias.[56]

Since silicon has a bandgap energy of 1.1 eV, absorption of light begins for wavelengths smaller than 1100 nm, and conversion of photons to signal charge takes place.[55,56] Conversely, if a photon wavelength is greater than 1100 nm, silicon is basically transparent. The absorption of photon flux follows the given relation, $\frac{d\varphi(x)}{dx} = -\alpha\varphi(x)$, where α is known as the absorption coefficient, and it is dependent on wavelength. Applying the boundary condition $\varphi(x = 0) = \varphi_0$, and solving the output is $\varphi(x) = \varphi_0 \exp(-\alpha x)$. Therefore, with the increased distance from the surface, the photon flux decays exponentially. Photon absorption causes the formation of electron−hole pairs in the semiconductor, which follow the above-mentioned relationship.[55]

3.2. Charge Accumulation or Collection. An electric field is created inside the substrate of the imager to collect the electrons that are produced by the photoelectric effect. Using gates at different voltages, an electric field is built within the imager to create a depletion region. The produced signal charge is accumulated in a charge collection region within a pixel. A regular photodiode works like a charge accumulation device, as shown in Figure 11b and c. Subsequently, the first n^+ zone is reset to a positive voltage and grounds the p zone. Then, holding the reverse-biased condition, the mixture becomes electrically floating. Excited electrons are collected at the n^+ region, resulting in the reduction of this zone's potential and holes drifting toward the grounded end. Here, the signal charge is an electron. In the case of a metal-oxide semiconductor (MOS) diode, applying a positive voltage to the gate electrode results in the downward bending of the energy band and the depletion of holes. Now the depletion zone is set to accumulate free charges.

For the photodiode, quantum efficiency (QE) and collection efficiency are the major description aspects. Quantum efficiency can be defined as "the percentage of photons hitting the photosensitive surface that produce an electron hole pair", while collection efficiency is "the fraction of the generated electron hole pair that contributes to a current flow external to the detector", whereas each factor is used to fine-tune the sensitivity of the photodiode. Additional vital photodiode considerations are thermal, dark current, and shot noise, which are material-dependent. Dark current is a comparatively weak electric current that flows through the photodiode through the photons that cannot penetrate the device. Such photosensing

https://doi.org/10.1021/acsmaterialslett.2c01011
ACS Materials Lett. 2023, 5, 1027−1060

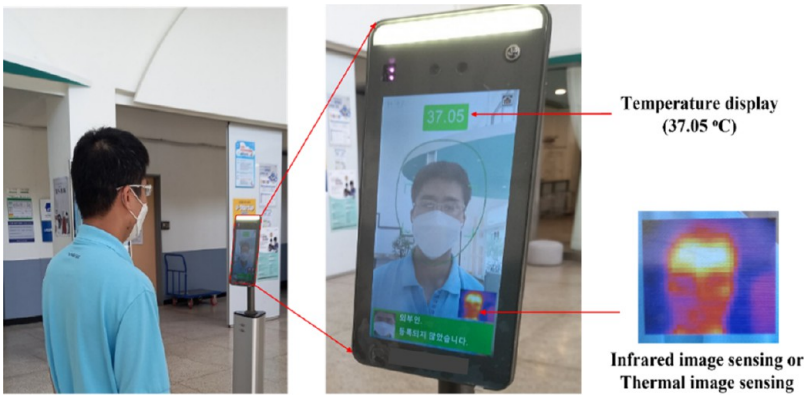

Figure 12. Temperature check and thermal image sensing device.

constraints are dependent on the type and construction of the junction. Electrons produced within the depletion zone are completely used as signal charges in both MOS diodes and reverse-biased photodiodes. Because there is no electric field present in the neutral region, only a small portion of the electrons produced inside the neutral region can reach the depletion region due to diffusion. Because of the recombination process, some of the electrons are lost before reaching the depletion zone.[57,58]

3.3. Image Formation and Scanning of an Image Array. Image sensors produce images by accumulating and determining the number of photoelectrons produced within the depletion zone of a pixel. The collected charges or the resultant signal voltage or current in an image sensor chip from a pixel must be delivered to the outside world. An image sensor can be a 1- or 2-dimensional array composed of a matrix of pixels. As the photons, which are incident on the pixel, are proportional to the number of photoelectrons, the matrix constituting the photoelectrons in every pixel creates a 1- or 2-dimensional image structure. The signals distributed in 2D space must be converted into signals with a temporal sequence. It is called "scanning", and this ability is essential for an image sensor. A single frame or a time-sequential frame with a duly large frame rate can be exhibited on a monitor, showing a 2D image and/or showing movements or more fluctuations in the field within the range. There are two types of scanning systems: (a) charge transfer scanning, and (b) $X-Y$ addressing scanning.

A charge transfer scheme transfers the charge from the H−CCD to the output amplifier, where it is converted to a voltage signal. This type of system requires nearly ideal efficiency for charge transfer; therefore, these technologies involve extremely tuned semiconductor construction and procedures. In most of the CMOS image sensors, which are based on an $X-Y$ addressing scheme, an operating transistor in a pixel converts the signal charge into a current or a voltage. A pixel signal is routed through a decoder, or a vertical scanner selects a row (Y) for a specific readout, and a horizontal scanner selects a column (X) to be displayed. When compared with the charge transfer scheme, the $X-Y$ addressing technique is significantly more adaptable in terms of obtaining a variety of readout modes.[56,59,60]

3.4. Charge Detection. For most CCDs and CISs, the charge detection principle is essentially the same. In the case of CCD image sensors, the detection of charges can be achieved by an output amplifier, whereas in CIS, it is accomplished within a pixel. A voltage buffer monitors a potential well that is fed by signal charge (Q_{sig}). The charge causes a change in potential, and the capacitor, connected to the potential well, functions as the charge-to-voltage converting capacitor. Floating diffusion charge detection is the most commonly used charge detection scheme. In a CCD image sensor, the charge detection can be achieved by a floating diffusion arrangement established at the terminal of the horizontal CCD register, whereas it is accomplished within a pixel for CIS active-pixel sensors (APSs).[61] The pixel readout circuit converts charge to voltage, after that, the signal accumulates within the pixel. In the display mode, the accumulated signal within the pixel is displayed on the programming gain amplifier (PGA) by the selection of a suitable pixel utilizing the column and row registers. The signal that is received from the pixel is amplified by the PGA, which has distinct gain settings. After the amplification, the signal is delivered to the analog to digital converter (ADC), where it is digitalized into a 10-bit value. Every pixel value is digitized by the ADC, preparing it for signal processing. The operation and timing of the pixel circuit are established by the pixel control block. The pixel selected to be read is decided by the row and column registers. The pixel display is completed in two steps: initially, the amount collected in the pixel is transported to the PGA input capacitor, and then the signal is amplified and digitized by PGA and ADC.[62]

4. REPRESENTATIVE IMAGE SENSING DEVICES AND THEIR ACTUAL APPLICATIONS

4.1. Quantum Dot-Based Infrared Image Sensing. Infrared image sensing (IRIS) or thermal image sensing (TIS) is operated on the basis of the detector and maps the surface temperature of an object without direct contact.[63] IRIS (or TIS) can provide image information in different environments such as invisible, low-light, low-visibility situations, as well as dark environments,[64] and has wide applications in telecommunication, national defense, motion detection, security inspection, surveillance, nondestructive inspection materials, and chemical detection.[65] Figure 12 demonstrates how IRIS (mode, ES-K7; product, Fast pass; Made in Korea) is applied to the detector of body-face temperature (thermal information) located at the University of Ulsan, Korea. The integrated thermal detector and camera measure the rising temperature or temperature differences due to heat radiation and can provide thermal information because of the coronavirus affection (Covid-19). Heat radiation and the distribution temperature of the body are then converted to visible images.

https://doi.org/10.1021/acsmaterialslett.2c01011
ACS Materials Lett. 2023, 5, 1027−1060

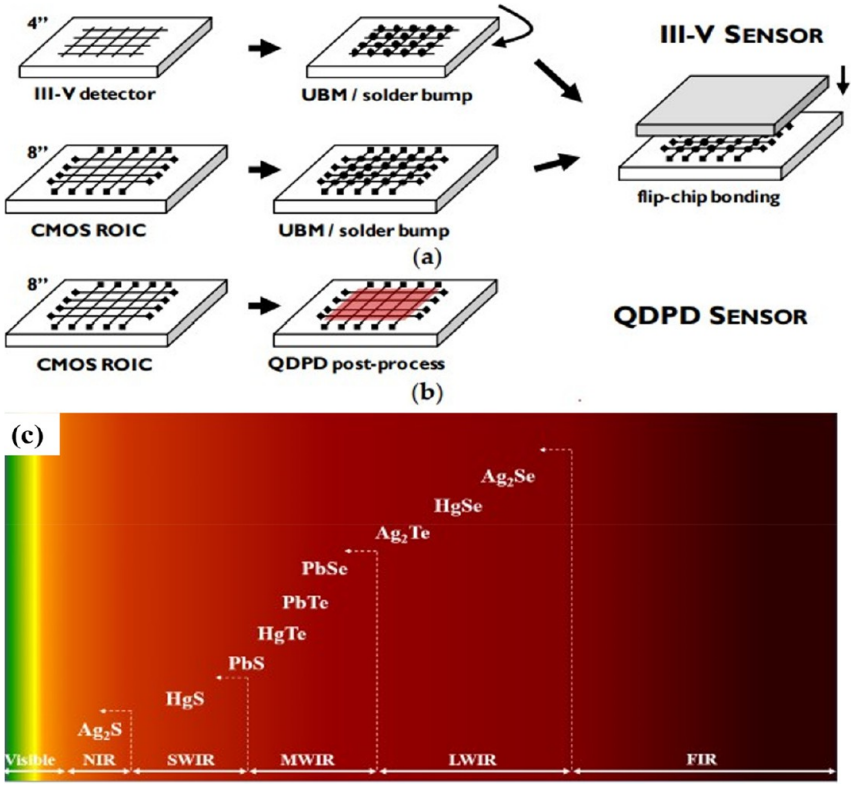

Figure 13. (a) Integration route for a hybrid III−V semiconductor materials, (b) monolithic QDs for the infrared image sensor. (a, b) Reproduced with permission from ref 68. Copyright 2017 MDPI. (c) Operation broad of quantum dot-based infrared image sensing. NIR-SWIR camera (HgS and PbS), SWIR MWIR camera (HgTe, PbTe, and PbSe), SWIR LWIR camera (Ag_2Se, HgSe, and Ag_2Te).

Infrared light includes near-infrared (NIR, 0.75−1.4 μm), short-wavelength infrared (SWIR, 1.4−3 μm), midwavelength infrared (MWIR, 3−8 μm), long-wavelength infrared (LWIR, 8−15 μm), very long wavelength infrared (VLWIR, 15−30 μm), and far-infrared (FIR, 30−100 μm), wherein the infrared image sensing requires sensitivity in infrared spectral regions from 0.75 to 100 μm.[66] Almost all infrared image sensing devices are made of narrow-gap traditional semiconductor materials such as HgCdTe (E_g 0−1.5 eV), InSb (E_g 0.17 eV), and InGaAs (E_g 0.36−1.45 eV).[63,67] The pixels of these materials are connected directly with complementary metal-oxide−semiconductor (CMOS) read-out integrated circuits (ROICs) via complicated processes, as shown in Figure 13a.[68] Traditional III−V semiconductor materials have advantages such as high stability and low product cost. However, they require high product costs, brittleness, and integration with the crystalline substrate. Materials, pixel arrays, and solder bump techniques limit the operating spectral range and pixel number.[68]

In QD-IRISDs, the III−V bulk (or thin-film) semiconductor materials are replaced by QDs or colloidal quantum dots (CQDs), as shown in Figure 13b.[68] Simple techniques such as screen-printing, sprinkling, and spin-coating methods were used to deposit QDs directly on the silicon ROIC. Quantum dot-based infrared image sensing devices (QD-IRISDs) have attracted much attention due to their high sensitivity sensors, high resolution, fast response, large spectral response, compatibility with a large-scale and flexible substrate, cost-effectiveness, and different operating temperatures.[69] Numerous studies have been published on the use of quantum dots made of lead chalcogenides (PbSe, PbS, and PbTe),[70−73] mercury chalcogenides (HgTe, HgS, and HgSe),[74−76] and silver chalcogenides (Ag_2S, Ag_2Se, and Ag_2Te)[77−79] materials as probe temperature, photodetector, and infrared image sensors. QDs exhibit large surface-to-volume, mechanically flexible, surface multifunctionalized, and narrow-gap properties that have demonstrated the potential of QDs for NIR-MWIR image sensors, as shown in Figure 13c.

The unique optical properties of QDs exhibit a size-dependent absorption spectrum range and an absorption coefficient (see Figure 13c). The absorption spectrum of Ag_2Se QDs was tuned from 4.8 to 15.4 μm via tuning the size of 5−28 nm.[77] HgTe QDs can work beyond LWIR, while HgSe can extend the absorption to THz. QDs can extend the absorption to a longer wavelength (from NIR − THz) due to the tunable bandgap, wherein the conduction band (CB) and valence band (VB) of QDs become discrete states. The bandgap and energy gap between states depend on QD size and shape, as shown in Figure 14a.[80] Moreover, the optical transitions can occur in both interband and intraband absorptions. Electron/hole pairs are generated due to the transitions from $1S_h$ to $1S_e$ (interband absorption) and from $1S_e$ to $1P_e$ (intraband absorption), and they are separated to form electrical signals, as shown in Figure 14b.[67] The absorption coefficient, absorption cross-section, and QD connecting can all have an effect on the optoelectronic current conversion process.[67] For ideal doping conditions (see Figure 14b(1−2)), due to the minimum number of holes and strongest optical absorption, QDs exhibit large amounts of excited electrons, slowing down recombination and prolonging their lifetime, which leads to the lowest dark conductivity and an increase in photocurrent. In the nonideal condition case (see Figure 14b(3−4)), the photocurrent depends on the carrier mobility of photoexcited electrons. Due to the quantum

https://doi.org/10.1021/acsmaterialslett.2c01011
ACS Materials Lett. 2023, 5, 1027−1060

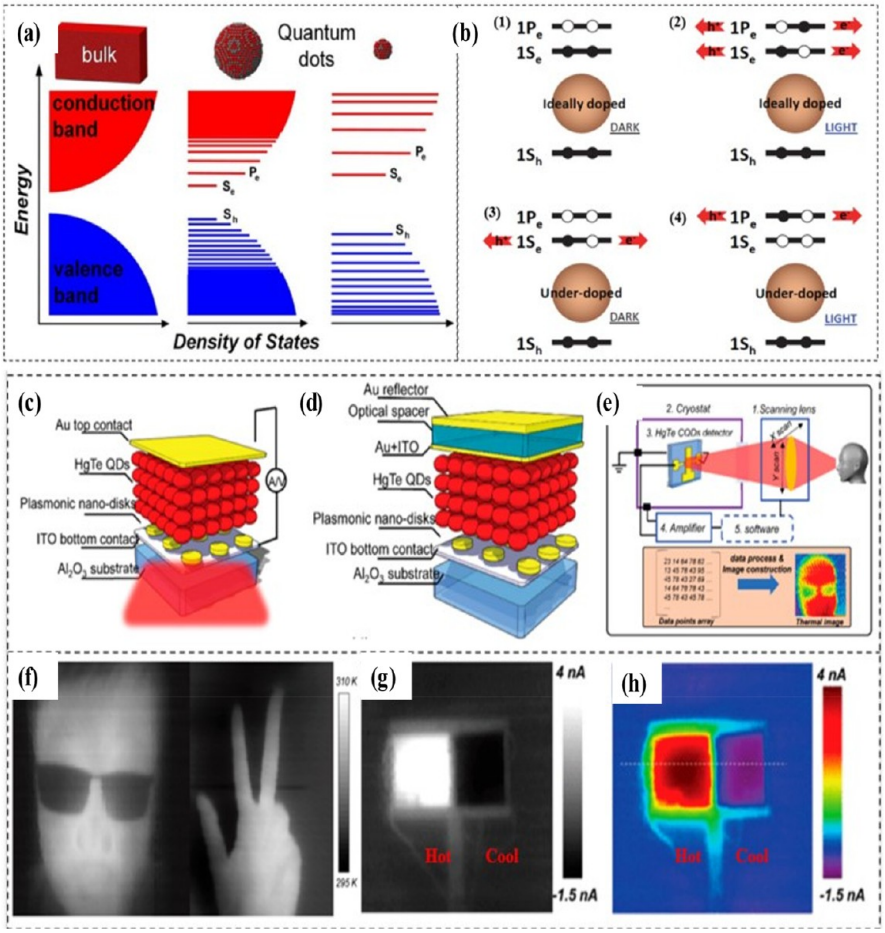

Figure 14. (a) Evolution of the electronic structure of inorganic semiconductors from bulk material to QDs of different size. Reproduced with permission from ref 80. Copyright 2016 AAAS. (b) carrier distribution and transport of intraband under dark and illumination CQDs for ideally doped (1, 2) and under-doped conditions (3, 4). Reproduced with permission from ref 67. Copyright 2019 Springer. Schematic diagram of HgTe CQDs MWIR detector with (c) plasmonic disks +30 nm Au contact, (d) interference structure + plasmonic disk array, and (e) thermal imaging system. Thermal images result of HgTe CQDs MWIR, (f) face and hand (detector operate at 90 K), (g) Peltier coolers in grayscale, and (h) rainbow color scheme. (c–h) Reproduced with permission from ref 83. Copyright 2018 American Chemical Society.

effects, the charge carriers are captured and scattered on the surface of QDs.[80]

PbX (X = S, Te, or Se) QDs have seen rapid development in photodetectors and infrared image sensor-based applications.[77] PbX QDs exhibit excellent light absorption and photoelectric properties. PbX QDs can tune the absorption range of PbS, PbTe, and PbSe to 2.5, 4.3, and 4.6 μm wavelengths, respectively.[70,71] PbS QDs have a large Bohr exciton of 18 nm and a high molar absorption coefficient of 1×10^6 $M^{-1}cm^{-1}$. Dong et al. prepared PbS QDs of 16 nm by the multiple injection method, which exhibit an absorption peak up to 2.53 μm.[73] PbS QDs just work in the NIR-SWIR region, while PbTe and PbSe IR cameras can work in the NIR-MWIR. The intrinsic gap of PbSe can be controlled in the range of 0.27 to 1.8 eV, leading to the blue shift from 4.6 μm to 690 nm.[70] Qiu et al. reported MWIR PbSe QDs for photodiodes operating at room temperature with an absorption range of up to 4.2 μm.[72]

The HgX (X = S, Te, Se) family is the substantive material with a fast time response, high absorption, and low dark current that was used in IRIS devices.[81,82] Compared with PbX QDs, HgX QDs allow a broader absorption range of IR from NIR to LIR (see Figure 12c).[83] HgTe and HgSe exhibit optical absorption and photoconductive response-ability in the broadband from SWIR to LWIR due to the intraband 1Se–1Pe transition.[74,81−83] Livache et al.[76] combined intraband absorption in the MWIR by a mixture of HgSe and HgTe nanocrystals (NCs). The broad absorption, time response, and dark current were affected by the HgTe content. Recent research indicates that the tunable crystal size of HgX NCs extends all the way to the far-infrared (FIR) or terahertz (THz) region. Goubet et al. synthesized the HgX NCs from 5 nm to above 200 nm size for tuning absorption that ranges up to THz.[84]

Among HgX, HgTe QD is the first material synthesized to be applied in IRIS, which indicates the best performance and fastest time response.[84] Guyot-Sionnest's research group developed sensitive infrared imaging using the HgTe CQDs due to the high results achieved using wide spectroscopy from SWIR to LWIR regions.[69,74,75,82,83,85,86] The HgTe CQDs were used by integrating architectures and different QD sizes, as shown in Figure 14. Figure 14c and d shows TISDs using two structures by integrating HgTe CQDs and plasmonic structures, such as plasmonic structure discs (see Figure 14c) and interference structures (see Figure 14d).[83] Light absorption and photocurrent can be increased by the integration of the plasmonics and QDs. Figure 14e shows the thermal imaging system (including five parts: the scanning

https://doi.org/10.1021/acsmaterialslett.2c01011
ACS Materials Lett. 2023, 5, 1027−1060

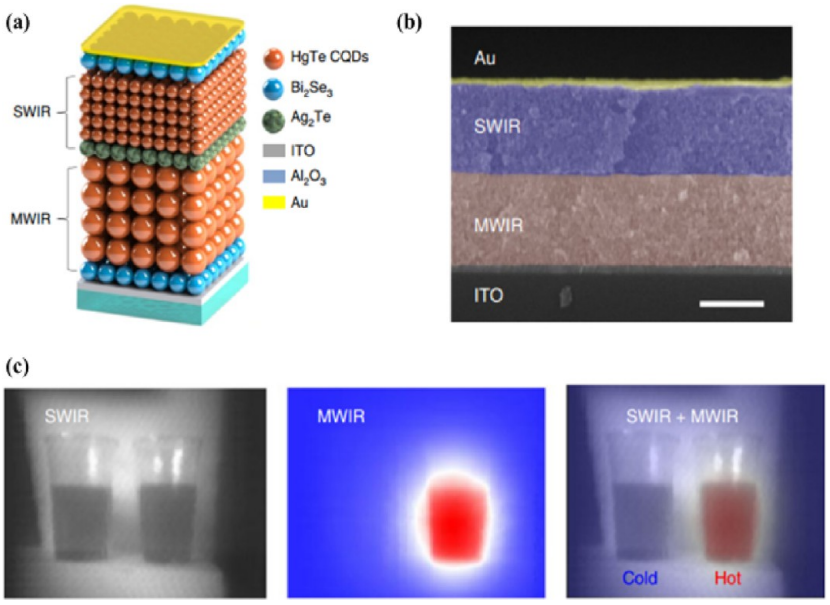

Figure 15. (a) Illustration of the structure of a dual-band CQD imaging device, (b) SEM image, and (c) SWIR, MWIR, and merged dual-band images of hot and cold water. (a–c) Reproduced with permission from ref 74. Copyright 2019 Nature Publishing Group.

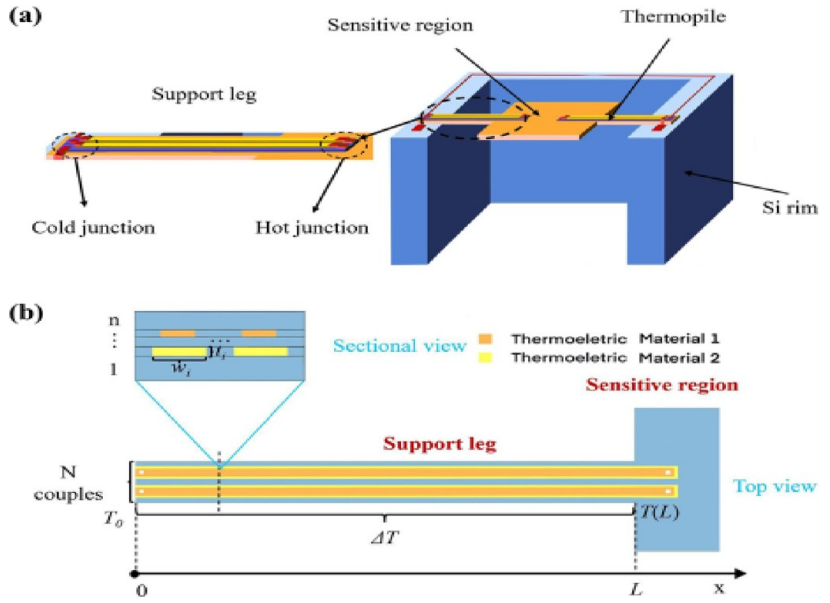

Figure 16. Thermopile IR sensor. (a) Schematic view and (b) top view and cross-section. (a, b) Reproduced with permission from ref 88. Copyright 2022 Elsevier.

lens, cryostat, HgTe detector, amplifier, and software), while Figure 14f–h shows the thermal image results, including folded fingers, hair, and the nose.[83] Due to the high response time, the thermal images can be detected at a high frame rate, while the temperature differences of Peltier (ΔT = 15 °C) are also demonstrated.

Figure 15a and b shows the architecture of the dual-band detector using the n–p–n structure and the cross-sectional SEM image. In this structure, different-sized HgTe QDs were used to tune the absorption (SWIR and MWIR) as a sensing material, while Bi_2Se_3, Ag_2Te, and Au play as the role of n-, p-type, and contact layers.[74] Infrared images of cold and hot water are shown in Figure 15c.[74] The single image identifies the water (SWIR) or determines the temperature of the water (MWIR), while the merged SWIR and MWIR images provide more information.[74]

The Ag_2X (X = S, Te, Se) QDs family has promising potential applications in IRIS due to the absorption range in the IR and high electrical conductivity. This family also consists of materials that are heavy metal-free with low toxicity.[87] Nevertheless, Ag_2X QDs are reported on IR photodetectors, while there is no research on the integration of Ag_2X QDs on the CMOS to fabricate QD-IRISDs. Reports show that Ag_2S exhibits absorption in the range 500–1000 nm, while Ag_2Se and Ag_2Te show MWIR region absorbance features. Mir et al.[78] reported the influence of reaction time on the optical properties of Ag_2S QDs. The samples with longer reaction times (20 and 60 min) show an absorption peak at 800 nm and up to 850 nm, compared to shoulder absorption at

https://doi.org/10.1021/acsmaterialslett.2c01011
ACS Materials Lett. 2023, 5, 1027–1060

650 nm in the sample with a 10 min reaction. Quyang et al. reported Ag_2Te QDs with a distinct absorption peak ranging from 1050 to 1450 nm.[79] Qu et al. reported tuning the energy from 0.26 to 0.08 eV by tuning the size of Ag_2Se QDs.[77]

4.2. Thermopile Image Sensing. Several working environments, including medical treatments, smart homes, space detections, and industrial monitoring, call for the employment of temperature sensors, gas sensors, vacuum sensors, biochemical sensors, thermal-power sensors, and flow sensors. These thermopile applications are numerous and widely used in body-temperature screening, especially as the 2019-nCoV widespread disease spreads globally beginning in 2020. Figure 16a shows a schematic view of a thermopile IR sensor.[88] They provide noncontact detection, mobility, simplicity of use, and low cost, wherein sensitivity is a vital characteristic to describe the performance of thermopiles among all other variables.[89]

It is effective to quickly test a subject's respiratory rate before they enter a space in order to evaluate potential dangers in their direction and control the spread of COVID-19. Researchers are looking into the possibility of thermopile-based respiratory screening, a novel yet cost-effective method of screening a subject by monitoring their respiration rate. Several image and signal processing techniques to determine the respiration rate are employed as low-resolution thermal recordings using a modified thermopile array system. A methodology based on autonomous region of interest selection yields a mean absolute error (MAE) of 0.8 breaths every 60 s for the purpose of developing and putting into practice a respiratory solution to stop the transmission of COVID-19 during the pandemic.[90] For many computer vision applications, such as MATLAB, recognizing children in thermal images utilizing thermopile array sensors (Th-AS) is essential, particularly for recognizing children left unsupervised in a parked car in extremely high temperatures. Many deadly incidents have been linked to careless parenting, and most parents have expressed regret over their children's incidents. This may be done by designing and setting up a thermal imaging camera utilizing a Th-AS as well as a Raspberry Pi as a microcontroller. The thermal image can then be processed using the background subtraction approach to remove the forefront or human item from the related image.[91]

There are numerous consumer and industrial uses for thermopile sensors (TH-S). The fundamental thermal parameter of TH-S is the Seebeck coefficient (SC). In TH-S, it is crucial to determine the SC of both the material and the thermocouple. The device consists of a substrate, a framework, four supporting legs, and a sensitive area with a resistor acting as a heater and a temperature sensor. Along with a thermopile sensor, several on-chip test structures are created. Figure 16b depicts the top view and cross-section of a thermopile IR sensor.[88] Its measurement results are examined and contrasted with those of the device, and the validity of its structure is confirmed by these results, which are compatible with one another.[92]

Researchers offer a numerical model for the effective design for optimization of a unique infrared (IR) detector array, which is built on a single silicon-on-insulator (SOI)-based microelectromechanical system (MEMS) membrane. The model, which is based on the finite element method (FEM), is used to look at how heat transfer at the pixel level affects the responsiveness and cross-talk performance of a thermopile array. Results demonstrate that adjusting a number of design components, such as pixel size, interpixel metal heat sinking tracks, and the addition of air gaps between pixels, can lead to the achievement of ideal operational conditions. Specifically, they discover that the combined impact of air gaps and copper heat sinking tracks can boost responsiveness by 6.4% while reducing pixel crosstalk by 65%, and a rising variety of low-cost industrial as well as consumer applications could benefit from the model's improved understanding of thermal effects in these devices.[93]

Thermopile sensors monitor temperature at a distance by spotting IR energy from an object. The amount of IR radiation increases with the temperature. Small thermocouples attached to a silicon chip make up the thermopile sensing element, which absorbs energy and generates an output signal. The production of the chip for a thermopile-based CMOS IR sensor array is made simpler by using a single Si membrane plus conventional CMOS Al layers for thermopile cold junction heat sinking. Noncontact distant temperature measurements are best suited for single-element thermopile sensors and thermopile arrays with poor spatial resolution. Temperature sensors for industrial process control and measurements of human body temperature with in-ear or forehead thermometers are the two most popular uses. The low thermal time constant of thermopile sensors enables fast observations. Thermopiles can also be operated at DC and do not require regular reactivation by an external shutter mechanism, making it possible to observe the temperature continuously. Literature study also reports thermopile arrays with 32 × 32, 80 × 64, and 120 × 84-pixel resolutions, beginning with 8 × 8 and 16 × 16 pixels. This enables customers to produce thermal images with various levels of spatial resolution for use in a variety of automation and security applications. Hot spot detection is another topic that has a variety of applications in fields like engineering, fire suppression, industrial safety, and consumer goods.[93,94]

Based on Beers' law and the nondispersive infrared (NDIR) gas detection principle, thermopile sensors can be used to measure gas concentrations. By employing TH-Ss, it is possible to determine the concentration of a certain gas by measuring the infrared radiation absorption at a particular wavelength. One thermopile and an infrared light source are all that complete this sensing setup. However, accuracy can be improved using two single or dual thermopile sensors, which prevent the infrared source output from rooting over time. TH-Ss can detect NDIR gases quickly and with a minimal volume, because of their tiny size and low thermal mass. For contactless temperature sensing, thermopiles are employed. A thermopile is used to convert the heat radiation that an object emits into a voltage output. The output range is tens or hundreds of millivolts or less. Thermopiles function as generators and sensors. It has been claimed that manufacturing of IR thermopile arrays on a single membrane is possible, although these arrays use unconventional components above or below the membrane. Due to the partial CMOS incompatibility of gold, bulk silicon layers or extra gold layers serving as heat sinks are two of the examples. The in-situ integration of composite nanoforests (CNFs) onto infrared thermopile sensors is accomplished using a micromachining-compatible approach that is suggested due to the CNFs' significant optical absorption. Their integration increases the sensitivity of the sensors by over 30% while essentially maintaining the reaction time. Such CNFs and their simple

https://doi.org/10.1021/acsmaterialslett.2c01011
ACS Materials Lett. 2023, 5, 1027−1060

integration method are anticipated to be applicable to other infrared devices, such as uncooled infrared focal plane arrays.[94]

4.3. THz Image Sensing. Since intra- and intermolecular vibrations fall within the THz spectrum, terahertz (THz) technology has received a lot of attention in several research fields over the years, particularly THz plasmonics for sensing applications. The use of metamaterials (MM), which are artificial structures on the subwavelength scale of the input light, can increase the sensitivity of free-space THz detection. These synthetic materials exhibit both strong electric field enhancement and great sensitivity to environmental changes. A polarization-insensitive THz metamaterial absorber (MMA) made of dielectric-metal disc antennas has been used to theoretically and experimentally examine residual herbicides and pesticides.[95] Figure 17 shows the terahertz radiation

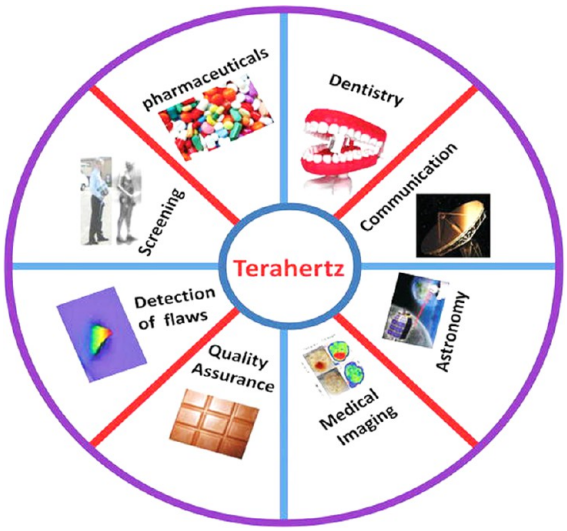

Figure 17. Application of terahertz radiation for detection of flaws in photovoltaic materials, medical imaging, screening, pharmaceuticals, quality control, dentistry, communication, and astronomy. Reproduced with permission from ref 96. Copyright 2017 IntechOpen, UK.

applications, and the findings demonstrate that THz MMA significantly increases sensitivity, with a limit of detection (LOD) of certain herbicides and pesticides reaching 5 ppm.[96] These findings suggest that the THz MMA platform could be a useful tool for highly sensitive THz applications in the regulation of food quality and safety and has the potential to be used to detect pesticide and herbicide residues in agricultural and food goods.[95]

THz imaging and spectroscopy have long been prized for in vivo biological applications due to the nonionizing, noninvasive nature of THz radiation and their high sensitivity to water. Due to the low THz wave penetration depth and high-water attenuation in biological samples, the skin is one of those that is primarily studied. A comprehensive skin model that can account for the interaction between THz and the skin is still required. This is important for revealing the optical properties of the skin from the recorded THz spectrum, and using the correct model, which is very important for ensuring the validity of the data and findings than simply ensuring compatibility between different works. Researchers compare the adaptability, accuracy, and limitations of the skin models utilized in the THz regime by demonstrating the majority of models to determine the skin's internal moisture profile, but there is also an anisotropic model that depicts structural changes to the skin's stratum corneum.[97]

Recent developments in THz technology-based image processing as well as related applications refer to THz as the region that is in the middle of infrared and microwave radiation, spanning the gap between optics and electronics. The interaction of materials in the submillimeter wavelength range (about 300 GHz to 3 THz) of a unique electromagnetic spectrum, which is indistinguishable from other spectroscopic methods, is the subject of THz image processing. Since neither microwave nor optical technology could completely overcome this enigmatic world with its countless undiscovered scientific resources, the THz regime, also known as the "THz gap", was recognized for a long time. THz imaging techniques have thus been successfully developed, and classic THz technology may concurrently acquire spectral and image data to address a variety of applications, including security, the aerospace industry, medicine, material science, biomedical imaging, and others. The development and commercialization of THz imaging systems are now widely acknowledged as an affordable alternative to relatively expensive components such as electron lasers, Smith-Purcell emitters, reverse wave oscillators, and synchrotrons. In order to increase its usefulness as a checkup

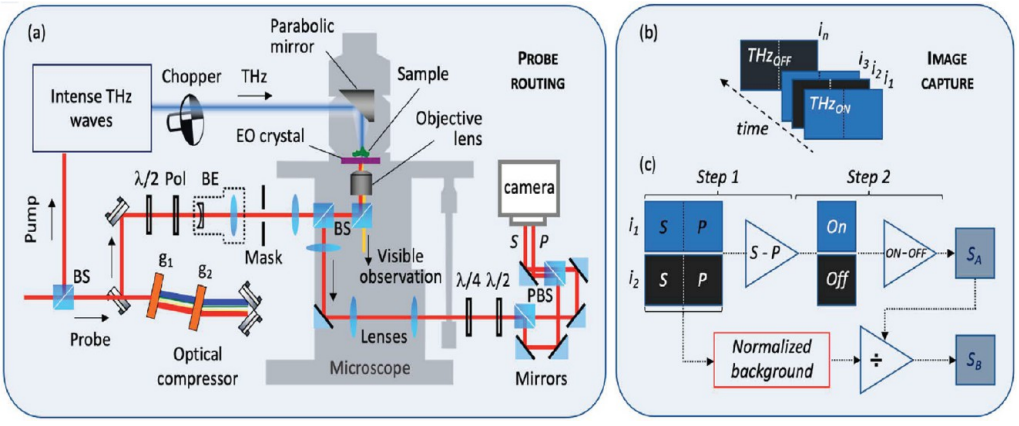

Figure 18. (a) Beam probing for two-dimensional near-field THz field measurements. (b) Aligning the acquisition order for dynamic background subtraction. (c) Dynamic background subtraction followed by the vertical S and horizontal P pictures subtraction operation (on−off images). (a−c) Reproduced with permission from ref 99. Copyright 2022 MDPI.

https://doi.org/10.1021/acsmaterialslett.2c01011
ACS Materials Lett. 2023, 5, 1027−1060

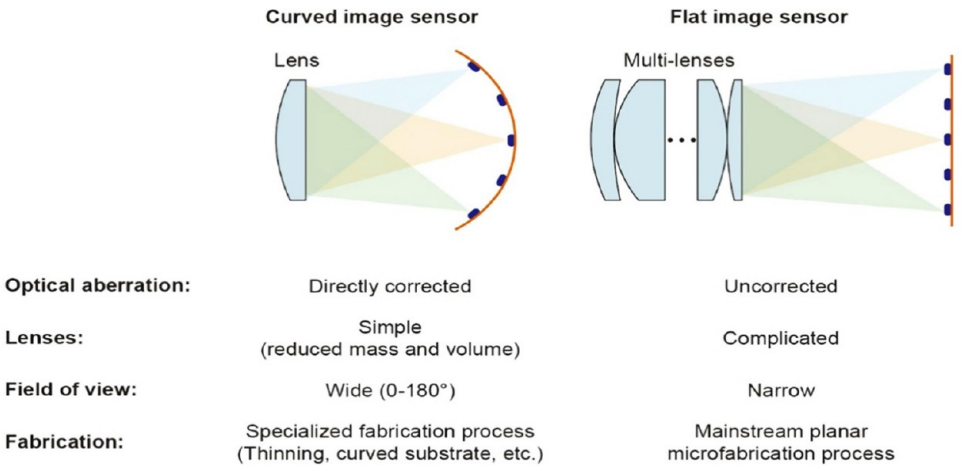

Figure 19. Comparison between curved and flat image sensors. Reproduced with permission from ref 107. Copyright 2022 Elsevier.

tool for different imaging applications, THz image processing attempts to identify solutions through the synthesis, modification, and detection of THz radiation. For instance, the ability to study the unique behavior of biomolecules is facilitated by the THz wave's increased sensitivity. The 3D structure of biological samples such as cancer tumors can be examined using cutting-edge digital image processing methods in conjunction with THz pulsed imaging (TPI). Additionally, the THz spectrum may have an effect on nonionizing radiation-based diode detectors used in the aerospace industry, as well as wireless network topologies (such as WLAN, WPAN, and D2D) and security screening. Figure 18 shows the vertical S and horizontal P picture subtraction operations (on−off images). THz waves are fully safe, unlike X-rays, and can penetrate clothing, items, and packages to identify the interior materials and chemicals in the fields of digital imaging and biomedical engineering, because THz imaging and detection technology make it possible to quickly identify opaque objects with distinct borders.[98,99]

Virus epidemics such as Ebola, Zika, MERS, and others have wreaked havoc on humanity in the last ten years, and the coronavirus (SARS-CoV-2) pandemic, as well as its constantly evolving variants, has put the entire technological advancement of healthcare in jeopardy. Although conventional methods of viral detection have been somewhat successful though they are expensive and time-consuming and require specialized human resources. The development of low-cost, noninvasive, and quick virus detection technology may be facilitated by terahertz-based biosensors. The current developments in terahertz technology-based biosensors for viruses, viral particles, and antigen detection are examined recently, along with future research directions in this area.[100] As a portable antenna test range, a silicon lens-integrated CMOS THz camera, a 26-dBi 0.852-THz standard gain horn antenna radiation source, and both single-frame low-resolution and multiframe super-resolution approaches are employed to acquire data. With the latter, a far-field radiation pattern can be measured with improved angular resolution. The source directivity is also calculated using both single-frame low-resolution and multiframe super-resolution radiation patterns. The highest directivity in two different radiation patterns is 25 and 25.8 dBi, respectively, with an accuracy of 1 and 0.2 dB, with better angular resolution in the latter resulting in improved accuracy.[101]

Since THz radiation is nonionizing, transparent to plastics and fibers, has a higher resolution than millimeter waves, and has a frequency that matches the typical absorption or vibration frequencies of some materials along with biomolecules, it has attracted attention of many researchers over the past one to two decades. The majority of commercial THz detectors for imaging are often made up of discrete components that are large but expensive due to the weak interaction between THz radiation and the majority of materials. For the purpose of improving absorption in the visible, infrared, and THz bands, metamaterials with an ultrathin thickness have also been studied. THz radiation absorption was also reported in a meta-material. As a result of converting a single-pixel sensor into a 5 × 5-pixel array with pixels of 30 m × 30 m, literature reports a thermal time constant of 68 ms and a minimum noise equivalent power of 37 pW $Hz^{-1/2}$. The metamaterial was directly fabricated in a six-metal-layer CMOS process, which also included insulating layers on top of metal, which were connected to electronics at the bottom by postprocessing techniques, using a high-quality processed pixel array that was designed to anticipate an absorption band with a center frequency of 2.5 THz. Using an aluminum cut-out "T" shape as a test specimen, the image of a metamaterial-based THz focal plane array demonstrates how the ultracompact THz sensor works in great detail at room temperature.[102]

The THz frequency band, which lies between microwaves and infrared, is the range of electromagnetic wave frequencies between 0.1 and 10 THz.[103] The THz signal is currently establishing itself as a prospective contender in the field of research for its many improved and diversified uses, including sensing, secure telecommunication, pharmaceutical drug testing, biomedical sensing, imaging, and environmental applications. PCF's advantageous geometrical structure and uniform guiding properties have suggested a number of sensing applications in the THz domain, including liquid chemical sensing, gas sensing, biosensing, RNA and DNA analysis, genetic diagnostics, cancer diagnosis, humidity, and temperature sensing, among others. The most crucial aspect is that the associated geometric parameters can be used to influence the optical behavior of the PCF sensor. Four different types of power detectors are implemented in 0.18-m CMOS technology for the THz image sensor application, as well as a common gate with or without supply voltage. At 332 GHz, the measured

https://doi.org/10.1021/acsmaterialslett.2c01011
ACS Materials Lett. 2023, 5, 1027−1060

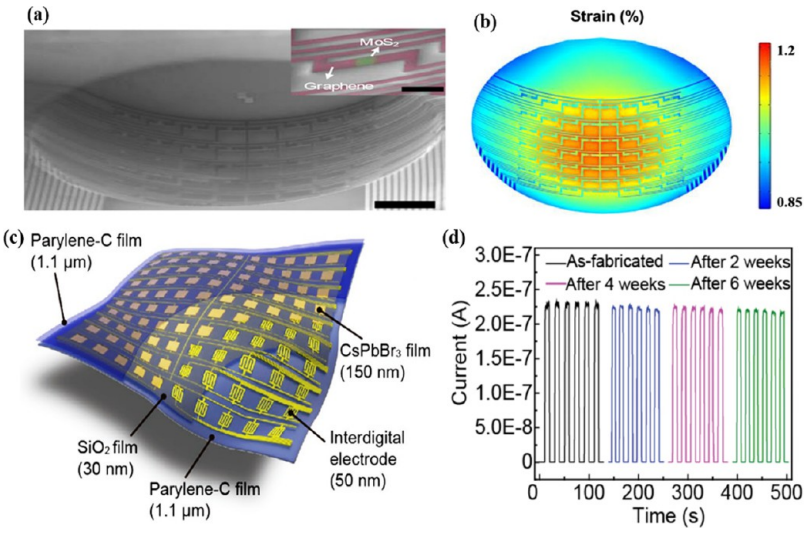

Figure 20. Ultrathin curved image sensor array of MoS_2-Graphene photodetector: (a) SEM image, (b) strain distribution through FEA. (a, b) Reproduced with permission from ref 112. Copyright 2021 American Chemical Society. For $CsPbBr_3$ thin film device: (c) schematic, and (d) *I*−*T* curve graph. (c, d) Reproduced with permission from ref 113. Copyright 2021 John Wiley and Sons, Inc.

responsivity is 632 kV/W, 13.2 kV/W, 16.2 kV/W, and 9.1 kV/W, and the proposed THz sensor has a 2 mm picture resolution.[104]

4.4. Curved Image Sensing Array. Joseph Petzval demonstrated the fact that a thick-lens optical framework focuses on an object that is placed on a curved image surface, whose curvature is demonstrated by the optical elements' morphological configuration and refractive indices. This design of field-flattening lenses has become the cornerstone of the modern optical imaging field. Multitasking optimization methodologies are used in modern frameworks to combine numerous optical elements to reduce aberration effects. Moreover, to enhance the lens design quality, arbitrary curved sensing systems are being used, which not only extend the lens optimization but also broaden the range of high-quality lenses. Numerous scientific reports are being investigated to explore the curved sensor devices' optical performance, including the illumination factor and modulation transfer function, particularly at the imaging field edges, which presents the impact of flat field systems on lens design.[105,106] In the present imaging sensor framework, multiple elements having opposing field-curvature properties are being used to reduce the field curvature, but it has the limitation that, with the addition of these elements, the mass and volume of the lens system increase, which gives rise to aberrations and therefore affects the device's performance. As a result, the degree of curvature must meet specific optical requirements such as the aperture, view field, and chromatic bandwidth in order to reap the significant benefits.

Figure 19 demonstrates the comparison of flat and curved image sensors, which strengthens the fact that a curved imaging lens design can minimize the aberration effects that are caused by the mismatch between the curved focal plane and the image sensor.[107] Moreover, a flat image sensor requires a complex configuration to fix the image distortion effects. For instance, a double glass lens uses a greater number of lenses for image focusing, while a plano-convex lens needs a single lens for the whole process, resulting in minimized distortion effects with high stability and a wide field of view with better image quality by employing a simple lens framework.

4.4.1. Fabrication Design. Curved image sensing devices can overcome the limitations of modern imaging devices with cost-effective techniques by matching their curvature to the focal plane. However, keeping in mind the challenging fabrication methodologies of these devices, presently, micro- and nanofabricated planar structures of CCD and CMOS devices are being used in image sensing fields. To introduce curved devices into the conventional industry, specialized fabrication methodologies such as deforming, transferring, and in-situ synthesis techniques have been reported.

4.4.1.1. Ultrathin Design. The planar device is deformed by pressing its spherical surface, which is an easy method of fabricating curved image sensors. However, this process causes some limitations in the mechanical failure of the device, which are introduced by the folding and wrinkling of the device by employing bending methodologies.[108] To overcome this effect, planar devices need to be flexible to bear mechanical bending and deformations.[109,110] One suitable method is the thinning of the film, which enhances the bending curvature. For instance, the increase in bending curvature was reported to be six times higher by reducing the film thickness from 1 μm to 1 nm.[111] Similarly, Thai et al. investigated the MoS_2-graphene thin film structured curved image sensor array, where they employed spherical surface bending by deformation techniques, which resulted in a wide photoresponse in the IR range.[112] Figure 20a presents the SEM analysis of a synthesized photodetector array on a spherical surface with a diameter of 6 mm and a depth of 400 μm, whereas the FEA method was used to analyze its strain distribution, as shown in Figure 20b.[112] Furthermore, Wu et al. investigated a 5-layered thin structured perovskite photodetector array using wafer-scale $CsPbBr_3$ as an active material, as shown in Figure 20c.[113] The device thickness was reported as 2.4 μm, which was advantageous for managing conformal contacts with undevelopable surfaces, including walnuts and fingerprints. As a further safety measure, an encapsulating layer of perylene-C was introduced, and this layer showed consistent photoresponsivity behavior for about a few weeks (see Figure 20d).[113]

https://doi.org/10.1021/acsmaterialslett.2c01011
ACS Materials Lett. 2023, 5, 1027−1060

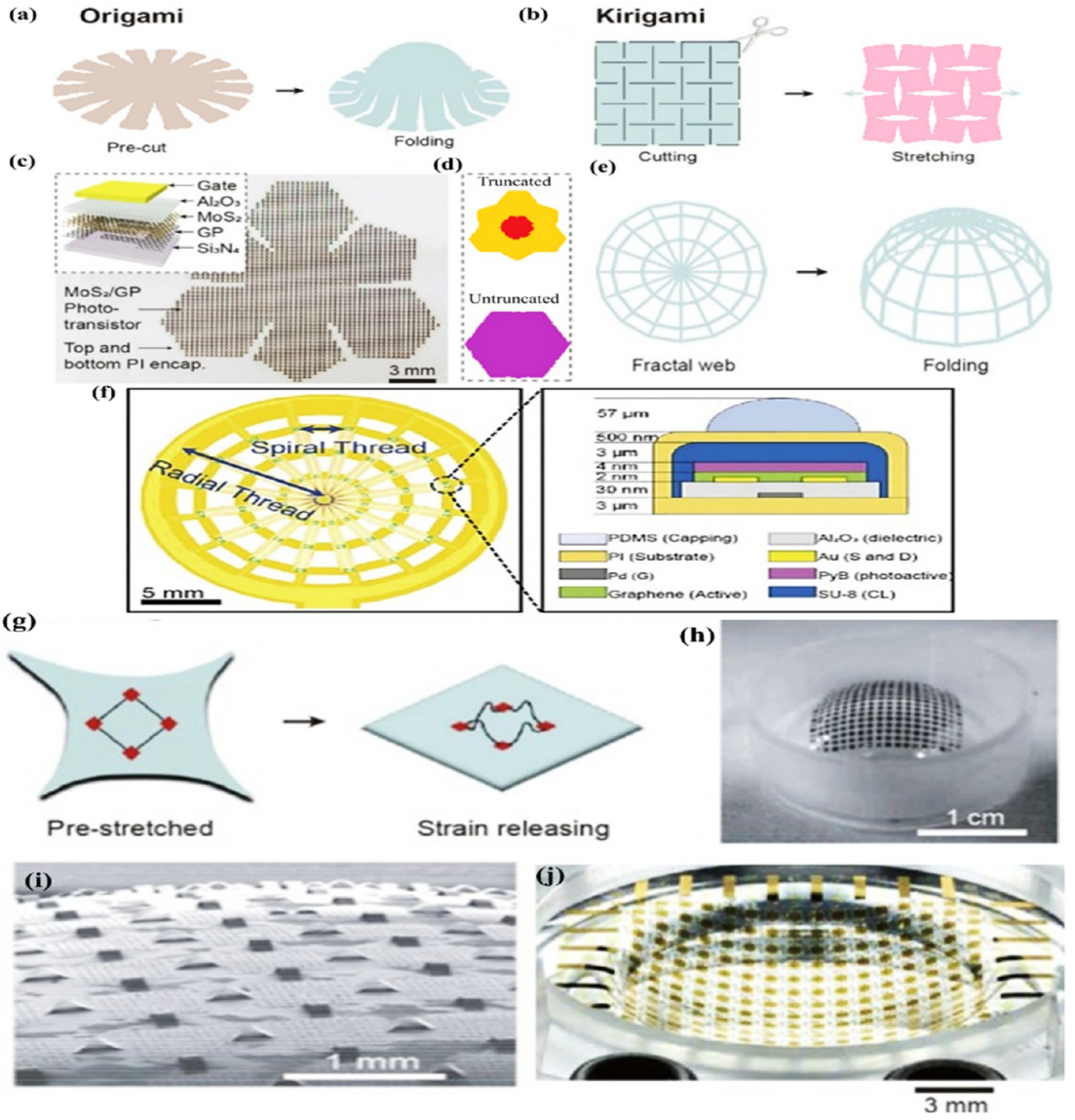

Figure 21. Schematic illustration of the: (a) origami design, (b) kirigami design. For MoS_2-graphene phototransistor: (c) optical image, (d) truncated and untruncated structure, and (e) fractal web schematic structure. (a–e) Reproduced with permission from ref 107. Copyright 2022 Elsevier. (f) Schematic illustration of pixel distribution in a fractal web structure. (f) Reproduced with permission from ref 127. Copyright 2020 John Wiley and Sons, Inc. (g) Schematic of Iceland bridge design. (g) Reproduced with permission from ref 107. Copyright 2022 Elsevier. Si photodetector on PDMS surface with: (h) Optical image and (i) SEM image. (h, i) Reproduced with permission from ref 128. Copyright 2008 Nature. (j) In hemisphere curved condition. Reproduced with permission from ref 114. Copyright 2011 PNAS.

4.4.1.2. Origami/Kirigami Design. Origami was named after a technique called paper folding, which is an easy method to transform a 2D planar material into a 3D structure by bending and folding techniques,[114−117] which have been investigated through micro- and fabrication processes by employing surface tension force.[118−120] Figure 21a presents a dome structure that was achieved by continuous folding of a 2D film.[107] Chen et al. reported a solar-blind 3D Ga_2O_3 material-based photodetector array that required eight times as much manual folding as a 2D film.[121] With this methodology, multipoint light imaging, spatial distribution, and tracking of the real-time light path are now possible. The kirigami structure, on the other hand, was named after paper cutting, which usually involves both cutting and folding methodologies. In some studies, there is no proper boundary mentioned between the kirigami and origami processes because they do not count the prepatterning procedures. However, if the planar object can withstand bending and twisting forces, some kirigami designs may allow for stretchability.[122,123] Blee et al. achieved graphene stretchability by applying the kirigami design to graphene structures, and efficient mechanical properties were also reported.[124] Figure 21b represents a 2D film structure by kirigami design that can be converted into a spherical surface to make uniform contact with curved surfaces owing to its maximum stretchability.[107,125] Similarly, Choi et al. studied a spherical curved image sensing device with high resolving power using MoS_2-graphene structure as an activating material with improved mechanical stability (see Figure 21c).[107,126] The theoretical analysis depicted a truncated design validity, which showed that the truncated design is a small circular pattern, whereas the untruncated design has more tensile strains with a large circular structure, as presented in Figure 21d.

https://doi.org/10.1021/acsmaterialslett.2c01011
ACS Materials Lett. 2023, 5, 1027−1060

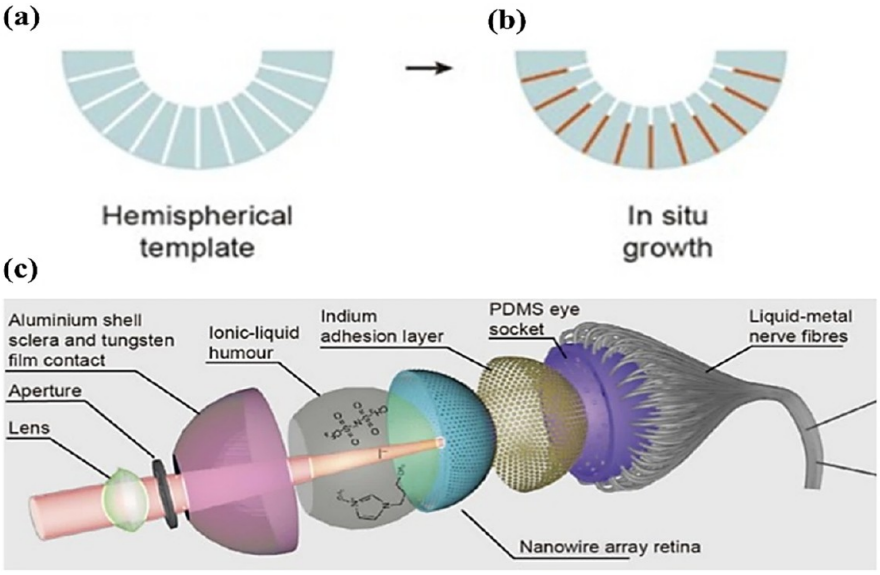

Figure 22. In situ growth of nanowires in a: (a) hemispherical template, (b) optical image of nanowires on a hemispherical template. (a, b) Reproduced with permission from ref 107 Copyright 2022 Elsevier. (c) Perovskite material-based active layer in which tungsten sheet acts as a counter electrode. Reproduced with permission from ref 135. Copyright 2020 Nature Publishing Group.

4.4.1.3. Fractal Web Structure. Naturally, spider webs follow a repeating structure that exhibits excellent environmental mechanical stress resistance,[129] which inspired the fractal web structure of image sensing devices. It has a few cuts to enhance the stretchability and strength of the structure with uniform strain distribution throughout the web structure.[130] Figure 21e presents the spherical fractal web structure without any mechanical mismatching in the design. Lee et al. investigated a 3D photodetector array structure in a spherical domelike shape by properly arranging the optical materials in the web structural form.[107] In their study, they assembled the photodetector elements on the web threads and connected them through Au serpentine along the thread, while the graphene doped with PyB was used as an active material in the transistor structure (see Figure 21f).[127] The fractal web structure laminated the device on a spherical dome and resulted in the effective properties.

4.4.1.4. Iceland Bridge Design. The Channel Island bridge structure is being used to design a stretchable framework of materials by employing the deformation of rigid materials into curved shapes.[131,132] Figure 21g demonstrates the formation of islands on a prestretched planar surface, interconnected with metal wire bridges to enhance their mechanical stability.[107,133] In the deattaching process, the substrate surface returns to its initial structure with the deformation of bridges while not affecting the mechanical and electrical stability of the structure. Figure 21h presents a photodetector array on a spherical substrate, in which an arc-shaped connection allows the substrate to deform from a 2D planar to a spherical structure (see Figure 21i).[128] Jung et al. investigated the Si-based spherical photodetector array, with the Si film separated by metal wires and transferred onto an elastomer substrate,[114] which deformed into a spherical shape with adjustable curvature, influenced by the water pressure substrate (see Figure 21j).[114]

4.4.2. Synthesis Strategies. The fabrication techniques for curved imaging sensing devices based on the strategy of first fabricating the device on a planar substrate and then shifting it to a curved surface resulted in increased external stress as well as a noticeable loss of efficiency.[134] To avoid this problem, photosensitive materials can be fabricated directly on the spherical substrate, so device damage through the transfer procedure can be avoided (Figure 22a,b).[107] The vapor phase deposition method was investigated by Gu et al. for the synthesis of $FAPbI_3$ perovskite nanowires inside the spherical substrate of a porous aluminum oxide membrane, demonstrating a 500 nm pitch with a high density of 4.6×10^8 cm^{-2}.[135] A spherical biometrical electrochemical eye was also proposed for proper electrical contact, where the perovskite acts as the active material following the tungsten sheet acting as the counter electrode (see Figure 22c).[135] Moreover, ionic fluid was filled up between the aluminum sphere and the porous aluminum oxide membrane, which contacts tungsten electrode and perovskite nanowire to collect the signals and their further transmission.

4.4.3. Applications. 4.4.3.1. Fisheye Zoom System. A commercial fisheye camera has a field of view of F/4, and a recent report was published to reduce the number of lenses used in this camera and to improve the device efficiency while keeping the field of view and back focal distance constant. The optical system was simplified by suppressing the field flattening lenses, which modified the optical performance of the device and improved its mechanical stability.[136] The configured device's optical performance is demonstrated in Figure 23 along with the conventional device (see Figure 23a,b).[137] While at 11.9 mm focal length, Figure 23c demonstrates the spot radius for both Canon and the new configured device, whereas Figure 23d represents their comparison in relative illumination, indicating that the improved configured device showed efficient optical performance by a factor of 2. As illustrated in Figure 23e and f with a zoom prototype and zoom acquisition incorporating efficient constructed patterns both at the center and at the edges of the image, a convex-shaped CMOS sensor of this configuration has been utilized commercially with the same electro-optical response.[137,138]

4.4.3.2. Compact Wide-Angle Camera. The conventional monocentric lenses have a broad field of view, high resolution, and high compactness with the curved substrate.[139] A study

https://doi.org/10.1021/acsmaterialslett.2c01011
ACS Materials Lett. 2023, 5, 1027−1060

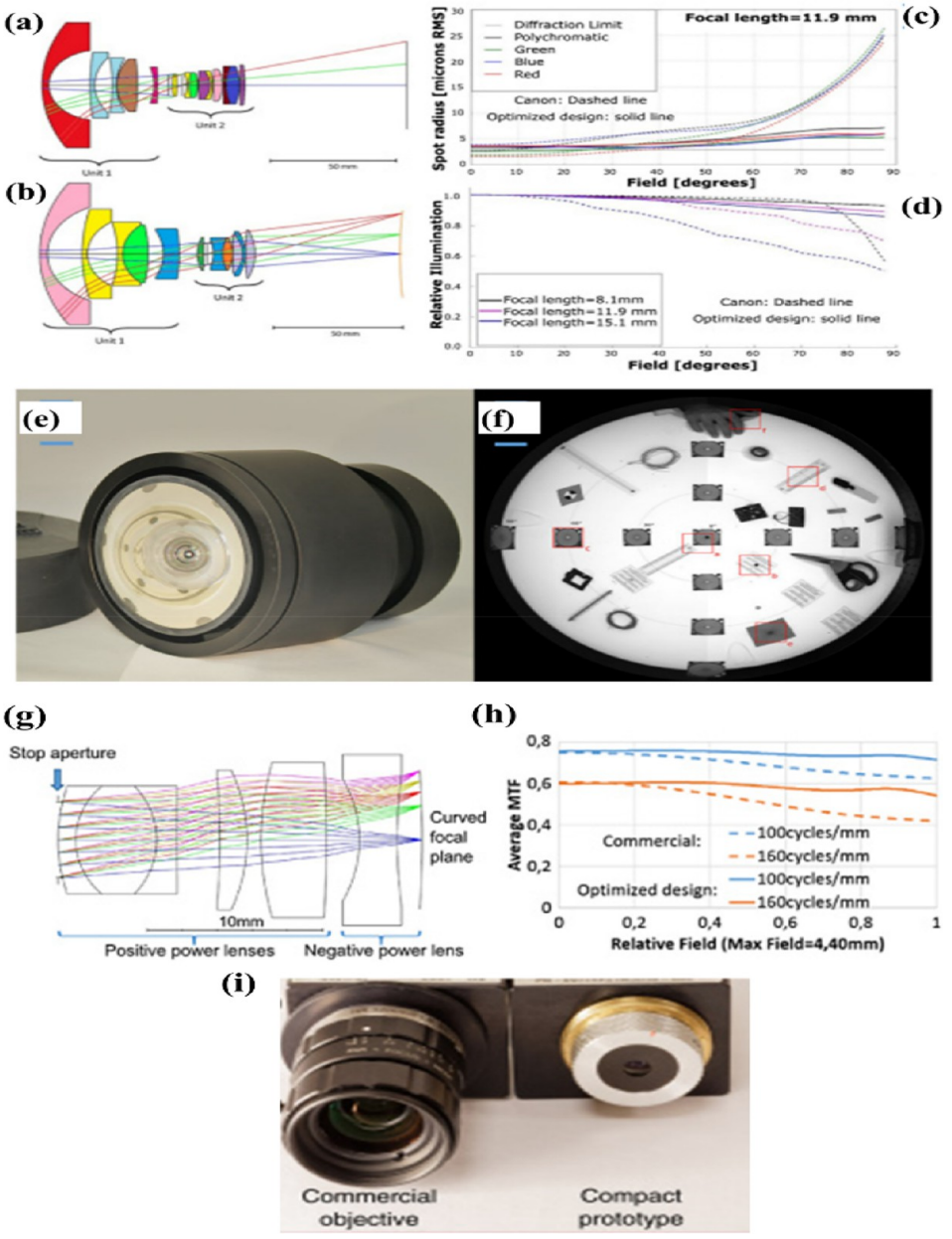

Figure 23. Optical layout of: (a) cannon object, (b) zoom camera, and their (c) spot radii, (d) optical relative illumination, (e) 8 mm focal length zoom prototype, (f) image acquisition, (g) compact system, (h) MTF comparison over field, and (i) comparison between prototype and commercial camera. (a–i) Reproduced with permission from ref 137. Copyright 2019 Optica Publishing Group.

was reported that improved the conventional device's performance and field of view while maintaining its high resolution. To achieve this improved performance, the subtended angle of the sensor was decreased by adding new spherical lenses, and hence the conventional lens system improved its field of view from 8 to 40 degrees (see Figure 23g).[137] Figure 23h demonstrates the modulation transfer function (MTF) comparison between commercial and upgraded sensor systems, wherein it shows that the MTFs of both lens systems are similar for the close-to-zero field, but at the edges, the upgraded lens system showed enhanced optical performance with a large gain in compactness. However, the existing commercial system offers a tunable iris, while the prototype system does not. The straylight issue was also reported to be resolved by adding an extra hood to avoid out-of-field straylight (see Figure 23i).[138]

4.5. Charge-Coupled Device-Based Image Sensors. In 1969, Willard Boyle and George E. Smith invented a charge-coupled device (CCD) that consists of a planar array of metal oxide semiconductor capacitors (MOSCAP) embedded into a semiconductor substrate, which can usually be a silicon surface. This arrangement forms an integrated circuit (IC), with each element acting as a pixel. This is basically a device that produces the packet of charge, transfers it within the IC, and then reads it by allowing the charge flow to obtain the output results. A charge amplifier is placed at the output stage, which reads the charge movement by providing voltage and thus processes it digitally.[140] Figure 24 represents the schematic of the CCD working, showing how light signals are detected, processed, and converted into electrical signals. However, a MOS capacitor consists of metal electrodes and a thin film made of insulating material, arranged on a semiconductor

https://doi.org/10.1021/acsmaterialslett.2c01011
ACS Materials Lett. 2023, 5, 1027−1060

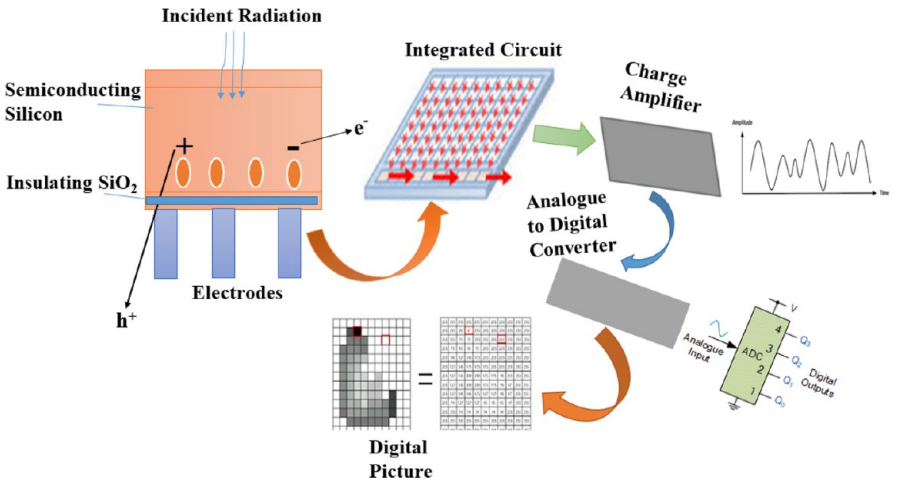

Figure 24. Schematic illustration for the working of a CCD.

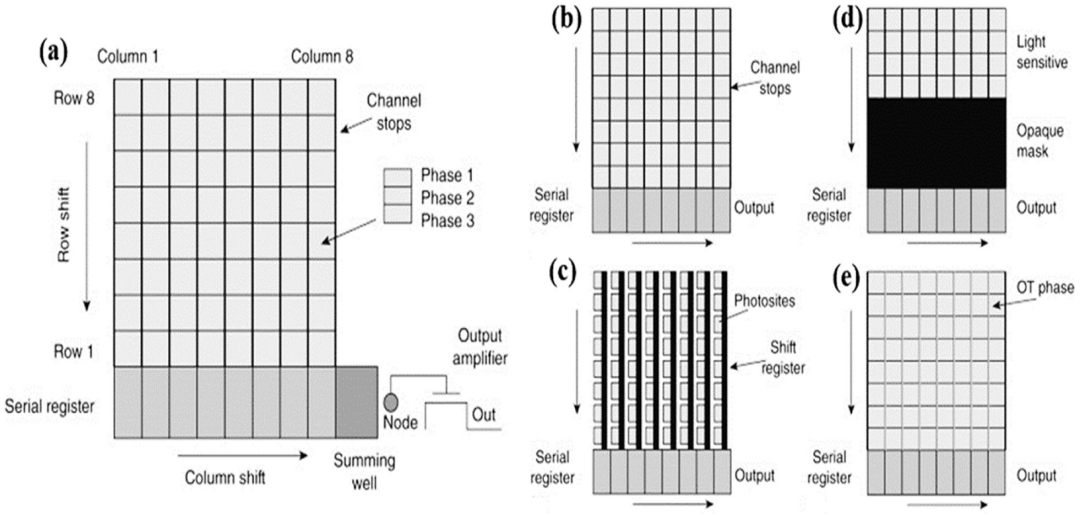

Figure 25. Design of a three-phase CCD. (a) Area array CCD architectures, (b) full frame CCD, (c) interline transfer, (d) frame transfer CCD, and (e) orthogonal transfer CCD. (a–e) Reproduced with permission from ref 144. Copyright 2014 Elsevier.

surface, where these materials act as a gate and a gate dielectric, respectively. The gate material can be made up of both metals and polycrystalline materials such as polycrystalline silicon, owing to its high efficiency and durability.[141]

4.5.1. Design, Layout, and Architecture. The pixel array in the CCD imaging sensor generates potential wells for charge storage and shifting in the form of charge packets, which are generally electron packets produced by the photoelectric effect. However, the voltage signal pattern is responsible for shifting the charge packets to the output edge, where an amplifier is placed to convert these charges into electrical signals, while the computing systems convert these signals into 2D digital images. These pixels consist of phases that are electrically linked to the applied voltage pattern, and here, each phase works like a MOS capacitor, having a repeating design in the form of rows and columns where each phase has the same applied voltage. Single-phase CCD devices, along with two-, three-, and four-phase devices, also exist, wherein, for more phases, more electrical connections are required in each direction. For example, three-phase CCD devices require electrical connections in both the *x*- and *y*-axis directions, requiring a total of six electrical connections.[142−144] A design of a 3-phase CCD is demonstrated in Figure 25a.[144]

4.5.2. Types of CCD Image Sensors. CCD devices have two main types based on linear and area array designs, wherein the linear arrays comprise the 1D structure of light-sensitive pixels, while the area array comprises 2D light-sensitive pixels. Compared with both of these, linear array devices are economical and have a fast procedure, whereas area array devices are mostly used in scientific imaging applications.[142,143]

4.5.2.1. Frame Transfer Type. One frame transfer (FT) type CCD consists of two vertical or parallel shift registers, one horizontal or serial shift register, storage, and an output section. Transparent electrodes are mainly used for photo-sensitive area detection, where the photoelectric process starts, and these generated electrical signals are collected in the potential well areas during the processing time. By employing vertical shift registers, the generated electrical signals are transferred to the storage area at high speed. Therefore, in this particular type, the vertical or parallel shift register serves as a photoelectric conversion device, while the stored signals are transferred to the output section by the horizontal or parallel shift register, where the photoelectric charge accumulation occurs at the photosensitive area (see Figure 25d).[144]

4.5.2.2. Full Frame Transfer Type. The full-frame transfer (FFT) type of a CCD device follows a similar design as the FT

https://doi.org/10.1021/acsmaterialslett.2c01011
ACS Materials Lett. 2023, 5, 1027−1060

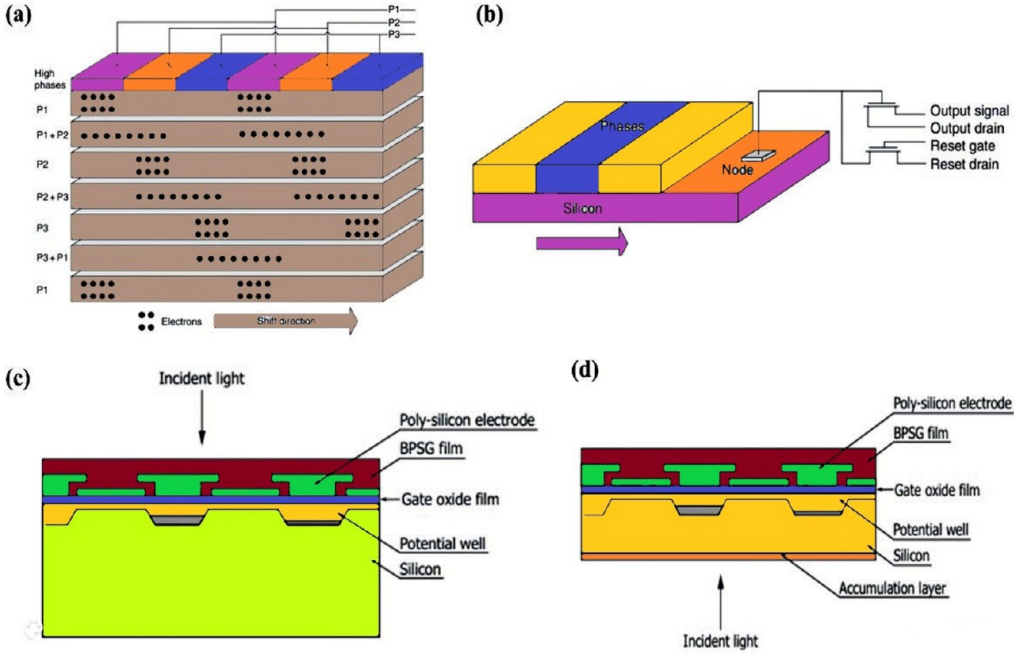

Figure 26. CCD working and illumination modes: (a) CCD clocking, (b) CCD voltage generation, (c) front illuminated CCD, and (d) back illuminated CCD. (a-d) adapted with permission from ref 144. Copyright 2014 Elsevier.

type with the difference that this type has no storage region. Therefore, it is employed through an external mechanism, which limits its applications. However, the working mechanism is the same for both of the mentioned CCD types. Like FT-type CCD, FFT also followed the charge collection in the potential well and shifted to the output region through horizontal columns during the closed period of external stimuli.[143] Moreover, like the FT type, FFT also does not have a storage section; hence, the pixel arrays are fabricated on the same chip size, making it useful for a range of applications, such as in the measurement camera framework (see Figure 25b).[144]

4.5.2.3. Interline Transfer Type. The interline transfer (IT) type of CCD devices can have both 1D and 2D structures. In a 1D design, the electrical signals are collected at the storage gate, shifted to the horizontal shift register, and then detected by the amplifier. For this type, both even and odd pixels are transferred to a separate horizontal support for the fabrication of a low-pitched photodiode array. However, for the 2D IT-CCD structure, the photosensitive area consists of photodiodes formed separately from the transfer section (see Figure 25c).[144] The IT type is different from FT in the sense that the charge shifting here is performed collectively for all of the pixels, while other operations of both types are the same.

4.5.2.4. Frame Interline Transfer and Orthogonal Transfer Type. The frame interline transfer (FIT) type CCD overcomes the IT-CCD limitations by adding the storage section to the IT-type CCD. The charge is transferred to the storage region at ultrahigh speed during signal processing from the photodiode to the vertical shift registers, enabling less smearing than IT-type CCD devices. Charge shifting along rows and columns can be accomplished with an orthogonal transfer CCD (OTCCD) by replacing the channel stops with an actively timed phase. A schematic of the OT-CCD is shown in Figure 25e.[144]

4.5.3. CCD Working Mechanism. During the integration or light exposure process, the photoelectrons are generated and collected, but not transferred anywhere. The channel stops can be employed to avoid charge spreading in relative columns. After the integration process, charge shifting occurs, followed by their collection in potential wells by applying the electrical connection, due to which they move toward the serial register. Hence, each serial register has its own output amplifier, which receives charges from its adjacent column. All the charges are shifted, which are then transferred out of the amplifier (see Figure 26a).[144] A serial register can have multiple output amplifiers to exit charges at high speeds.

After the integration process, these photogenerated charges are transferred to the output amplifier where they are detected, and the output voltage is generated (see Figure 26b) according to the relation: $V = Nq/C$, wherein V is the generated voltage, N is the number of electrons, q is the charge on an electron, and C is the node capacitance. According to this relation, a single electron can generate about 1−50 μV of the output voltage based on the value of capacitance. This photogenerated voltage can be buffered by an external amplifier for the generation of measurable voltage throughout the resistor as a part of the CCD camera controller, which can be easily amplified and converted into digital signals through an analog-to-digital converter, hence forming a digital image.

4.5.4. Illumination Modes. During the integration process, there are two illumination modes of the CCD imaging devices. CCD devices are typically designed to be illuminated directly on the circuit pattern from the front side of the device. This mode of illumination is known as "front-illuminated CCD", having their light input surface on the front side of the substrate, where the active elements such as electrodes, gate oxides, and active films are fabricated, which reflect and absorb light in an effective manner (see Figure 26c).[144] However, the quantum efficiency of the device is limited to 40% in the visible range and is not sensitive in the UV range.

Back-illuminated CCDs are designed to improve the device's efficiency by overcoming the limitations of front-illuminated CCDs. In a back-illuminated CCD, light falls on a device from

https://doi.org/10.1021/acsmaterialslett.2c01011
ACS Materials Lett. 2023, 5, 1027−1060

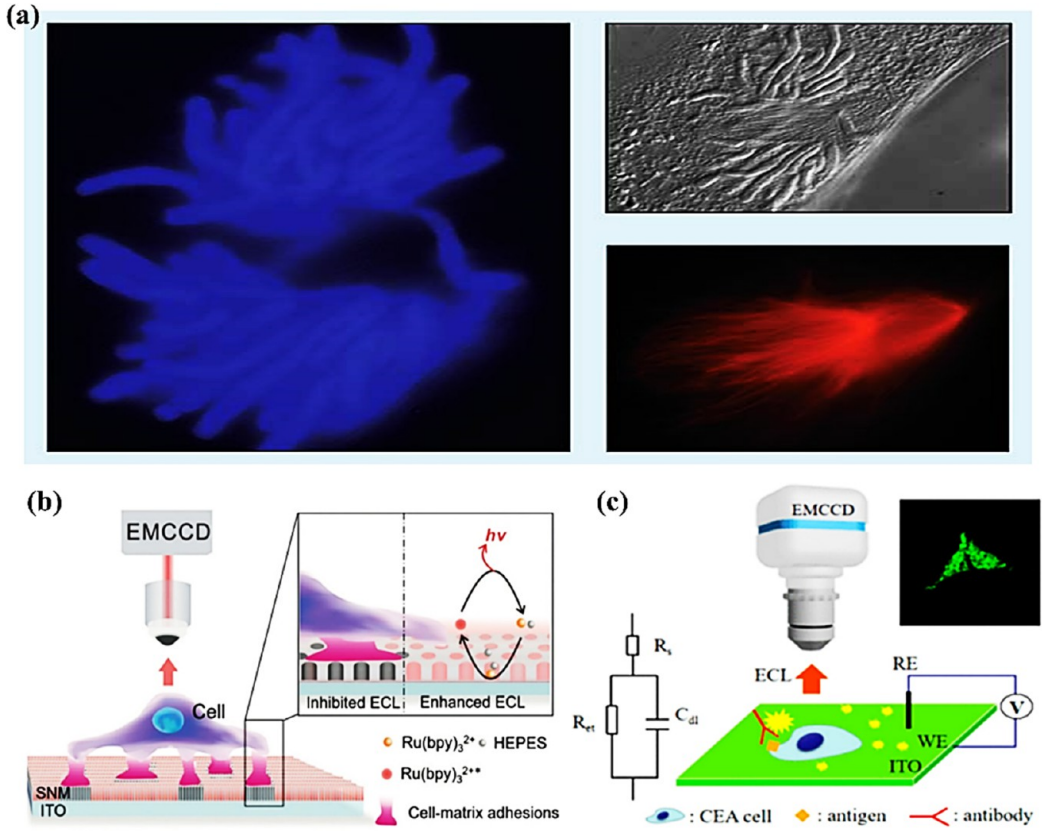

Figure 27. (a) Epithelial lung cell microscopy by a CCD camera. Reproduced with permission from ref 147. Copyright 2023 Photonics Media. Electron multiplying CCD camera applications in (b) cell matrix adhesion Reproduced with permission from ref 149. Copyright 2019 John Wiley and Sons, Inc. (c) CEA cell observation. Reproduced with permission from ref 150. Copyright 2019 American Chemical Society.

the backside, where there is no interaction with active elements, such as electrodes, active layers, and metal wiring.[145] Hence, a wide spectral range and high efficiency, along with high sensitivity and low noise, can be obtained (see Figure 26d).[144] Moreover, these CCD designs are sensitive to not only the UV region but also the near IR, X-rays, and electron beams.

4.5.5. Applications. The use of CCD devices in industrial and scientific applications is continuously increasing. Acting as photodiodes, CCDs capture light photons to employ them for detection applications and to form a digital image, hence enabling their efficient applications in the medical, physics, materials science, chemistry, and astronomy fields as photodetectors and imaging cameras. As image sensing devices, CCDs offer a range of attractive approaches, including cyclic voltammetry, for efficient applications, where the device sensitivity can be improved by multiple charge transfer accumulation cycles.[146] In life sciences applications, CCD cameras can take contrasted cell images, which helps them collect images of biomolecules with fluorophore doping. This technology has evolved in X-ray tomography systems to take tissue and bone images for analysis. Figure 27a shows the microscope CCD image of lung cells with contrast imaging methods.[147] Moreover, these features of the CCD camera also offer high-speed imaging up to the range of 0.1 to 20 MHz in modern microscopes. Furthermore, since 1970, CCD has found applications in astronomical instruments, where all celestial bodies that reflect light, whether stars, planets, or galaxies can be imaged using this method.[148]

The CCD camera is much more efficient than photomultiplier tubes, owing to its features of fast imaging, high resolution, and multichannel detection ability, due to which it finds applications in electrochemiluminescence (ECL) imaging and analysis. Ding et al. studied the contrast luminescence area for living cell adhesion on the electrode surface using an electron multiplying CCD camera, where the $Ru(bpy)_3$-2 and N-(2-hydroxyethyl) piperazine-*N*′-2-ethanesulfonic acid (HEPES) reaction generates ECL by applying voltage, which was modified by the silica nanochannel membrane, as shown in Figure 27b.[149] Furthermore, the visualization of living cells on the electrode surface and plasma membrane was investigated by Zhang et al., based on ECL microscopy in which the CEA cell was visualized at very low concentrations of about 1 pg, which finds applications in cancer diagnosis, to observe the experimental membrane in detail, schematically presented in Figure 27c.[150] CCD devices are also used in signal detection to produce the resulting digital images. A prostate-specific antigen biomarker was reported by Cao et al., with a detection limit of 31 pg/mL.[151] Moreover, Yu et al. also reported a near-IR field range immunosensor to label proteins with a methionine linker with high sensitivity and a detection range of 1 fg/mL.[152] These studies show that CCD devices also find applications in protein characterization at the single-cell level.

4.6. Neural Network Image Sensing. The human ability to perceive shapes is extremely powerful and evolutionarily beneficial. Our capability to distinguish sights, sounds, and objects and classify them on the basis of their various features is essential for functioning in our world. Still, our capability for

https://doi.org/10.1021/acsmaterialslett.2c01011
ACS Materials Lett. 2023, 5, 1027−1060

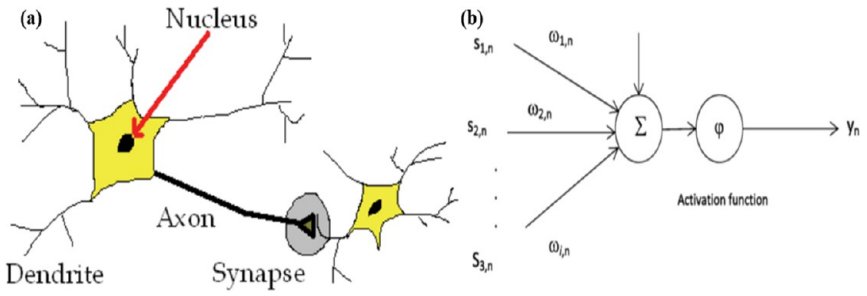

Figure 28. Biological neurons in contrast to artificial neurons. (a) Neurons with synapses in the brain. Reproduced with permission from ref 154. Copyright 2009 IntechOpen, UK. (b) Elementary model of a neural network. Reproduced with permission from ref 155. Copyright 2022 IntechOpen, UK.

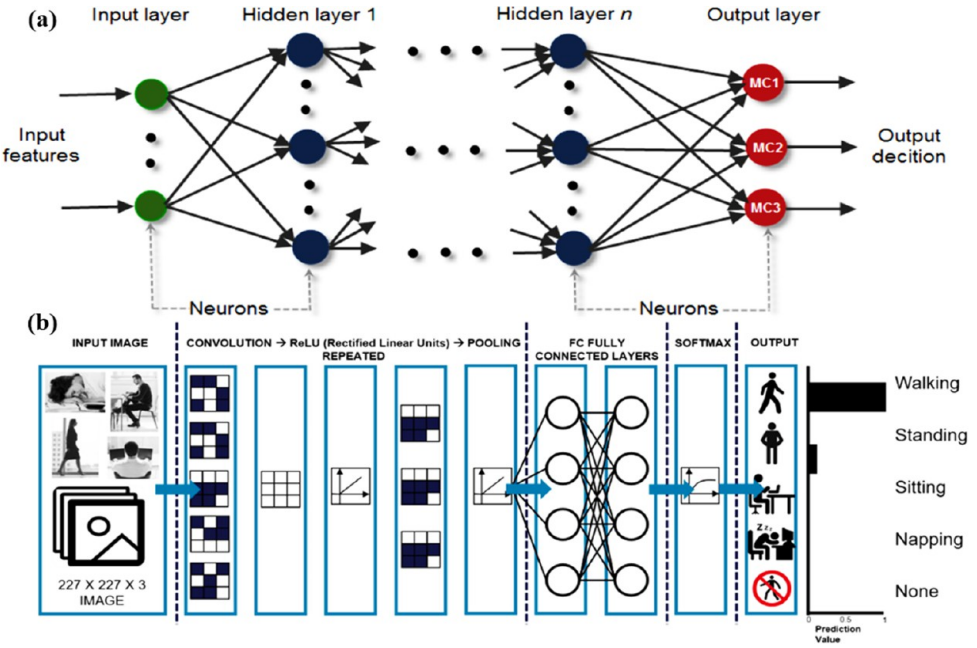

Figure 29. (a) Fully connected multilayer neural network. Reproduced with permission from ref 159. Copyright 2012 Walter de Gruyter GmbH and Co. (b) CNN-based model for activity detection and recognition. Reproduced with permission from ref 162. Copyright 2020 Elsevier.

categorization has limits: speed, noise, intensity, and clutter are all elements that alter our ability to distinguish shapes. Scientists have established a computational perspective for pattern recognition. In a few cases, researchers have also attempted to mock human categorization systems. Neural networks are referred to as a type of computer algorithm generally termed "artificial intelligence. They received a major popularity wave just in the past decade, when competitive models were finally implemented following technological improvements. The ability to teach machine skills similar to those of the human brain has been shown to be beneficial in a wide range of applications, ranging from image recognition to patient diagnosis. As a result, the artificial neural network is not limited to human-like abilities such as speech or image recognition but can also be used to learn disease diagnostics by learning massive amounts of data. Such systems have been established to achieve human or even superhuman attainments in various fields like image recognition, face authentication, the generation of human-like features for cinematic special effects, self-driving cars, automatic translation, speech recognition, medical diagnosis, game playing, and many other activities that have for a long time been considered exclusive to humans.[153−157]

Basically, there are two types of artificial neural networks: a feed-forward network, which can be single or multilayer perceptions or a recurrent network, consisting of: (i) input layers, (ii) hidden layers, and (iii) output layers. From the input to the output, the computation is accomplished layer by layer. For recurrent networks, signals possess the capability to move in loops forward and backward in the network.[155] Neural networks are modeled nearly after the human brain and its capability to distinguish patterns. In association with the notions of the nervous system for humans, the sections of the neural network take on the similar label of the neuron with a synapse, as shown in Figure 28a.[154]

As in the brain, neurons process and transmit information to the next neuron via a synapse. The synapse in the brain is basically a complicated connection in which a single neuron is linked to thousands of other neurons that commonly transfer signals to other neurons.[155] An artificial neuron can be considered an operating system that combines the weighted inputs collectively and, by using an activation function, produces an output as shown in Figure 28b.[155,156] A neural

https://doi.org/10.1021/acsmaterialslett.2c01011
ACS Materials Lett. 2023, 5, 1027−1060

network is composed of artificial neurons. These neurons are generally arranged into layers. In a fully connected feed-forward multilayer network, every output layer of neurons is transferred as input to each neuron of the following layer. Therefore, just a few layers process the original input data, whereas the processed data is received from other associated neurons. Every single neuron has a number of weights equivalent to the number of neurons in the previous layer.[157] A multilayer network consists of three types of layers, which include an input layer, one or more hidden layers, and an output layer. The input layer normally transfers data without modification. The computation takes place inside the hidden layers, whereas the function of the output layer is to convert the hidden layer computations to an output, for instance, a categorization. A feed-forward network with multilayers can function as a universal approximator at least through one hidden layer, such that it is feasibly built to compute nearly every function.[158] A fully connected multilayered neural network is shown in Figure 29a.[159]

A significant, but computer-intensive aspect of neural networks is their learning capacity. In order to make a neural network more accurate, it can be improved and trained by learning algorithms. The learning or training algorithms include training models that can work out challenging difficulties once the regular computer algorithms are insufficient. These training neural networks are expressed in two stages: initially the training period and later the recollection phase.[159] The training phase is just about weight change, and then the recollection phase is when the network is established and reaches stability with weights closest to the best possible rules the algorithm is skilled to achieve. The distinctiveness of neural networks is that they start working with absolutely no knowledge of their ascribed task and steadily learn the rules through many trials and errors. A computer programmer does not need to identify every case and solution that the machine may encounter; they simply need to lay the right foundation for the algorithm to progress and complete the given task.[160]

Today, the technology of automatic image detection is extensively used, wherein skin cancer can be reliably diagnosed by these computer programs, which are used in self-driving cars for navigation or to control robots. So far, everything has been established for the assessment of image information taken through regular cameras, which is inefficient. In particular, while the recorded number of images per second is very high, it becomes hard to handle the generation of large volumes of data. In the past few years, neural networks have seen various applications in the field of automatic image recognition, mainly owing to their functioning being equal, if not greater, than that of humans. Still, in addition to great success and attainments, they also faced numerous challenges.[161]

For challenges of image detection and identification, deep learning has been extensively employed to resolve difficulties of different types such as face identification,[163,164] speech identification,[165,166] traffic signs,[167] observation and recognition of pedestrians,[14] and the detection of several objects.[168] RBM and SAEs have been used in the biomedical field to solve problems with abnormality identification and categorization in electrocardiogram (ECG),[169,170] electro-ocular-gram (EOG),[171,172] electroencephalogram (EEG),[173] and electromyogram (EMG).[174] A convolutional neural network (CNN), a technique based on deep learning, is commonly used for image classification, and is a special case of a neural network.[175] In our brain, neurons are arranged into layers and connected to other layers of neurons. The manner in which these neurons are linked depends on the structure of each layer, and there is a specific function for each layer, such as a convolutional layer, a pooling layer, or a flattening layer. In the same way, a CNN is assembled and functions. A CNN-based model for activity detection is shown in Figure 29b.[162] For image handling, it is normal to use several convolutional layers. The first layer in an image processing network, known as the input layer, gets the pixel values from an image as an input, and the last layer (the output layer), which delivers the result for the required task, for example, if the task is to categorize an image into one of ten different classes, the output layer contains a vector of length 10 with the probability of the image being classified into each class. The layers between the input and the output layers are termed as hidden layers, and a CNN consisting of hidden layers is called a Deep CNN.[176]

Convolutional neural networks collect input images, which are convoluted using kernels or filters to obtain characteristics. To convolve a $N \times N$ image, a $f \times f$ filter is used, and this process of image convolution acquires the exact features of the whole image.[177] The window moves subsequently after every process, and the characters are acquired by means of feature maps. These maps take the localized receptive field of the image and run it by the allocated weights and biases.[178−183] Basically, CNN defines a function from an input (images to an output) and probability for a certain number of classes, and the attributes of this function can be trained using a large collection of identified images known as the ImageNet data set.

Alex Krizhevsky presented the construction of a CNN for image classification,[180] and his work known as AlexNet is widely regarded as a major breakthrough for CNN, with the large-scale visual recognition challenge (ILSVRC) in ImageNet being one of the reasons.[184] After AlexNet, many more architectures were proposed for image classification, including ZFNet[177] and VGG16.[185] These types of networks have been used as an essential elements in architectures designed for object detection. Recently, at TU Wien Vienna,[186] an ultrafast image sensor with an integrated neural network that can be used to identify specific items was built. Scientists working at TU Wien consequently carried out a special process by working with a specific 2D material and constructing an image sensor that could be used to identify individual items. This chip serves as an artificial neural network with a training capability. The information does not require it to be displayed and evaluated at a computer. However, the chip delivers data by itself regarding whatever it is by quickly detecting it within nanoseconds. A neuron network is digitally modeled, and the intensity of one network node changes another, and so on, until the network displays the required behavior. In general, image information is read pixel by pixel and then evaluated by the computer. The neural network is directly integrated through its AI into the hardware of such an image sensor, which results in much faster object identification.[186] The chip is manufactured and developed at TU Wien. It is constructed on photodetectors formed with tungsten diselenide, a very fine material comprising just three layers of atoms. The separate photodetector, the pixel in the camera system, connects to a limited number of output components that can support the outcome of item identification. Furthermore, the signal collected by a specific detector alters the output signal, which can be accomplished simply by adjusting the local electric field in the direction of the photodetector. With the

https://doi.org/10.1021/acsmaterialslett.2c01011
ACS Materials Lett. 2023, 5, 1027−1060

support of a computer program, this variation is accomplished externally. Sensors can be used to record various letters and, step by step, change the sensitivity of the individual pixels until a specific letter leads precisely to a matching output signal. This is exactly the way a neural network within the chip is designed by creating certain powerful or weaker links in the network. After this learning procedure is finished, the computer is no longer required and the neural network is able to function itself. In the event that a specific signal is put forward to the sensor, it produces the skilled output signal in a period of 50 ns. In general, the chip can also be prepared to distinguish apples from bananas. This chip has many uses in scientific experiments or for more specific purposes. This technology could be conveniently employed when a very high speed is essential. For example, it can be used for particle detection and other research fields where short events are probed.[126,187]

5. PERSPECTIVE AND CHALLENGES

Image sensing devices are used in a variety of scientific and commercial applications. However, they face some major challenges that need to be addressed to improve the device efficiency. This technology has become a reflection of the changes that occurred during the Cambrian era in our daily lives due to the ability of mobile devices to quickly process, copy, and save several images and huge amounts of imaging data without affecting the performance of memories that act like the brain. The size of image sensing technology continued to advance due to the advent of new image sensors, with more than 100 million pixels reported in 2019. The growth of the black box camera market is in the process of development for automobiles, in addition to the current mobile applications. Additionally, the COVID-19 epidemic, which heralded in the "contact-free" era, has expedited diversification and given a boost to the electronic device industry. Though the pandemic will eventually come to an end, the tendency will persist. As new technologies are introduced, image sensors with exceptional qualities in terms of good resolution, increased sensitivity, high efficiency, low noise, and vibrant colors are constantly being launched. New sorts of structures with improved sensitivity and specificity are being used. Tremendous research has been conducted to produce high-performance image sensing. The development of nanostructured materials for image sensing has increased the sensitivity, responsiveness, and detectivity of image sensors. The continuous development of 0D, 1D, 2D, and 3D materials greatly improved the image sensors' physicochemical properties and associated characteristics. However, the selectivity and reliability of nanostructured-based image sensors need attention, and they can be further improved by the use of functionalities and fabrication processes. Numerous methods for the fabrication of nanostructured materials have been developed recently. In vivo imaging sensors that can be permanently injected into living systems to perform in vivo analyses are a major domain that is still in its early stages of development. These nanosensors may be able to sense, transmit, and capture in vivo data and transfer it into external systems, resulting in real-time image sensing of drug response, toxicity, and environmental effects.

the COVID-19 epidemic, which heralded in the "contact-free" era, has expedited diversification and given a boost to the electronic device industry

Presently, curved image sensors face a lack of fabrication techniques for highly curved devices with high resolution. Many printing technologies have been introduced that require printing on a planar surface and then folding or molding it to the curved shape of the device. Furthermore, the conversion of 2D devices to 3D has been proposed, but these strategies offer low pixel density and large pixel dimensions, which are limited by the device's folding and stretching. The field of view and volume of the imaging system are also a great challenge for high-quality curved imaging devices, which require a high lens curvature and ultimately result in a total increase in volume. In the case of CCD, the major drawback is the shrinking of pixels, which must be addressed for efficient scientific and industrial imaging applications with a large dynamic range. Hence, a very large area of CCDs is required, which will continue to grow. Miniaturized portable devices with easy manipulation software and cost-effective instrumentation methodologies are one of the other challenges for next-generation CCD devices. Therefore, the ideal technologies are needed to demonstrate some comparable performance to that of the existing commercially available devices.

In the case of QD image sensors, they bring about many advances in thermal infrared image sensing. However, there are many significant challenges in application such as the toxicity of QDs. QDs are active in the infrared region and also contain toxic heavy metals, such as lead, cadmium, and mercury, which have a direct impact on the environment and health. Therefore, the aim of future research is to achieve QDs, or low-dimensional, nontoxic, heavy metal-free QDs, such as graphene QDs, carbon nanotubes, and carbon QDs. Consequently, these materials have low absorption, a short cycle life, and rapid performance degradation.[188] Despite considerable research efforts, reducing noise for real-time operation and improving the integration between QDs and the circuit ROIC wafer are the challenges that still need further research to bring QD-IRISDs out of the laboratory for commercialization.

It is also important to consider the negative aspects of in vivo image sensors, where the main issue is the long-term adverse effects of nanostructured materials remaining in the body. The toxicity is influenced by the nanomaterial's chemical (particle charge), physical (particle size), and biocompatibility (material) features. The goal is to create biocompatible particles that cause cytotoxicity only at extremely high doses. It is therefore critical that the toxic effects of nanostructured materials be minimized by using appropriate materials for their synthesis. With the advent of new classes of intelligent nanostructured materials with distinctive and controllable features, it is anticipated that more and more effective and focused nanoimage sensors will appear. It could be possible to design sensors that can detect extremely low analyte concentrations for minimally invasive studies for a broad range of applications. Additionally, it is predicted that the price of individual sensors will drop dramatically and, in the end, consumers will find them easier to use. In the future, innovation in image sensors may improve vision, infrared imaging, and optoelectronics, and these advancements in image sensing technology will considerably improve people's daily lives and certainly have a positive impact on a number of

https://doi.org/10.1021/acsmaterialslett.2c01011
ACS Materials Lett. 2023, 5, 1027−1060

industries, including manufacturing, healthcare, clinical procedures, nature conservation, the military, homeland protection, the network, and communications. Moreover, scientists are working on innovative fabrication strategies to tune the intrinsic properties of active materials at the nanoscale regime, which are supposed to eliminate the defect density and allow the maximum efficiency of the device with fast responsiveness. The miniaturization of sensors to maintain their sensitivity and selectivity is also a major challenge that can be addressed by employing environmentally friendly, inexpensive, and sustainable substrates with high adaptation ability that allow for large-scale production with easy printing ability. Moreover, the stability of the image sensors for long-term use in system monitoring at the nanoscale needs to be addressed. The research is still going on to incorporate innovative concepts and designs for the development of nanostructured image sensors that can be practically implemented to improve image sensing, which will allow the next generation of sensing devices to be a part of the Internet of things revolution with high satisfaction and comfort.

scientists are working on innovative fabrication strategies to tune the intrinsic properties of active materials at the nanoscale regime, which are supposed to eliminate the defect density and allow the maximum efficiency of the device with fast responsiveness

AUTHOR INFORMATION

Corresponding Authors

Muhammad Aamir Iqbal − *School of Materials Science and Engineering, Zhejiang University, Hangzhou 310027, China;* orcid.org/0000-0002-5031-5305; Email: aamir.hum@gmail.com

Vinoth Kumar Ponnusamy − *Department of Medicinal and Applied Chemistry and Research Center for Precision Environmental Medicine, Kaohsiung Medical University (KMU), Kaohsiung City 807, Taiwan; Department of Medical Research, Kaohsiung Medical University Hospital (KMUH), Kaohsiung City 807, Taiwan; Department of Chemistry, National Sun Yat-sen University, Kaohsiung 804, Taiwan*; Email: kumar@kmu.edu.tw

Phuong V. Pham − *Department of Physics, College of Science, National Sun Yat-Sen University, Kaohsiung 80424, Taiwan;* orcid.org/0000-0001-7951-1329; Email: phuongpham@mail.nsysu.edu.tw

Authors

Maria Malik − *Centre of Excellence in Solid State Physics, University of the Punjab, Lahore 54590, Pakistan*

Top Khac Le − *Faculty of Materials Science and Technology, University of Science, Ho Chi Minh City 700000, Vietnam; Vietnam National University, Ho Chi Minh City 700000, Vietnam*

Nadia Anwar − *School of Materials Science and Engineering, Tsinghua University, Beijing 100084, China; Department of Physics, The University of Lahore, Lahore 54000, Pakistan*

Sunila Bakhsh − *Department of Physics, Balochistan University of Information Technology, Engineering and Management Sciences, Quetta 08770, Pakistan*

Wajeehah Shahid − *Department of Physics, The University of Lahore, Lahore 54000, Pakistan*

Samiah Shahid − *Institute of Molecular Biology and Biotechnology, The University of Lahore, Lahore 54000, Pakistan*

Shaheen Irfan − *Department of Physics, The University of Lahore, Lahore 54000, Pakistan*

Mohammed Al-Bahrani − *Chemical Engineering and Petroleum Industries Department, Al-Mustaqbal University College, Babylon 51001, Iraq*

Kareem Morsy − *Biology Department, College of Science, King Khalid University, Abha 61421, Saudi Arabia*

Huy-Binh Do − *Faculty of Applied Science, Ho Chi Minh City University of Technology and Education, Thu Duc City 700000, Vietnam*

Complete contact information is available at: https://pubs.acs.org/10.1021/acsmaterialslett.2c01011

Author Contributions

[θ]Muhammad Aamir Iqbal, Maria Malik, and Top Khac Le share first authorship with equal contributions. [ϕ] Sunila Bakhsh, Wajeehah Shahid, Samiah Shahid, and Shaheen Irfan have equal contributions and share third authorship.CRediT: **Muhammad Aamir Iqbal** conceptualization, methodology, project administration, resources, writing-original draft, writing-review & editing; **Maria Malik** writing-original draft, writing-review & editing; **Top Khac Le** writing-original draft, writing-review & editing; **Nadia Anwar** writing-original draft, writing-review & editing; **Wajeehah Shahid** writing-original draft; **Sunila Bakhsh** editing, proofreading; **Samiah Shahid** writing-original draft; **Shaheen Irfan** writing-original draft; **Mohammed Al-Bahrani** proofreading, resources; **Kareem Morsy** proofreading, funding; **Huy-Binh Do** review & editing; **Vinoth Kumar Ponnusamy** funding acquisition, project administration, review; **Phuong V. Pham** conceptualization, funding acquisition, methodology, project administration, resources, writing-original draft, writing-review & editing.

Notes

The authors declare no competing financial interest.

Biographies

Muhammad Aamir Iqbal is a senior postgraduate researcher at School of Materials Science and Engineering, Zhejiang University, China. His research interests include optoelectronics, nanophotonics, optical glasses, plasmonics, materials modeling, density functional theory, photocatalysis, and green synthesis.

Maria Malik is a Lecturer of Physics at the University of Education, Lahore, Pakistan. She has completed her M.S. degree in Nanotechnology from the University of the Punjab, Lahore Pakistan, with distinction. Her research interests include materials engineering, nanomaterials synthesis, and optoelectronic device applications of nanomaterials.

Top Khac Le is currently a lecturer of Faculty of Materials Science and Technology, University of Science, Vietnam National University HCM City (US − VNUHCM). He earned his Ph.D. degree in Physics from the University of Ulsan, South Korea. He then spent three years as a Postdoctoral Researcher in Energy Harvest Storage Research Center (EHSRC, Department of Physics, University of Ulsan). His research interests include micronano materials synthesis

https://doi.org/10.1021/acsmaterialslett.2c01011
ACS Materials Lett. 2023, 5, 1027−1060

techniques, physical properties of vanadium oxides, and other metal oxide semiconductor materials. He also has interests in micronano applications in energy, photocatalysis, solar cells, chromogenic materials, optoelectronics, and thermoelectrics.

Nadia Anwar is a doctoral researcher at the School of Materials Science and Engineering, Tsinghua University, Beijing, China. She has also worked as a lecturer in physics at the University of Lahore, Pakistan. She has expertise in thin film fabrication and nanoparticles synthesis via PVD techniques and chemical methods. She did simulation and modelling of single layer, bilayer, and multilayer and fabricated thin films according to optoelectronic applications for solar cells and optical filters, nanoelectronics, and electrochemical sensing.

Sunila Bakhsh is working as an assistant professor in the Department of Physics at the Balochistan University of Information Technology, Engineering, and Management Science in Quetta. Her current research field is condensed matter physics and computational physics. She also has research interests in prediction algorithms, computations, and their applications in multidisciplinary areas.

Wajeehah Shahid has been associated with teaching for the last ten years. She is working as an Assistant Professor (Physics) at the University of Lahore in Lahore, Pakistan, after obtaining her Ph.D. in 2022. She has published more than 20 articles. She is working mainly on materials science, including photocatalytic applications and biomedical applications, as well as theoretical applications in various fields of physics.

Samiah Shahid is working as an Assistant Professor at the Institute of Molecular Biology and Biotechnology at the University of Lahore, Lahore, Pakistan. She obtained her Ph.D. from the University of the Punjab, Lahore, Pakistan. She is actively participating in research and has more than 15 research publications, with research focusing on cancer diagnosis and treatment.

Shaheen Irfan is an Assistant Professor at Department of Physics, The University of Lahore and her research interests include Biosynthesis, Theoretical Physics, and High Energy Physics. Her Ph.D. research is affiliated with Texas Tech University, Lubbock, Texas, USA.

Mohammed Al-Bahrani earned an M.Sc. in mechanical engineering before earning a Ph.D. in self-sensing nanocomposite materials from Plymouth University in 2019. Before getting his Ph.D., he worked as a senior engineer in the oil and gas field, in particular at an oil refinery company. Presently, he serves in the same oil company and, in addition to that, works as a researcher in the energy and research unit at Al-Mustaqbal University. His professional interests focus on research in the fields of energy, self-sensing nanocomposites, smart multifunctional materials, self-heating materials, and nanotechnology. He has over 45 research articles published in high-impact journals with a good reputation, and he has presented his work at numerous conferences.

Kareem Morsy is an experienced researcher and has published many quality research articles. He is currently working at Biology Department, Faculty of Science, King Khalid University, Saudi Arabia.

Huy-Binh Do is currently a lecturer with HCMC University of Technology and Education. He received the Ph.D. degree from National Chiao Tung University, Hsinchu, Taiwan in 2017 and worked as a postdoctoral research fellow there for a year. He was a Research Associate at Sheffield University (the UK) from 2018−2019. His research interests are in RF and power devices including InGaAs, GaN, and Ga_2O_3 MOSFETs. He also has an interest in 2D materials. His current work includes a new class of RF and power devices as well as a new approach to fabricate 2D materials.

Vinoth Kumar Ponnusamy is currently working as an Associate Professor in the Department of Medicinal and Applied Chemistry, Kaohsiung Medical University (KMU), Taiwan, and has been leading the Nano and Green Analytical Technology laboratory since 2016. His researches are mainly focused on novel nanomaterials, sample preparations, green analytical methodologies, chromatographic and mass spectrometric analysis, and analytical method developments and application towards clinical, food, drugs, and environmental analysis. In 2017, Prof. Kumar also joined into the Research Center of Precision Environmental Medicine, KMU, as a core research faculty to lead the research in the area of human biomonitoring projects, especially on monitoring/analysis of drugs, biomarkers, and biometabolites. So far, he has published (authored and coauthored) more than 140 SCI publications (H-index of 32), two book chapters, 150 international and national conference presentations, and 40 invited keynote speaker lectures at various international conferences. Currently, he is also acting as an Associate Editor in *Frontiers in Chemistry* (Analytical Chemistry Section) journal and editorial board member in several other journals.

Phuong V. Pham is an Assistant Professor at College of Science, National Sun Yat-Sen University (NSYSU), Taiwan. He is pioneering scientist in materials science and electronics/optoelectronics. He has been a former senior scientist at the Hangzhou Global Scientific and Technological Innovation Center (HIC), Zhejiang University, China. He earned a Ph.D. degree in SKKU Advanced Institute of Nanotechnology (SAINT), Sungkyunkwan University (SKKU), South Korea. Then he spent a few years as a Postdoctoral Researcher and Research Fellow at the School of Advanced Materials Science and Engineering, SKKU, and at Center for Multidimensional Carbon Materials (CMCM) (Director: Prof. Rodney Ruoff), Institute for Basic Science (IBS), South Korea, respectively. He is a recipient of NSF Career Award and National Postdoctoral Award for the Excellent Young Scientists, China. His research interest focuses on low-dimensional materials, 2D material synthesis, twistronics, strain-tronics, 2D heterostructures, doping technique development, nanocomposites, block copolymer, plasma engineering for flexible displays, sensors, photodetectors, transistors, OLED, and wearable electronics.

■ ACKNOWLEDGMENTS

The authors acknowledge the support provided by Prof. Xiaofeng Liu, and Zhejiang University, China, while extending their appreciation to the Deanship of Scientific Research at King Khalid University for supporting this work through large groups (project under grant number R.G.P.2/1/44). This research was also funded by Ministry of Science and Technology, Taiwan, grant number-"MOST110-2113-M-037-009" and by the Research Center for Precision Environmental Medicine, Kaohsiung Medical University, Kaohsiung, Taiwan from "The Featured Areas Research Center Program within the framework of the Higher Education Sprout Project" by the Ministry of Education (MOE) in Taiwan.

■ REFERENCES

(1) Lee, G. J.; Choi, C.; Kim, D. H.; Song, Y. M. Bioinspired artificial eyes: optic components, digital cameras, and visual prostheses. *Adv. Funct. Mater.* **2018**, *28*, 1705202.

(2) Imbrogno, A. *Pulsed laser deposition based nanodecoration of carbon-based nanomaterials, their characterizations, and integration into third generation photovoltaic devices*. Doctoral dissertation, Université du Québec, Institut national de la recherche scientifique, 2018.

(3) Bouvier, M. *Study and design of an energy efficient perception module combining event-based image sensors and spiking neural network*

https://doi.org/10.1021/acsmaterialslett.2c01011
ACS Materials Lett. 2023, 5, 1027−1060

with 3D integration technologies. Doctoral dissertation, Université Grenoble Alpes, 2021.
(4) Behera, A.; Aich, S.; Theivasanthi, T. Magnetron sputtering for development of nanostructured materials. In Design, Fabrication, and Characterization of Multifunctional Nanomaterials. *Elsevier sci.* **2022**, 177−199.
(5) Gubala, V.; Johnston, L. J.; Liu, Z.; Krug, H.; Moore, C. J.; Ober, C. K.; Vert, M. Engineered nanomaterials and human health: Part 1. Preparation, functionalization and characterization (IUPAC Technical Report). *Pure Appl. Chem.* **2018**, *90*, 1283−1324.
(6) Cahyadi, W. A.; Chung, Y. H.; Ghassemlooy, Z.; Hassan, N. B. Optical camera communications: Principles, modulations, potential and challenges. *Electronics* **2020**, *9*, 1339.
(7) Theuwissen, A. J. CMOS image sensors: State-of-the-art. *Solid-State Electron.* **2008**, *52*, 1401−1406.
(8) Ding, M.; Guo, Z.; Chen, X.; Ma, X.; Zhou, L. Surface/Interface engineering for constructing advanced nanostructured photodetectors with improved performance: A brief review. *Nanomaterials* **2020**, *10*, 362.
(9) Ghosh, S.; Porwal, S.; Singh, T. Investigation of the role of back contact work function for hole transporting layer free perovskite solar cells applications. *Optik* **2022**, *256*, 168749.
(10) Liu, X.; Zheng, J.; Niu, C.; Liu, T.; Huang, Q.; Li, M.; Cheng, B.; et al. Sn content gradient GeSn with strain controlled for high performance GeSn mid-infrared photodetectors. *Photonics Research* **2022**, *10*, 1567−1574.
(11) Fontaine, R. The state-of-the-art of mainstream CMOS image sensors. In *Proceedings of the International Image Sensors Workshop*; IISW, 2015; pp 6−12.
(12) Li, L.; Ye, S.; Qu, J.; Zhou, F.; Song, J.; Shen, G. Recent advances in perovskite photodetectors for image sensing. *Small* **2021**, *17*, 2005606.
(13) Chai, Y. In-sensor computing for machine vision. *News and Views, Nature* **2020**, *579*, 32−33.
(14) Ganasala, P.; Prasad, A. D. Contrast enhanced multi sensor image fusion based on guided image filter and NSST. *IEEE Sens. J.* **2020**, *20*, 939−946.
(15) Kastek, M.; Piatkowski, T.; Zyczkowski, M.; Chamberland, M.; Lagueux, P.; Farley, V. Hyperspectral imaging infrared sensor used for enviromental monitoring. *Acta Phys. Polym., A* **2013**, *124*, 463−467.
(16) Fang, Q.; Mahmoud, S. S.; Gu, X.; Fu, J. A novel multistandard compliant hand function assessment method using an infrared imaging device. *IEEE J. Biomed Health Inform.* **2019**, *23*, 758−765.
(17) Seitz, P. Solid-State Image Sensing. In Computer Vision and Applications. *Elsevier sci.* **2000**, 111−151.
(18) Gove, R. J. CMOS image sensor technology advances for mobile devices. In High Performance Silicon Imaging. *Elsevier sci.* **2020**, 185−240.
(19) Yan, M.; Huang, X.; Yu, H. *CMOS Integrated Lab-on-a-Chip System for Personalized Biomedical Diagnosis*; John Wiley & Sons, 2018; pp 142−168.
(20) Swain, P.; Mark, D. Curved CCD detector devices and arrays for multispectral astrophysical applications and terrestrial stereo panoramic cameras. In *Optical and Infrared Detectors for Astronomy*; SPIE, 2004; Vol. *5499*, pp 281−301.
(21) Fossum, E. R. CMOS image sensors: Electronic camera-on-a-chip. *IEEE Trans. Electron Devices* **1997**, *44*, 1689−1698.
(22) Catrysse, P. B.; Wandell, B. A. Roadmap for CMOS image sensors: Moore meets Planck and Sommerfeld. In Digital Photography. *SPIE* **2005**, *5678*, 1−13.
(23) Anzagira, L.; Fossum, E. R. Color filter array patterns for small-pixel image sensors with substantial cross talk. *J. Opt Soc. Am. A* **2015**, *32*, 28−34.
(24) Sasagawa, K.; Yamaguchi, T.; Haruta, M.; Sunaga, Y.; Takehara, H.; Takehara, H.; Ohta, J.; et al. An implantable CMOS image sensor with self-reset pixels for functional brain imaging. *IEEE Trans. Electron Devices* **2016**, *63*, 215−222.
(25) Jourdon, J.; Lhostis, S.; Moreau, S.; Chossat, J.; Arnoux, M.; Sart, C.; Henrion, Y.; Lamontagne, P.; Arnaud, L.; Bresson, N. Hybrid bonding for 3D stacked image sensors: impact of pitch shrinkage on interconnect robustness. *IEEE International Electron Devices Meeting (IEDM)* **2018**, 731−734.
(26) Imura, S.; Mineo, K.; Honda, Y.; Arai, T.; Miyakawa, K.; Watabe, T.; Kubota, M.; Nishimoto, K.; Sugiyama, M.; Nanba, M. J. S. R. Enhanced image sensing with avalanche multiplication in hybrid structure of crystalline selenium photoconversion layer and CMOSFETs. *Sci. Rep.* **2020**, *10*, 1−9.
(27) Lou, Z.; Shen, G. J. S. S. Flexible image sensors with semiconducting nanowires for biomimic visual applications. *Small Struct.* **2021**, *2*, 2000152.
(28) Wu, W.; Wang, X.; Han, X.; Yang, Z.; Gao, G.; Zhang, Y.; Hu, J.; Tan, Y.; Pan, A.; Pan, C. Flexible photodetector arrays based on patterned $CH_3NH_3PbI_{3-x}Cl_x$ perovskite film for real-time photosensing and imaging. *Adv. Mater.* **2019**, *31*, 1805913.
(29) Yashiro, W.; Shirasawa, T.; Kamezawa, C.; Voegeli, W.; Arakawa, E.; Kajiwara, K. A Multi-Beam X-Ray Imaging Detector Using a Branched Optical Fiber Bundle. *Jpn. J. Appl. Phys.* **2020**, *59*, 38003.
(30) Wang, H.; Sun, Y.; Chen, J.; Wang, F.; Han, R.; Zhang, C.; Kong, J.; Li, L.; Yang, J. A Review of Perovskite-Based Photodetectors and Their Applications. *Nanomaterials* **2022**, *12*, 4390.
(31) Chen, H.; Liu, H.; Zhang, Z.; Hu, K.; Fang, X. Nanostructured photodetectors: from ultraviolet to terahertz. *Adv. Mater.* **2016**, *28*, 403−433.
(32) Zhao, Y.; Zhu, K. J. Organic−inorganic hybrid lead halide perovskites for optoelectronic and electronic applications. *Chem. Soc. Rev.* **2016**, *45*, 655−689.
(33) Noah, N. M. Design and synthesis of nanostructured materials for sensor applications. *J. Nanomater.* **2020**, *2020*, 1−20.
(34) Lobnik, A.; Turel, M.; Urek, Š. K.; Košak, A. Nanostructured materials use in sensors: their benefits and drawbacks. In *Carbon and Oxide Nanostructures*; Springer, 2010; pp 307−354.
(35) Rehman, A. U.; Wu, Y.; Tran, H. D.; Vazquez-Prada, K.; Liu, Y.; Adelnia, H.; Ta, H. T.; et al. Silver/iron oxide nano-popcorns for imaging and therapy. *ACS Appl. Nano Mater.* **2021**, *4*, 10136−10147.
(36) Pham, P. V.; Bodepudi, S. C.; Shehzad, K.; Liu, Y.; Xu, Y.; Yu, B.; Duan, X. 2D heterostructures for ubiquitous electronics and optoelectronics: Principles, opportunities, and challenges. *Chem. Soc. Rev.* **2022**, *122*, 6514−6613.
(37) Farooq, U.; Min-Dianey, K. A.; Rajagopalan, P.; Malik, M.; Kongnine, D. M.; Choi, J. R.; Pham, P. V. Photodetection Tuning with High Absorptivity Using Stacked 2D Heterostructure Films. *Nanomaterials* **2022**, *12*, 712.
(38) Min-Dianey, K. A.; Le, T. K.; Qadir, A.; M'Bouana, N. L. P.; Malik, M.; Kim, S. W.; Choi, J. R.; Pham, P. V. The ripple effect of graphite nanofilm on stretchable polydimethylsiloxane for optical sensing. *Nanomaterials* **2021**, *11*, 2934.
(39) Min-Dianey, K. A. A.; Le, T. K.; Choi, J. R.; Pham, P. V. Advanced optical detection through the use of a deformably transferred nanofilm. *Nanomaterials* **2021**, *11*, 816.
(40) Hoeser, T.; Kuenzer, C. Object detection and image segmentation with deep learning on earth observation data: A review-part i: Evolution and recent trends. *Remote Sensing* **2020**, *12*, 1667.
(41) Wang, J.; Xiao, X.; Javidi, B. Three-dimensional integral imaging with flexible sensing. *Opt. Lett.* **2014**, *39*, 6855−6858.
(42) Berzinš, J.; Fasold, S.; Pertsch, T.; Bäumer, S. M.; Setzpfandt, F. Submicrometer nanostructure-based RGB filters for CMOS image sensors. *ACS Photonics* **2019**, *6*, 1018−1025.
(43) Xu, T.; Shi, H.; Wu, Y. K.; Kaplan, A. F.; Ok, J. G.; Guo, L. J. J. S. Structural colors: from plasmonic to carbon nanostructures. *Small* **2011**, *7*, 3128−3136.
(44) Graydon, O. A colourful future? *Nat. Photon* **2015**, *9*, 487−488.
(45) Kumar, K.; Duan, H.; Hegde, R. S.; Koh, S. C.; Wei, J. N.; Yang, J. K. Printing colour at the optical diffraction limit. *Nat. Nanotechnol.* **2012**, *7*, 557−561.

https://doi.org/10.1021/acsmaterialslett.2c01011
ACS Materials Lett. 2023, 5, 1027−1060

(46) Ni, X.; Emani, N. K.; Kildishev, A. V.; Boltasseva, A.; Shalaev, V. M. Broadband Light Bending with Plasmonic Nanoantennas. *Science* **2012**, *335*, 427.
(47) Li, L.; Li, T.; Tang, X.-M.; Wang, S.-M.; Wang, Q.-J.; Zhu, S.-N. Plasmonic polarization generator in well-routed beaming. *Light Sci. Appl.* **2015**, *4*, e330−e330.
(48) Zheng, G.; Mühlenbernd, H.; Kenney, M.; Li, G.; Zentgraf, T.; Zhang, S. Metasurface holograms reaching 80% efficiency. *Nat. Nanotechnol.* **2015**, *10*, 308−312.
(49) Chen, Q.; Hu, X.; Wen, L.; Yu, Y.; Cumming, D. Nanophotonic image sensors. *Small* **2016**, *12*, 4922−4935.
(50) Dave, S. R.; Gao, X. Monodisperse magnetic nanoparticles for biodetection, imaging, and drug delivery: a versatile and evolving technology. *Wiley Interdiscip. Rev. Nanomed.* **2009**, *1*, 583−609.
(51) Li, L.; Lou, Z.; Shen, G. Flexible broadband image sensors with SnS quantum dots/Zn_2SnO_4 nanowires hybrid nanostructures. *Adv. Funct. Mater.* **2018**, *28*, 1705389.
(52) Murari, K.; Etienne-Cummings, R.; Thakor, N.; Cauwenberghs, G. Which photodiode to use: A comparison of CMOS-compatible structures. *IEEE Sens. J.* **2009**, *9*, 752−760.
(53) Matalon, A. *Searching for Light Dark Matter with DAMIC at SNOLAB and DAMIC-M: Investigations into Radioactive Backgrounds and Silicon Charge-Coupled Devices*. Doctoral dissertation, Sorbonne Université; University of Chicago, 2021.
(54) Ng, D. C.; Tokuda, T.; Shiosaka, S.; Tano, Y.; Ohta, J. Implantable microimagers. *Sensors* **2008**, *8*, 3183−3204.
(55) Kuroda, T. *Essential principles of image sensors*; CRC Press, 2017.
(56) Nakamura, J. *Image sensors and signal processing for digital still cameras*; CRC Press, 2017.
(57) Fossum, E. R.; Hondongwa, D. B. A review of the pinned photodiode for CCD and CMOS image sensors. *IEEE J. Electron Devices Soc.* **2014**, *2*, 33−43.
(58) Green, M. A.; Keevers, M. J. Optical Properties of Intrinsic Silicon at 300 K. *Prog. Photovolt.: Res. Appl.* **1995**, *3*, 189−192.
(59) Sheppard, C. J. R.; Castello, M.; Tortarolo, G.; Vicidomini, G.; Diaspro, A. Image Formation in Image Scanning Microscopy, Including the Case of Two-Photon Excitation. *J. Opt. Soc. Am. A* **2017**, *34*, 1339−1350.
(60) Green, M. A. Self-consistent optical parameters of intrinsic silicon at 300 K including temperature coefficients. *Sol. Energy Mater. Sol. Cells* **2008**, *92*, 1305−1310.
(61) Kosonocky, W.; Carnes, J. Two-phase charge-coupled devices with overlapping polysilicon and aluminum gates. *RCA Review* **1973**, *34*, 164−202.
(62) Stevanovic, N.; Hillebrand, M.; Hosticka, B. J.; Teuner, A. A CMOS image sensor for high-speed imaging. *Digest of Technical Papers, IEEE International Solid-State Circuits Conference*; IEEE, 2000; pp 104−105.
(63) Norton, P. R. Infrared Image Sensors. *Opt. Eng.* **1991**, *30*, 1649−1663.
(64) Ackerman, M. M. Bringing colloidal quantum dots to detector technologies. *Information Display* **2020**, *36*, 19−23.
(65) Havens, K. J.; Sharp, E. *Thermal imaging techniques to survey and monitor animals in the wild: A methodology*; Academic Press, 2015; pp 121−141.
(66) Lu, H.; Carroll, G. M.; Neale, N. R.; Beard, M. C. Infrared quantum dots: Progress, challenges, and opportunities. *ACS Nano* **2019**, *13*, 939−953.
(67) Hafiz, S. B.; Scimeca, M.; Sahu, A.; Ko, D.-K. Colloidal quantum dots for thermal infrared sensing and imaging. *Nano Convergence* **2019**, *6*, 1−22.
(68) Malinowski, P. E.; Georgitzikis, E.; Maes, J.; Vamvaka, I.; Frazzica, F.; Van Olmen, J.; De Moor, P.; Heremans, P.; Hens, Z.; Cheyns, D. Thin-Film Quantum Dot Photodiode for Monolithic Infrared Image Sensors. *Sensors* **2017**, *17*, 2867.
(69) Keuleyan, S.; Lhuillier, E.; Brajuskovic, V.; Guyot-Sionnest, P. Mid-infrared HgTe colloidal quantum dot photodetectors. *Nat. Photon* **2011**, *5*, 489−493.
(70) Gupta, M. C.; Harrison, J. T.; Islam, M. T. Photoconductive PbSe thin films for infrared imaging. *Mater. Adv.* **2021**, *2*, 3133−3160.
(71) Yin, X.; Zhang, C.; Guo, Y.; Yang, Y.; Xing, Y.; Que, W. PbS QD-based photodetectors: future-oriented near-infrared detection technology. *J. Mater. Chem. C* **2021**, *9*, 417−438.
(72) Qiu, J.; Weng, B.; McDowell, L. L.; Shi, Z. Low-cost uncooled MWIR PbSe quantum dots photodiodes. *RSC Adv.* **2019**, *9*, 42516−42523.
(73) Dong, C.; Liu, S.; Barange, N.; Lee, J.; Pardue, T.; Yi, X.; Yin, S.; So, F. Long-wavelength lead sulfide quantum dots sensing up to 2600 nm for short-wavelength infrared photodetectors. *ACS Appl. Mater. Interfaces* **2019**, *11*, 44451−44457.
(74) Tang, X.; Ackerman, M. M.; Chen, M.; Guyot-Sionnest, P. Dual-band infrared imaging using stacked colloidal quantum dot photodiodes. *Nat. Photonics* **2019**, *13*, 277−282.
(75) Ackerman, M. M.; Tang, X.; Guyot-Sionnest, P. Fast and sensitive colloidal quantum dot mid-wave infrared photodetectors. *ACS Nano* **2018**, *12*, 7264−7271.
(76) Livache, C.; Martinez, B.; Goubet, N.; Gréboval, C.; Qu, J.; Chu, A.; Royer, S.; Ithurria, S.; Silly, M. G.; Dubertret, B.; et al. A Colloidal Quantum Dot Infrared Photodetector and Its Use for Intraband Detection. *Nat. commun.* **2019**, *10*, 1−10.
(77) Qu, J.; Goubet, N.; Livache, C.; Martinez, B.; Amelot, D.; Gréboval, C.; Chu, A.; Ramade, J.; Cruguel, H.; Ithurria, S.; et al. Intraband Mid-Infrared Transitions in Ag_2Se Nanocrystals: Potential and Limitations for Hg-Free Low-Cost Photodetection. *J. Phys. Chem. C* **2018**, *122*, 18161−18167.
(78) Mir, W. J.; Swarnkar, A.; Sharma, R.; Katti, A.; Adarsh, K.; Nag, A. Origin of unusual excitonic absorption and emission from colloidal Ag_2S nanocrystals: ultrafast photophysics and solar cell. *J. Phys. Chem. Lett.* **2015**, *6*, 3915−3922.
(79) Ouyang, J.; Graddage, N.; Lu, J.; Zhong, Y.; Chu, T.-Y.; Zhang, Y.; Wu, X.; Kodra, O.; Li, Z.; Tao, Y.; et al. Ag_2Te Colloidal Quantum Dots for Near-Infrared-II Photodetectors. *ACS Appl. Nano Mater.* **2021**, *4*, 13587−13601.
(80) Kagan, C. R.; Lifshitz, E.; Sargent, E. H.; Talapin, D. V. J. S. Building devices from colloidal quantum dots. *Science* **2016**, *353*, aac5523.
(81) Tang, X.; Wu, G. f.; Lai, K. W. C. Plasmon resonance enhanced colloidal HgSe quantum dot filterless narrowband photodetectors for mid-wave infrared. *J. Mater. Chem. C* **2017**, *5*, 362−369.
(82) Chen, M.; Lan, X.; Tang, X.; Wang, Y.; Hudson, M. H.; Talapin, D. V.; Guyot-Sionnest, P. High carrier mobility in HgTe quantum dot solids improves mid-IR photodetectors. *ACS Photonics* **2019**, *6*, 2358−2365.
(83) Tang, X.; Ackerman, M. M.; Guyot-Sionnest, P. Thermal imaging with plasmon resonance enhanced HgTe colloidal quantum dot photovoltaic devices. *ACS Nano* **2018**, *12*, 7362−7370.
(84) Goubet, N.; Jagtap, A.; Livache, C.; Martinez, B.; Portalès, H.; Xu, X. Z.; Lobo, R. P.; Dubertret, B.; Lhuillier, E. Terahertz HgTe nanocrystals: beyond confinement. *J. Am. Chem. Soc.* **2018**, *140*, 5033−5036.
(85) Tang, X.; Ackerman, M. M.; Shen, G.; Guyot-Sionnest, P. Towards infrared electronic eyes: flexible colloidal quantum dot photovoltaic detectors enhanced by resonant cavity. *Small* **2019**, *15*, 1804920.
(86) Buurma, C.; Pimpinella, R. E.; Ciani, A. J.; Feldman, J. S.; Grein, C. H.; Guyot-Sionnest, P. MWIR imaging with low cost colloidal quantum dot films. In *Optical Sensing, Imaging, and Photon Counting: Nanostructured Devices and Applications*; SPIE, 2016; pp 9933, 993303.
(87) Liu, Z. Y.; Liu, A. A.; Fu, H.; Cheng, Q. Y.; Zhang, M. Y.; Pan, M. M.; Pang, D. W.; et al. Breaking through the size control dilemma of silver chalcogenide quantum dots via trialkylphosphine-induced ripening: leading to Ag_2Te emitting from 950 to 2100 nm. *J. Am. Chem. Soc.* **2021**, *143*, 12867−12877.
(88) Yuan, T.; Fu, J.; Lu, Y.; Hou, Y.; Huang, P.; Chen, D. An Effective Self-Test Method for Extracting Thermal Parameters of Thermopile IR Sensors. *Measurement* **2022**, *194*, 110967.

https://doi.org/10.1021/acsmaterialslett.2c01011
ACS Materials Lett. 2023, 5, 1027−1060

(89) Li, H.; Xu, G.; Zhang, C.; Mao, H.; Zhou, N.; Chen, D. A Sensitivity Controllable Thermopile Infrared Sensor by Monolithic Integration of a N-channel Metal Oxide Semiconductor. *ECS J. Solid State Sci. Technol.* **2021**, *10*, No. 097002.
(90) Zhan, Q.; Wang, W.; Ding, X. Examination of Potential of Thermopile-Based Contactless Respiratory Gating. *Sensors* **2021**, *21*, 5525.
(91) Ali, N. J.; Mustapha, N. A. C. Thermopile array sensor for children detection in automobile application. *Int. Conf. Comput. Commun. Eng.* **2021**, 223−227.
(92) Huang, P.; Fu, J.; Lu, Y.; Liu, J.; Zhang, J.; Chen, D. An on-chip test structure to measure the Seebeck coefficient of thermopile sensors. *J. Micromech. Microeng.* **2022**, *32*, No. 015004.
(93) Dai, Y.; Ali, S. Z.; Hopper, R.; Popa, D.; Udrea, F. Modeling of CMOS Single Membrane Thermopile Detector Arrays. *IEEE Sens. J.* **2022**, *22*, 1366−1373.
(94) Shi, M.; Dai, X.; Liu, Y.; Zhou, N.; Zhang, C.; Ni, Y.; Mao, H.; Chen, D. Infrared Thermopile Sensors with in-Situ Integration of Composite Nanoforests for Enhanced Optical Absorption. *Proc. IEEE Int. Conf. Micro Electro Mech. Syst.* **2021**, 282−285.
(95) Tantiwanichapan, K.; Durmaz, H. Herbicide/pesticide sensing with metamaterial absorber in THz regime. *Sens. Actuator A Phys.* **2021**, *331*, 112960.
(96) Uddin, J. Terahertz Spectroscopy: A Cutting Edge Technology. *IntechOpen* **2017**, DOI: 10.5772/62805.
(97) Wang, J.; Lindley-Hatcher, H.; Chen, X.; Pickwell-MacPherson, E. THz sensing of human skin: a review of skin modeling approaches. *Sensors* **2021**, *21*, 3624.
(98) Kundu, B. K. THz Image Processing and Its Applications. *Generation, Detection and Processing of Terahertz Signals*; Springer, 2022; pp 123−137.
(99) Blanchard, F.; Arikawa, T.; Tanaka, K. Real-time megapixel electro-optical imaging of THz beams with probe power normalization. *Sensors* **2022**, *22*, 4482.
(100) Akter, N.; Hasan, M. M.; Pala, N. A review of THz technologies for rapid sensing and detection of viruses including sars-cov-2. *Biosensors* **2021**, *11*, 349.
(101) Zatta, R.; Jagtap, V. S.; Grzyb, J.; Pfeiffer, U. R. CMOS THz camera used as compact antenna test range. *IEEE Third International Workshop on Mobile Terahertz Systems (IWMTS)* **2020**, 1−4.
(102) Rahman, M.; Mou, F. A.; Bhuiyan, M. I. H.; Islam, M. R. Refractometric THz sensing of blood components in a photonic crystal fiber platform. *Braz. J. Phys.* **2022**, *52*, 1−12.
(103) Yu, C.; Fan, S.; Sun, Y.; Pickwell-MacPherson, E. The Potential of Terahertz Imaging for Cancer Diagnosis: A Review of Investigations to Date. *Quant. Imaging Med. Surg.* **2012**, *2*, 33.
(104) Lai, C. W.; Chen, W. C.; Yan, T. C.; Li, C. H.; Kuo, C. N. The experimental study of THz image sensor in 0.18 μm CMOS technology. *IEEE Asia-Pacific Microwave Conference*; IEEE, 2014; pp 148−150.
(105) Reshidko, D.; Sasian, J. Optical analysis of miniature lenses with curved imaging surfaces. *Appl. Opt.* **2015**, *54*, E216−E223.
(106) Stamenov, I.; Agurok, I. P.; Ford, J. E. Optimization of two-glass monocentric lenses for compact panoramic imagers: general aberration analysis and specific designs. *Appl. Opt.* **2012**, *51*, 7648−7661.
(107) Gao, W.; Xu, Z.; Han, X.; Pan, C. Recent advances in curved image sensor arrays for bioinspired vision system. *Nano Today* **2022**, *42*, 101366.
(108) Zhou, K.; Zhao, Y.; Sun, X.; Yuan, Z.; Zheng, G.; Dai, K.; Mi, L.; Pan, C.; Liu, C.; Shen, C. Ultra-stretchable triboelectric nanogenerator as high-sensitive and self-powered electronic skins for energy harvesting and tactile sensing. *Nano Energy* **2020**, *70*, 104546.
(109) Zhou, K.; Xu, W.; Yu, Y.; Zhai, W.; Yuan, Z.; Dai, K.; Zheng, G.; Mi, L.; Pan, C.; Liu, C.; et al. Tunable and Nacre-Mimetic Multifunctional Electronic Skins for Highly Stretchable Contact-Noncontact Sensing. *Small* **2021**, *17*, 2100542.
(110) Sun, J.; Chang, Y.; Dong, L.; Zhang, K.; Hua, Q.; Zang, J.; Chen, Q.; Shang, Y.; Pan, C.; Shan, C. MXene Enhanced Self-Powered Alternating Current Electroluminescence Devices for Patterned Flexible Displays. *Nano Energy* **2021**, *86*, 106077.
(111) Zang, J.; Liu, F. Modified Timoshenko formula for bending of ultrathin strained bilayer films. *Appl. Phys. Lett.* **2008**, *92*, No. 021905.
(112) Thai, K. Y.; Park, I.; Kim, B. J.; Hoang, A. T.; Na, Y.; Park, C. U.; Chae, Y.; Ahn, J. H. MoS_2/Graphene photodetector array with strain-modulated photoresponse up to the near-infrared regime. *ACS Nano* **2021**, *15*, 12836−12846.
(113) Wu, W.; Han, X.; Li, J.; Wang, X.; Zhang, Y.; Huo, Z.; Chen, Q.; Sun, X.; Xu, Z.; Tan, Y.; et al. Ultrathin and conformable lead halide perovskite photodetector arrays for potential application in retina-like vision sensing. *Adv. Mater.* **2021**, *33*, 2006006.
(114) Jung, I.; Xiao, J.; Malyarchuk, V.; Lu, C.; Li, M.; Liu, Z.; Yoon, J.; Huang, Y.; Rogers, J. Dynamically tunable hemispherical electronic eye camera system with adjustable zoom capability. *Proc. Natl. Acad. Sci. U. S. A.* **2011**, *108*, 1788−1793.
(115) Chen, S.; Chen, J.; Zhang, X.; Li, Z.-Y.; Li, J. Kirigami/origami: unfolding the new regime of advanced 3D microfabrication/nanofabrication with "folding". *Light Sci. Appl.* **2020**, *9*, 1−19.
(116) Rogers, J.; Huang, Y.; Schmidt, O. G.; Gracias, D. H. Origami mems and nems. *MRS Bull.* **2016**, *41*, 123−129.
(117) Pandey, S.; Ewing, M.; Kunas, A.; Nguyen, N.; Gracias, D. H.; Menon, G. Algorithmic design of self-folding polyhedra. *Proc. Natl. Acad. Sci. U. S. A.* **2011**, *108*, 19885−19890.
(118) Chen, H.; Zhang, X. L.; Zhang, Y. Y.; Wang, D.; Bao, D. L.; Que, Y.; Gao, H. J.; et al. Atomically precise, custom-design origami graphene nanostructures. *Science* **2019**, *365*, 1036−1040.
(119) Liu, Z.; Du, H.; Li, J.; Lu, L.; Li, Z.-Y.; Fang, N. X. Nano-kirigami with giant optical chirality. *Sci. Adv.* **2018**, *4*, eaat4436.
(120) Malik, M.; Iqbal, M. A.; Choi, J. R.; Pham, P. V. 2D Materials for Efficient Photodetection: Overview, Mechanisms, Performance and UV-IR Range Applications. *Front. Chem.* **2022**, *10*, 1−28.
(121) Chen, Y.; Lu, Y.; Liao, M.; Tian, Y.; Liu, Q.; Gao, C.; Yang, X.; Shan, C. 3D solar-blind Ga_2O_3 photodetector array realized via origami method. *Adv. Funct. Mater.* **2019**, *29*, 1906040.
(122) Li, J.; Liu, Z. Focused-Ion-Beam-Based Nano-Kirigami: From Art to Photonics. *Nanophotonics* **2018**, *7*, 1637−1650.
(123) Han, X.; Seo, K. J.; Qiang, Y.; Li, Z.; Vinnikova, S.; Zhong, Y.; Zhao, X.; Hao, P.; Wang, S.; Fang, H. Nanomeshed Si Nanomembranes. *npj Flex. Electron.* **2019**, *3*, 1−8.
(124) Blees, M. K.; Barnard, A. W.; Rose, P. A.; Roberts, S. P.; McGill, K. L.; Huang, P. Y.; McEuen, P. L.; et al. Graphene kirigami. *Nature* **2015**, *524*, 204−207.
(125) Rao, Z.; Lu, Y.; Li, Z.; Sim, K.; Ma, Z.; Xiao, J.; Yu, C. Curvy, shape-adaptive imagers based on printed optoelectronic pixels with a kirigami design. *Nat. Electron.* **2021**, *4*, 513−521.
(126) Choi, C.; Choi, M. K.; Liu, S.; Kim, M.; Park, O. K.; Im, C.; Kim, D. H.; et al. Human eye-inspired soft optoelectronic device using high-density MoS_2-graphene curved image sensor array. *Nat. commun.* **2017**, *8*, 1−11.
(127) Lee, E. K.; Baruah, R. K.; Leem, J. W.; Park, W.; Kim, B. H.; Urbas, A.; Ku, Z.; Kim, Y. L.; Alam, M. A.; Lee, C. H. Fractal Web Design of a Hemispherical Photodetector Array with Organic-Dye-Sensitized Graphene Hybrid Composites. *Adv. Mater.* **2020**, *32*, 2004456.
(128) Ko, H. C.; Stoykovich, M. P.; Song, J.; Malyarchuk, V.; Choi, W. M.; Yu, C. J.; Rogers, J. A.; et al. A hemispherical electronic eye camera based on compressible silicon optoelectronics. *Nature* **2008**, *454*, 748−753.
(129) He, Q.; Feng, J.; Chen, Y.; Zhou, H. Mechanical properties of spider-web hierarchical honeycombs subjected to out-of-plane impact loading. *J. Sandw. Struct. Mater.* **2020**, *22*, 771−796.
(130) Liu, X.; Liu, D.; Lee, J. H.; Zheng, Q.; Du, X.; Zhang, X.; Kim, J. K.; et al. Spider-web-inspired stretchable graphene woven fabric for highly sensitive, transparent, wearable strain sensors. *ACS Appl. Mater. Interfaces* **2019**, *11*, 2282−2294.

(131) Liu, W.; Zou, Q.; Zheng, C.; Jin, C. Metal-assisted transfer strategy for construction of 2D and 3D nanostructures on an elastic substrate. *ACS Nano* **2019**, *13*, 440−448.
(132) Zhao, H.; Li, K.; Han, M.; Zhu, F.; Vázquez-Guardado, A.; Guo, P.; Rogers, J. A.; et al. Buckling and twisting of advanced materials into morphable 3D mesostructures. *Proc. Natl. Acad. Sci. U. S. A.* **2019**, *116*, 13239−13248.
(133) Hua, Q.; Sun, J.; Liu, H.; Bao, R.; Yu, R.; Zhai, J.; Pan, C.; Wang, Z. L. Skin-inspired highly stretchable and conformable matrix networks for multifunctional sensing. *Nat. Commun.* **2018**, *9*, 1−11.
(134) Carlson, A.; Bowen, A. M.; Huang, Y.; Nuzzo, R. G.; Rogers, J. A. Transfer printing techniques for materials assembly and micro/nanodevice fabrication. *Adv. Mater.* **2012**, *24*, 5284−5318.
(135) Gu, L.; Poddar, S.; Lin, Y.; Long, Z.; Zhang, D.; Zhang, Q.; Fan, Z.; et al. A biomimetic eye with a hemispherical perovskite nanowire array retina. *Nature* **2020**, *581*, 278−282.
(136) Ravi Kumar, V.; Klingner, M.; Yogamani, S.; Bach, M.; Milz, S.; Fingscheidt, T.; Mader, P. SVDistNet: Self-supervised near-field distance estimation on surround view fisheye cameras. *IEEE Trans. Intell. Transp. Syst.* **2022**, *23*, 10252−10261.
(137) Gaschet, C.; Jahn, W.; Chambion, B.; Hugot, E.; Behaghel, T.; Lombardo, S.; Henry, D.; et al. Methodology to design optical systems with curved sensors. *Appl. Opt.* **2019**, *58*, 973−978.
(138) Chambion, B.; Gaschet, C.; Behaghel, T.; Vandeneynde, A.; Caplet, S.; Gétin, S.; Ferrari, M. Curved sensors for compact high-resolution wide-field designs: prototype demonstration and optical characterization. *Photonic Instrumentation Engineering V, SPIE* **2018**, *10539*, 240−249.
(139) Stamenov, I.; Arianpour, A.; Olivas, S. J.; Agurok, I. P.; Johnson, A. R.; Stack, R. A.; Morrison, R. L.; Ford, J. E. Panoramic Monocentric Imaging Using Fiber-Coupled Focal Planes. *Opt. express* **2014**, *22*, 31708−31721.
(140) Amelio, G. F.; Tompsett, M. F.; Smith, G. E. Experimental verification of the charge coupled device concept. *Bell Syst. Technol. J.* **1970**, *49*, 593−600.
(141) Bigas, M.; Cabruja, E.; Forest, J.; Salvi, J. Review of CMOS image sensors. *Microelectron. J.* **2006**, *37*, 433−451.
(142) Theuwissen, A. J. *Solid-state imaging with charge-coupled devices* **2006**. DOI: 10.1007/0-306-47119-1
(143) Jahne, B. *Practical Handbook on Image Processing for Scientific and Technical Applications*; CRC Press, 2004.
(144) Lesser, M. Charge coupled device (CCD) image sensors. *High Performance Silicon Imaging*; Elsevier, 2014; pp 78−97.
(145) Pain, B.; Cunningham, T.; Nikzad, S.; Hoenk, M.; Jones, T.; Wrigley, C.; Hancock, B. A back-illuminated megapixel CMOS image sensor. *IEEE Workshop on Charge-Coupled Devices and Advanced Image Sensors*; IEEE, 2005.
(146) Lee, H.; Song, C.; Hong, Y. S.; Kim, M.; Cho, H. R.; Kang, T.; Kim, D. H.; et al. Wearable/disposable sweat-based glucose monitoring device with multistage transdermal drug delivery module. *Sci. adv.* **2017**, *3*, e1601314.
(147) *Detectors: CCDs for Life-Science Applications*; Photonics Media, 2023. https://www.photonics.com/Articles/Detectors_CCDs_for_Life-Science_Applications/a25141.
(148) Wong, H. S.; Yao, Y. L.; Schlig, E. S. TDI charge-coupled devices: design and applications. *IBM J. Res. Dev.* **1992**, *36*, 83−106.
(149) Ding, H.; Guo, W.; Su, B. Imaging cell-matrix adhesions and collective migration of living cells by electrochemiluminescence microscopy. *Angew. Chem., Int. Ed.* **2020**, *132*, 457−464.
(150) Zhang, J.; Jin, R.; Jiang, D.; Chen, H. Y. Electrochemiluminescence-Based Capacitance Microscopy for Label-Free Imaging of Antigens on the Cellular Plasma Membrane. *J. Am. Chem. Soc.* **2019**, *141*, 10294−10299.
(151) Cao, J. T.; Wang, Y. L.; Zhang, J. J.; Dong, Y. X.; Liu, F. R.; Ren, S. W.; Liu, Y. M. Immuno-electrochemiluminescent imaging of a single cell based on functional nanoprobes of heterogeneous Ru (bpy) 32+@ SiO_2/Au nanoparticles. *Anal. Chem.* **2018**, *90*, 10334−10339.
(152) Yu, L.; Zhang, Q.; Kang, Q.; Zhang, B.; Shen, D.; Zou, G. Near-Infrared Electrochemiluminescence Immunoassay with Biocompatible Au Nanoclusters as Tags. *Anal. Chem.* **2020**, *92*, 7581−7587.
(153) Fawzi, A.; Moosavi-Dezfooli, S. M.; Frossard, P.; Soatto, S. Classification regions of deep neural networks. *arXiv preprint arXiv:1705.09552*, 2017.
(154) Sibai, F. N.; Shehhi, A.; Shehhi, S.; Shehhi, B.; Salami, N. Designing and Training Feed-Forward Artificial Neural Networks for Secure Access Authorization. *Pattern Recognition* **2009**, 29 DOI: 10.5772/7526.
(155) Sanchez-Ruiz, F. J. Reactive Distillation Modeling Using Artificial Neural Networks. *IntechOpen* **2022**. DOI: 10.5772/intechopen.101261.
(156) Sangeetha, T.; Meenal, C. Digital Implementation of Artificial Neural Network for Function Approximation and Pressure control applications. *IOSR J. Electron. Commun. Eng.* **2013**, *5*, 34.
(157) Bishop, C. M.; Nasrabadi, N. M. *Pattern recognition and machine learning*; Springer, 2006; Vol. *4*, p 738.
(158) Hornik, K. Approximation capabilities of multilayer feedforward network. *Neural networks* **1991**, *4*, 251−257.
(159) Ebrahimi, E.; Mollazade, K.; Arefi, A. An Expert System for Classification of Potato Tubers Using Image Processing and Artificial Neural Networks. *Int. J. Food Eng.* **2012**, *8*. DOI: 10.1515/1556-3758.2656
(160) Szegedy, C.; Zaremba, W.; Sutskever, I.; Bruna, J.; Erhan, D.; Goodfellow, I.; Fergus, R. J. Intriguing properties of neural networks. *arXiv preprint arXiv:1312.6199*, 2013.
(161) Nielsen, M. A. *Neural networks and deep learning*; Determination press, 2015; Vol. *25*.
(162) Tien, P. W.; Wei, S.; Calautit, J. K.; Darkwa, J.; Wood, C. A vision-based deep learning approach for the detection and prediction of occupancy heat emissions for demand-driven control solutions. *Energy Build.* **2020**, *226*, 110386.
(163) Menotti, D.; Chiachia, G.; Pinto, A.; Schwartz, W. R.; Pedrini, H.; Falcao, A. X.; Rocha, A. Deep representations for iris, face, and fingerprint spoofing detection. *IEEE Trans. Inf. Forensics Secur.* **2015**, *10*, 864−879.
(164) Gao, S.; Zhang, Y.; Jia, K.; Lu, J.; Zhang, Y. Single sample face recognition via learning deep supervised autoencoders. *IEEE Trans. Inf. Forensics Secur.* **2015**, *10*, 2108−2118.
(165) Cai, M.; Shi, Y.; Liu, J. Deep maxout neural networks for speech recognition. *IEEE Workshop on Automatic Speech Recognition and Understanding* **2013**, 291−296.
(166) Kundu, S.; Mantena, G.; Qian, Y.; Tan, T.; Delcroix, M.; Sim, K. C. Joint acoustic factor learning for robust deep neural network based automatic speech recognition. *IEEE International Conference on Acoustics, Speech and Signal Processing*; IEEE, 2016; pp 5025−5029.
(167) Li, C.; Yang, C. The research on traffic sign recognition based on deep learning. *IEEE 16th International Symposium on Communications and Information Technologies (ISCIT)*; IEEE, 2016; pp 156−161.
(168) Nataprawira, J.; Gu, Y.; Goncharenko, I.; Kamijo, S. Pedestrian detection using multispectral images and a deep neural network. *Sensors* **2021**, *21*, 2536.
(169) Wang, X.; Yang, M.; Zhu, S.; Lin, Y. Regionlets for generic object detection. *Proceedings of the IEEE international conference on computer vision*; IEEE, 2013; pp 17−24.
(170) Muduli, P. R.; Gunukula, R. R.; Mukherjee, A. A deep learning approach to fetal-ECG signal reconstruction. *2016 Twenty Second National Conference on Communication (NCC)*; IEEE, 2016; pp 1−6.
(171) Zhou, L.; Yan, Y.; Qin, X.; Yuan, C.; Que, D.; Wang, L. Deep learning-based classification of massive electrocardiography data. *IEEE Advanced Information Management, Communicates, Electronic and Automation Control Conference (IMCEC)*; IEEE, 2016; pp 780−785.
(172) Du, L. H.; Liu, W.; Zheng, W. L.; Lu, B. L. Detecting Driving Fatigue with Multimodal Deep Learning. *8th International IEEE/EMBS Conference on Neural Engineering (NER)*; IEEE, 2017; pp 74−77.

(173) Xia, B.; Li, Q.; Jia, J.; Wang, J.; Chaudhary, U.; Ramos-Murguialday, A.; Birbaumer, N. Electrooculogram based sleep stage classification using deep belief network. *IEEE International Joint Conference on Neural Networks (IJCNN)*; IEEE, 2015; pp 1−5.
(174) Fraiwan, L.; Lweesy, K. Neonatal sleep state identification using deep learning autoencoders. *IEEE 13th International Colloquium on Signal Processing & its Applications (CSPA)*; IEEE, 2017; pp 228−231.
(175) Rojas, R. *Neural networks: a systematic introduction*; Springer Science & Business Media, 2013.
(176) Goodfellow, I.; Bengio, Y.; Courville, A. *Deep learning*; MIT press, 2016.
(177) Zeiler, M. D.; Fergus, R. Visualizing and understanding convolutional networks. *13th European conference on computer vision*; Springer, 2014; pp 818−833.
(178) Kriegeskorte, N.; Golan, T. Neural Network Models and Deep Learning. *Curr. Biol.* **2019**, *29*, R231−R236.
(179) Nebauer, C. Evaluation of Convolutional Neural Networks for Visual Recognition. *IEEE transactions on neural networks* **1998**, *9*, 685−696.
(180) Krizhevsky, A.; Sutskever, I.; Hinton, G. E. Imagenet classification with deep convolutional neural networks. *Communications of the ACM* **2017**, *60*, 84−90.
(181) Chauhan, R.; Ghanshala, K. K.; Joshi, R. Convolutional neural network (CNN) for image detection and recognition. *First International Conference on Secure Cyber Computing and Communication (ICSCCC)*; IEEE, 2018; pp 278−282.
(182) Rashid, T. A. Convolutional neural networks based method for improving facial expression recognition. *The international symposium on intelligent systems technologies and applications*; Springer, 2016, *530*, pp 73−84.
(183) Guo, Y.; Liu, Y.; Oerlemans, A.; Lao, S.; Wu, S.; Lew, M. S. Deep learning for visual understanding: A review. *Neurocomputing* **2016**, *187*, 27−48.
(184) Alom, M. Z.; Taha, T. M.; Yakopcic, C.; Westberg, S.; Sidike, P.; Nasrin, M. S.; Van Esesn, B. C.; Awwal, A. A. S.; Asari, V. K. The history began from alexnet: A comprehensive survey on deep learning approaches. *arXiv preprint arXiv:1803.01164*, 2018.
(185) Simonyan, K.; Zisserman, A. Very deep convolutional networks for large-scale image recognition. *arXiv preprint arXiv:1409.1556*, 2014.
(186) Mennel, L.; Symonowicz, J.; Wachter, S.; Polyushkin, D. K.; Molina-Mendoza, A. J.; Mueller, T. Ultrafast machine vision with 2D material neural network image sensors. *Nature* **2020**, *579*, 62−66.
(187) Zhou, F.; Zhou, Z.; Chen, J.; Choy, T. H.; Wang, J.; Zhang, N.; Chai, Y.; et al. Optoelectronic resistive random access memory for neuromorphic vision sensors. *Nat. Nanotechnol.* **2019**, *14*, 776−782.
(188) Sun, Y.; Chang, H.; Hu, J.; Wang, Y.; Weng, Y.; Zhang, C.; Xiao, L.; et al. Large-scale multifunctional carbon nanotube thin film as effective mid-infrared radiation modulator with long-term stability. *Adv. Opt. Mater.* **2021**, *9*, 2001216.

https://doi.org/10.1021/acsmaterialslett.2c01011
ACS Materials Lett. 2023, 5, 1027−1060